

NORTHWESTERN UNIVERSITY

*Neural Mechanisms Underlying Hand/Arm Impairment and Intervention-Induced Improvements
Post-Stroke*

A DISSERTATION

SUBMITTED TO THE GRADUATE SCHOOL
IN PARTIAL FULFILLMENT OF THE REQUIRMENTS

For the degree

DOCTOR OF PHILOSOPHY

Field of Neuroscience

By

Kevin B. Wilkins

EVANSTON, ILLINOIS

September 2019

Abstract

Individuals following a stroke suffer from a host of movement impairments that affect the upper extremity. Hand use is often significantly compromised, especially in individuals with more severe impairments, which makes it difficult for individuals to participate in activities of daily living. One of the major goals of rehabilitation is to understand the neural mechanisms underlying these impairments and then target them in order to improve hand and arm function. Unfortunately, many individuals with more severe impairments are typically excluded from traditional hand and arm therapy due to a lack of residual hand function.

One reason for this observed difficulty in opening the hand is the loss of independent joint control. The most debilitating form of this for hand opening is termed the ‘flexion synergy’, in which activation of the shoulder abductors, such as during lifting, leads to involuntary coactivation of elbow, wrist, and finger flexors. Consequently, hand opening ability, which is already impaired due to extensor weakness, is further exacerbated due to involuntary wrist/finger coactivation. Whereas weakness is thought to be due to damage to ipsilesional CST, this loss of independent joint control may be due to an increased compensatory reliance on uncrossed contralesional cortico-bulbospinal pathways that innervate the paretic arm but bias towards flexors and lack the resolution to individually activate muscles.

The goal of this dissertation is to examine the neural mechanisms underlying the negative impact of lifting on hand opening ability in individuals following a stroke and any subsequent neural changes following participation in a device-assisted task-specific arm/hand intervention. We combined structural imaging of cortical gray matter, functional imaging related to the hand/arm,

and robotics to uncover both the neural mechanisms of impairment and subsequent behavioral improvements following an intervention. We first investigated functional cortical activity changes for the hand in isolation compared to in conjunction with the shoulder in healthy individuals who do not display any negative impact of lifting on hand opening ability. We found that increasing the complexity of the task from a simple hand opening to a multi-joint hand opening while lifting led to an increase in cortico-cortico coupling between both the contralateral and ipsilateral hemisphere relative to the moving arm during the motor preparation phase, but that it did not alter the predominant reliance on contralateral motor cortices at movement execution. Meanwhile, for individuals with stroke, the addition of lifting during attempted hand opening led to an increase in activity in the ipsilateral (i.e., contralesional) hemisphere, specifically in ipsilateral secondary motor regions. This increased activity in ipsilateral secondary motor areas was associated with a decrease in hand opening ability, suggesting that a compensatory reliance on these regions (and their descending projections) may be detrimental to hand opening. Furthermore, individuals following a stroke showed a systematic increase in gray matter density in ipsilateral secondary motor areas compared to controls, implying a long-term compensatory reliance on these regions. Finally, we investigated the neural changes following a device-assisted task-specific hand arm intervention that improved hand function. Following the intervention, individuals displayed an increased reliance on the ipsilesional sensorimotor cortices for both hand opening in isolation and hand opening while lifting. This increased reliance included a reduction in contralesional primary sensorimotor cortex activity and an increase in ipsilesional primary sensorimotor cortex activity at movement execution. Furthermore, these changes at movement execution were accompanied by complementary changes in coupling during motor preparation, including a reduction in interhemispheric M1 coupling and a change in coupling within ipsilesional M1. In addition,

individuals exhibited structural changes in the sensorimotor cortex, including an increase in gray matter density in ipsilesional primary sensorimotor cortex and a decrease in contralesional primary sensorimotor cortex.

This work demonstrates that the negative impact of lifting on hand opening may be at least partially attributed to an increased reliance on contralesional secondary motor areas. This fits within the framework proposing that compensatory use of contralesional cortico-bulbospinal tracts may result in the loss of independent joint control, since these tracts primarily originate from secondary motor areas. Furthermore, this work confirms that even individuals with severe motor impairments maintain the ability to reengage residual ipsilesional resources if engaged in an effective intervention. Considering the detrimental effect of the contralesional hemisphere on hand opening, reengaging the ipsilesional sensorimotor cortex appears crucial for any potential recovery of the hand.

Acknowledgements

This dissertation would not have been possible without the mentorship, support, and guidance I received from all of those I have been in touch with over the last five years. First, and foremost, I want to thank my advisor Dr. Jun Yao for her unwavering support throughout the entirety of my time at Northwestern. You taught me more things than I can count and helped shape me into the scientist, researcher, and person I am today. I will be forever grateful for all of the things you have done for me, and I look forward to maintaining our relationship far into the future.

I would also like to thank Dr. Jules Dewald, who has served as my scientific mentor from the very beginning. You were always willing to help my scientific development and growth in any way you could, and for that I will be always be grateful.

I would also like to thank the rest of my committee, Dr. Lee Miller and Dr. Carson Ingo who provided invaluable feedback and guidance to help tailor and improve my research project. Your expertise was instrumental in helping develop and interpret the results of my projects, while helping me further my development as a scientist.

To the Dewald Lab and PTHMS department, thank you for your friendship, mentorship, advice, feedback, and support. Carolina, you have been so helpful from the very first day I joined the lab and a true friend. You never hesitated to help me whenever I was in need, and it was a joy to be around you. Ana Maria, Mike, Netta, and Yuan, thank you for all of your suggestions and feedback of my work over the past few years. You helped me develop my scientific instincts and learn how to see questions and answers from multiple points of view. Special thanks to Erin and Brad for all

of your help over the years. Thank you to Meriel, Rachel, Lindsay, Yiyun, Ben, Nayo, Jordan, Al, Ed, Jackie, Kacey, Miranda, Mary, Steve, Grace, Vatsala, Drew, Thomas, Ray, Dylan, Mark, and all the other past and present students for being such supportive friends and great people. It was a joy getting the chance to work with you, and I hope you all the best in the future.

To all of the participants who gave their own time to come and be a part of my research projects, whether it was for just one experiment, or for a two-month intervention. This work would not have been possible without your help. You inspire me every single day to try and come in and make a difference.

To my parents and grandparents, thank you for your love and support through the good times and the bad. You have always been there for me no matter what and provided me with the chance to come to Northwestern in the first place. Thank you to my sister, Christine, for being the best friend I could every ask for. No matter the distance, I know I could and can always count on you.

Lastly, I want to thank Liz Lydon. You have been my rock for the last 8 years. I don't know where I would be without your love and support. I can't wait to see where and what our future adventures bring us.

Table of Contents

Abstract	2
Acknowledgements.....	5
List of Figures	10
Lift of Tables.....	11
1. Introduction.....	12
Problem Statement	12
Research Goals	13
Research Aims	14
Dissertation Outline	14
2. Background and Literature Review	15
Healthy Motor System.....	15
Cortical Regions	15
Descending Motor Tracts.....	18
Motor Impairments Following a Stroke	20
Neural Mechanisms of Motor Impairment.....	22
Weakness.....	22
Loss of Independent Joint Control.....	24
Behavioral Recovery Following a Stroke	26
Neural Mechanisms of Recovery.....	30
Summary.....	34
3. Neural Effects of Lifting on Hand Opening in Healthy Individuals	35
Abstract.....	35
Introduction	36
Materials and Methods	39
Participants.....	39
Experimental Design.....	39
Data Analysis.....	41
Statistical Analysis.....	47
Results	47
Behavioral Results	47
Bayesian model selection and model fit.....	48
Default motor networks for the two tasks	51
Task-related differences in coupling.....	53
Cortical Activity Related to Movement Execution.....	55
Discussion	55
Common Networks During Single- and Multi-Joint Movements	56

	8
Distinct Networks During Single- and Multi-Joint Movements	57
Potential Role of the Ipsilateral Hemisphere.....	61
No Change in Cortical Activity Related to Movement Execution.....	62
Limitations	62
Conclusion.....	64
4. Ipsilateral Secondary Motor Areas Drive the Negative Impact of Lifting on Hand Opening Ability Post-Stroke.....	65
Abstract.....	65
Introduction	66
Materials and Methods	69
Participants	69
Experimental Protocols.....	70
Data Analysis.....	73
Statistical Analysis.....	76
Results	77
Differences in Gray Matter Density in Ipsilateral Sensorimotor Cortex	77
Impact of Shoulder Abduction on Hand Opening Ability Post Stroke.....	79
Impact of Shoulder Abduction on Cortical Activity.....	80
Relationship Between Cortical Activity and Hand Opening Ability.....	83
Relationship Between Cortical Activity and Cortical Structure.....	83
Cortico-Cortico Coupling.....	84
Discussion	86
Clinical Implications.....	92
Limitations	92
5. Neural Plasticity in Moderate to Severe Chronic Stroke Following a Device-Assisted Task-Specific Arm/Hand Intervention	94
Abstract.....	94
Introduction	95
Materials and Methods	99
Participants	99
Experimental Protocols.....	100
Intervention	100
Pre- and Post-Intervention Tests	101
Clinical Assessments	101
Structural Imaging of the Brain.....	102
Functional Imaging Related to Hand Opening	102
Data Analysis.....	103
Reorganization of Cortical Activity Related to Movement Execution.....	103
Dynamic causal modeling for induced responses.....	105
Definition of model space.....	105
DCM Preprocessing.....	107
Calculation of coupling parameters.....	108
Bayesian model selection	109

	9
Inference on coupling parameters	110
Structural Changes in GM Density	110
Statistical Analysis.....	111
Results	111
Changes in arm/hand function following EMG-FES task-specific training.....	111
Cortical reorganization related to the hand and arm	112
Bayesian model selection and model fit.....	114
Intervention-induced changes in coupling parameters.....	116
.....	118
Intervention-induced changes in gray matter density.....	118
Discussion	120
Shift Toward Ipsilesional Hemisphere	120
Changes in Cortical Activity Driving LI Shift	122
Increased Gray Matter Density in Ipsilesional Sensorimotor Cortex.....	126
Limitations	128
Conclusion.....	129
6. Discussion.....	131
Thesis Summary	131
Neural Mechanisms Underlying the Negative Impact of Lifting on Hand Opening Ability	132
Neural Changes Following an Intervention	137
Future Directions.....	139
Conclusion.....	143
References	145
Appendix.....	166
EEG Analysis	166
Dynamic Causal Modeling for Induced Responses	166
Pressure Analysis.....	169
Gray Matter Density Analysis	170

List of Figures

Figure 3.1.....	43
Figure 3.2.....	48
Figure 3.3.....	50
Figure 3.4.....	50
Figure 3.5.....	51
Figure 3.6.....	52
Figure 3.7.....	55
Figure 4.1.....	70
Figure 4.2.....	78
Figure 4.3.....	79
Figure 4.4.....	80
Figure 4.5.....	81
Figure 4.6.....	82
Figure 4.7.....	83
Figure 4.8.....	84
Figure 4.9.....	84
Figure 5.1.....	100
Figure 5.2.....	101
Figure 5.3.....	108
Figure 5.4.....	113
Figure 5.5.....	114
Figure 5.6.....	115
Figure 5.7.....	116
Figure 5.8.....	118
Figure 5.9.....	119

Lift of Tables

Table 3.1. Coordinates for Motor Network	42
Table 3.2. Exceedance probabilities for each family.....	49
Table 3.3. Exceedance probabilities for each model.....	49
Table 3.4. Significant default frequency-to-frequency coupling.....	53
Table 3.5. Significant differences in frequency-to-frequency coupling between tasks.....	54
Table 4.1. Participant Demographics	70
Table 4.2. Significant default frequency-to-frequency coupling.....	85
Table 5.1. Participant Demographics and Clinical Characteristics	106
Table 5.2. Coordinates of Motor Network	106
Table 5.3. Exceedance probabilities for each model.....	115
Table 5.4. Brain regions exhibiting changes in Gray Matter Density	120

1. Introduction

Problem Statement

Stroke is currently the leading cause of disability in the United States, with over 800,000 individuals experiencing a stroke every year (Mozaffarian et al. 2015). Approximately two thirds of survivors then receive rehabilitation services of some nature following their hospitalization to improve function (Buntin et al. 2010). This formal rehabilitation is commonly concluded 3-4 months following a stroke but does not always lead to a full recovery. Roughly 50% of individuals will experience some form of hemiparesis contributing to the motor impairment in the upper limb (Roger et al. 2012), and unfortunately greater than 40% of stroke survivors still report participation restrictions, such as difficulty with autonomy, engagement, and fulfilling societal roles, 4 years after their stroke and almost 80% report not feeling fully recovered (Gadidi et al. 2011).

Motor impairments following a stroke impact both the upper and lower extremity. A recent survey found that for the upper extremity, stroke survivors reported the largest gap between their desired function and actual function for the paretic hand compared to the rest of the arm (Sullivan et al. Accepted). This matches clinical observations in which the distal portion of the limb, such as the hand, tends to be more impaired than more proximal portions of the limb such as the shoulder or elbow. Additionally, the observed impairment is greater for finger/wrist extension (i.e., opening) compared to finger/wrist flexion (i.e., closing) once in the chronic phase (Conrad and Kamper 2012). The observed hand impairment is due to a combination of issues, including weakness of the finger extensor muscles, hypertonicity of the finger/wrist flexor muscles, and the loss of independent joint control, in which movements such as lifting or reaching lead to involuntary coactivation of wrist/finger flexors. A better understanding of the neural mechanisms underlying

the observed hand impairment following a stroke may lead to more targeted interventions and evaluation of recovery potential.

Unfortunately, evidence for significant improvements in hand function following stroke rehabilitation is still lacking, particularly for individuals with more severe impairments. In fact, individuals with more severe impairments are often excluded from typical hand-targeted interventions due to an inability to voluntarily perform the necessary movements required to participate. Consequently, we still do not know what capacity these individuals may have for improving hand function if involved in an effective intervention. However, recent advances in assistive devices, including robotic, mechanical, and electrical stimulation devices offer a means with which to include this population in intensive hand therapy for the first time, and have shown promising results. The question remains, though, whether the underlying neural mechanisms of behavioral improvements following effective interventions mirrors that from more traditional therapy in individuals with mild impairments and addresses the underlying mechanisms of the initial observed impairment.

Research Goals

The goal of this dissertation is to examine the neural mechanisms underlying hand impairment and subsequent intervention-induced improvements in individuals with moderate to severe chronic hemiparetic stroke. In order to carry out this goal, we need a comprehensive understanding of the healthy condition, what may go wrong following a stroke, and how an intervention bridges the gap between the two. Understanding this interaction offers a path towards building more effective interventions that may improve upper extremity functions in individuals with more severe

impairments. At the impairment level, I will focus on the neural mechanisms underlying the loss of independent joint control and its negative impact on hand function in particular. Meanwhile, at the intervention-level, I will evaluate the behavioral and neural effects of a device-assisted task-specific hand/arm longitudinal training.

Research Aims

In order to accomplish the goal stated above, I carried out the following three research aims:

- 1) Quantified the effect of lifting on cortical activity related to hand opening in healthy individuals
- 2) Explored the neural mechanisms underlying the negative impact of lifting on hand opening following a stroke
- 3) Investigated neural changes following a device-assisted task-specific intervention in individuals with moderate to severe chronic hemiparetic stroke

Dissertation Outline

Chapter 2 will provide background information covering the healthy motor system, behavioral impairments following stroke, the neural mechanisms underlying those impairments, behavioral recovery following a stroke, and the neural mechanisms underlying that recovery. Chapter 3 will use healthy controls to evaluate how the addition of lifting typically impacts cortical activity related to hand opening under normal circumstances. Chapter 4 will then show how this cortical activity differs in individuals following a stroke, both functionally and structurally, and how this relates to the observed behavioral impairment. Chapter 5 will then show how the observed neural differences change following an effective hand-arm intervention. Finally, Chapter 6 will provide a discussion of the overall results, potential future directions, and conclusion of the thesis.

2. Background and Literature Review

Healthy Motor System

Successful movement entails the integration of high-level goals into a motor output to control the activation of muscles in a precise manner. This includes the combination of cortical and subcortical interactions in the motor preparation phase, followed by the actual motor command to activate muscle. Unfortunately, damage to any portion of this chain of events can lead to altered or impaired motor behavior. Although this process is not limited to only sensorimotor cortical regions, as the basal ganglia, cerebellum, brainstem, and other cortical regions are known to be involved, the following section will focus primarily on the sensorimotor cortical regions and the descending pathways that carry these signals to the spinal cord.

Cortical Regions

Primary Motor Cortex (M1)

The primary motor cortex (M1) is located posterior to the supplementary motor area and premotor cortex, including the precentral gyrus up to the central sulcus. M1 is a major source of descending motor commands for voluntary movement going back to electrical stimulation experiments in the 1890s (Beevor and Horsley 1890). Further studies showed the importance of M1 for movement execution by finding that M1 modulated its firing rate near movement onset and displayed a relationship with force production and movement direction in monkeys (Evarts 1968; Georgopoulos et al. 1982). More recent approaches have started looking at the neuronal population as a whole, rather than individual neurons in an attempt to explain how M1 is involved in the generation of movement. It seems that patterns of activity confined to low-dimensional space can explain behavior quite well (Gallego et al. 2017), which may alleviate some of the difficulties with

predicting movement patterns from individual neurons (Churchland et al. 2012). This finding may underlie the success at attempting to decode movement intention from M1 population activity despite access to only a small portion of M1 neurons (Bouton et al. 2016).

Activity in M1 is related to motor output, as approximately 50% of the Corticospinal Tract (CST) originates from M1. This potential role of M1 during motor output fits in line with results from fMRI in humans showing increases in blood-oxygen-level-dependent imaging in contralateral M1 during hand closing (Grefkes et al. 2008a). However, it is worth noting that the majority of corticobulbar and CST neurons do not synapse directly on motoneurons and instead project to brainstem and spinal interneurons which can have inhibitory connections to motoneurons (Ebbesen and Brecht 2017). This suggests that M1 may also be playing a role in movement suppression in addition to its role in movement execution. M1 also receives projections from secondary motor areas and subcortical regions, further complicating its role in movement preparation and execution (Morecraft and Van Hoesen 1993; Muakkassa and Strick 1979).

Supplementary Motor Area (SMA)

The supplementary motor area (SMA) is located on the medial aspect of the human brain, specifically in the dorsomedial frontal cortex and anterior to the leg representation of M1 (Nachev et al. 2008). The SMA sends and receives projections from/to primary motor cortex (Jurgens 1984), frontal cortex (Arikuni et al. 1988), parietal cortex (Jurgens 1984), basal ganglia (Jurgens 1984), thalamus (Matelli et al. 1989; Schell and Strick 1984), and also sends descending projections to the spinal cord (Maier et al. 2002). Therefore, it has been implicated in both the

shaping of motor planning prior to movement, as well as movement execution. SMA is traditionally thought to be primarily involved in self-initiated movements (Tanji 2001). However, additional work in monkeys has shown that it is also involved externally cued movements (Kurata and Wise 1988; Romo and Schultz 1987). It seems to be especially important during the motor planning of movement since it shows increases in firing rates prior to hand movements (Brinkman and Porter 1979; Tanji and Kurata 1982). This can also be captured in humans using electroencephalography (EEG), in which a ‘readiness’ potential is observed, especially for self-initiated movements, over central sensorimotor cortex corresponding to SMA roughly 0.8-1.0 seconds prior to movement onset (Deecke and Kornhuber 1978; Jahanshahi et al. 1995). Importantly, this activity in SMA precedes activity in primary motor cortex during a distal hand task, suggesting that SMA may be providing information to primary motor cortex to shape motor output (Huang et al. 2004).

Premotor Cortex (PM)

The premotor cortex is typically categorized into two specific regions: dorsal premotor cortex (PMd) and ventral premotor cortex (PMv). The PM is located on the lateral surface of the cortex posterior to prefrontal cortex and anterior to the precentral gyrus (Barbas and Pandya 1987). In addition to connections with M1, the PM is connected to the parietal cortex (Tanne-Gariepy et al. 2002; Wise et al. 1997), thalamus (Matelli et al. 1989), and other cortical and subcortical regions. Similar to SMA, PM has been implicated in both the planning and execution of movement due to the presence of cortical-cortical connections in addition to descending projections to the spinal cord (Dum and Strick 1991). Early hypotheses implicated the PM as a mechanism of shaping motor output from primary motor cortex rather than direct control of muscles; however, further

work has demonstrated the intrinsic role within PM for planning goal-directed movements (Wise 1985). Unlike SMA which has been more widely associated with self-initiated movements, PM is thought to be crucial for planning and executing visually-cued movements. In particular, PM activity is especially prominent for reaching and grasping type movements (Takahashi et al. 2017).

Additional Motor-Related Cortical Regions

Motor-related cortical activity is not limited to M1, SMA, and PM. For instance, the posterior parietal cortex is a well-accepted part of the motor system. This includes anterior intraparietal area, lateral intraparietal area, inferior parietal lobule, and other subregions within the parietal lobe. However, its primary role is in visuomotor transformation and sensory integration (Fogassi and Luppino 2005). Since this thesis will primarily focus on self-initiated movements that are not visually-guided, where posterior parietal cortex is less likely to play a significant role, I will not focus on this region.

Descending Motor Tracts

Corticospinal Tract (CST)

The corticospinal tract (CST) is the primary descending motor tract of the brain, particularly for more distal movements, with origins predominantly from M1, but also spanning PM, SMA, S1, and cingulate (Dum and Strick 2002; Ralston and Ralston 1985) in layer V of the cortex. The majority of the CST (80-90%) crosses over at the level of the medulla to control the limb opposite of the sensorimotor cortex origin (lateral CST), whereas the remaining tract projects ipsilaterally (ventral CST). The CST has the fastest conduction time of the motor tracts due to its monosynaptic nature, synapsing directly on alpha motor neurons in the ventral horn or interneurons that influence

those alpha motor neurons. Importantly, the CST seems to be especially important to the primate, with increasing importance to humans as compared to monkeys (Lemon 2008). Whereas the lateral CST seems to play a crucial role in distal movements of the forelimb, uncrossed ventral CST lacks strong connections to distal portions of the limb and primarily innervates axial muscles (Zaaimi et al. 2018).

Reticulospinal Tract (RST)

The reticulospinal tract (RST) originates in the medial reticular formation nuclei in the pons and medulla, such as the nucleus reticularis gigantocellularis and pontis caudalis, sending both ipsilateral and contralateral projections to the spinal cord (Fukushima et al. 1979). M1 sends connections primarily to contralateral reticular formation, whereas SMA and PM send connections primarily to ipsilateral reticular formation, which has been confirmed through anterograde tracers and cortical stimulation (Fregosi et al. 2017; Montgomery et al. 2013). Although the RST is typically implicated in postural control and more proximal muscles, it also makes mono- and di-synaptic connections to the forearm (Riddle et al. 2009). However, these connections are substantially weaker than CST connections (only ~10-20% in strength) (Baker 2011; Riddle et al. 2009). RST preferentially activates flexor muscles ipsilaterally and extensor muscles contralaterally (Davidson et al. 2007), with innervations that spread across multiple spinal segments (Matsuyama et al. 1999; Matsuyama et al. 1997).

Additional Motor Tracts

In addition to the CST and RST, studies in monkeys have revealed the existence of additional motor tracts including rubrospinal, vestibulospinal, and tectospinal tract. The rubrospinal tract,

originating from the magnocellular red nucleus, plays a role in reaching and grasping in monkeys (Lemon 2008). However, functional evidence of its use in humans is limited (Nathan and Smith 1955). Meanwhile, the vestibulospinal tract originates in the vestibular nucleus and is important for postural adjustments and head movements. Lastly, the tectospinal tract descends from the superior colliculus through the contralateral anterior funiculus to cervical levels of the spinal cord. Although it is assumed to be important in the reflex responsible for turning the head in response to various sensory stimuli, little is known about its function in humans. Given the greater evidence implicating the CST and RST in upper extremity motor behavior in humans, the majority of this thesis will focus on these pathways.

Motor Impairments Following a Stroke

Several motor impairments are observed following a stroke. Individuals often display one or more of the following: muscle weakness, loss of independent joint controls (also referred to as synergy), and excessive muscle tone (also referred to as hyperactive stretch reflexes or spasticity).

Muscle weakness, or the inability to fully activate a muscle (leading to a loss of force generation), is the most common impairment observed following a stroke (Sathian et al. 2011). It gives rise to the nomenclature “hemiparetic,” which refers to the weakness observed on one side of the body. At the level of the motor unit, this weakness has been hypothesized to be at least partially due to a combination of a reduction in the discharge rate of motor units, a more limited range of motoneuron recruitment, and inability to increase motor unit discharge rate during increasing voluntary force production (Gemperline et al. 1995). In the upper extremity, this weakness is greater at the level of the hand as compared to more proximal muscles such as the elbow in individuals in the chronic phase (Garmirian et al. 2018). Additionally, at the level of the hand,

weakness is greater for extensor muscles compared to flexor muscles (Conrad and Kamper 2012). This paresis leads to slower, less accurate, and less efficient movements compared to healthy individuals (Lang et al. 2005; Lang et al. 2006).

The loss of independent joint control (sometimes referred to as loss of fractionated movement or synergy) refers to the inability to voluntarily move segments of the limb independently of other segments. In the upper extremity, this decreased ability to selectively activate muscles is most commonly seen in the case of the flexion synergy where activation of shoulder abductors leads to involuntary coactivation of elbow, wrist, and finger flexors (Dewald et al. 1995; Miller and Dewald 2012; Sukal et al. 2007). The flexion synergy leads a reduction in reaching ability due to involuntary activation of the biceps, and a reduction in hand opening ability due to involuntary activation of the finger flexors. In fact, in individuals with more severe impairments, this involuntary coactivation of the finger flexors during shoulder abduction can lead to individuals closing their hand when they are actually attempting to open (Lan et al. 2017). In the upper extremity, there is also the less common extension synergy, in which shoulder adduction leads to elbow extension, but still with wrist/finger flexion (McPherson and Dewald 2019). The loss of independent joint control in the upper extremity makes many activities of daily living that are already difficult due to the presence of weakness, practically impossible due to the involuntary flexor coactivation of elbow, wrist, and finger muscles making it difficult to reach and open the hand.

Abnormal muscle tone, typically in the form of hypertonicity, refers to the abnormal resistance of the muscle to passive elongation or stretch (Bohannon and Smith 1987). This hypertonicity,

sometimes referred to clinically as spasticity, is velocity-dependent, with faster stretches inducing greater resistance. Consequently, the limb may be harder to move, and range of motion may be limited. However, in individuals with moderate to severe chronic stroke, the functional implications of spasticity may be limited since individuals often cannot move their limb fast enough to induce this resistance when having to deal with the weight of their limb (McPherson et al. 2017). This fits well with the clinical finding that patients with spasticity are not more impaired in voluntary control than those without spasticity, nor do they recover less (O'Dwyer et al. 1996).

It is worth noting that although these clinical impairments can be observed in isolation, they are typically highly correlated. For instance, the severity of paresis or weakness is highly correlated with the loss of independent joint control (Lang and Beebe 2007) and the degree of spasticity or abnormal muscle tone (Lang and Beebe 2007). This is thought to be due to the similarities and interconnectedness of their underlying neural mechanisms, which will be expanded upon in the next section. However, at the level of the hand, weakness in grip strength and extension accounts for the greatest portion of variance between individuals with moderate and severe chronic impairments compared to biomechanical changes or spasticity (Kamper et al., 2006).

Neural Mechanisms of Motor Impairment

Weakness

The observed weakness following stroke is a consequence of damage to corticofugal pathways within the lesioned hemisphere (Stinear et al. 2007). Lawrence and Kuypers were among the first to show that damage to the corticospinal tract, as induced by pyramidal tract lesions, leads to a combination of loss of dexterity and weakness distally in monkeys (Lawrence and Kuypers 1968).

Although corticobulbar tracts could compensate for postural stability and even behaviors more reliant on power grasps, such as climbing, these initial lesion studies showed the necessity of CST for hand function. This is likely due to the fact that the CST is the only motor pathway sufficiently innervating the extensor muscles of the wrist and fingers. Therefore, there is limited ability for other pathways to substantially compensate for hand function (particularly opening and individuation) following extensive damage to the CST (Baker et al. 2015).

In humans, transcranial magnetic stimulation (TMS) and diffusion tensor imaging (DTI) allow us to investigate the structural integrity of the CST. Not surprisingly, individuals following a stroke show reduced integrity of CST as measured by both TMS and DTI, which is associated with a loss of hand strength (Archer et al. 2017; Lotze et al. 2012; Schulz et al. 2012; Thickbroom et al. 2002). Similar measures examining the amount of lesion load on the CST also find that greater overlap of the lesion and CST is associated with higher levels of impairment (Zhu et al. 2010).

Potentially as a consequence of damage to the CST, individuals with stroke have reduced motor output from ipsilesional primary motor cortex (Buetefisch et al. 2018), and this paucity of activity is significantly associated with poorer outcomes (Favre et al. 2014). In compensation of this reduced output from the ipsilesional hemisphere, individuals often display increased activity in the contralesional hemisphere when attempting to move the paretic hand/arm (Rehme et al. 2012; Ward et al. 2003). Activation of the contralesional hemisphere during movement is associated with worse motor outcomes and is typically greater in individuals with more extensive damage to the ipsilesional CST (Lotze et al. 2012).

Loss of Independent Joint Control

The loss of input from corticofugal tracts from the lesioned hemisphere does not in isolation explain the abnormal coupling and resulting loss of independent joint control often observed following a stroke. Evidence from monkey lesion experiments shows that following damage to CST, ipsilateral reticulospinal tract connections to the paretic arm are strengthened (Zaaimi et al. 2012). However, these changes are only seen in connections to the wrist flexors and intrinsic hand muscles, but not wrist extensor muscles. In fact, these ipsilateral reticulospinal tracts preferentially innervate flexor muscles of the arm. Given that these tracts spread across multiple segments of the spinal cord (Matsuyama et al. 1999; Matsuyama et al. 1997; Peterson et al. 1975), they cannot specifically activate individual muscles with the same resolution as CST, and instead lead to coactivation across joints. Thus, the observed loss of independent joint control may be a consequence of increased reliance on ipsilateral reticulospinal tract following damage to CST.

Although the evidence implicating RST in impairment in humans is still in its early stages, one possibility is that the frequently observed contralesional cortical activity may reflect use of ipsilateral corticobulbar tracts, such as the cortico-reticulospinal tract, in an effort to control the paretic arm. This is supported by the finding that progressively increasing the shoulder abduction load during reaching, which exacerbates the flexion synergy, leads to a progressive increase in contralesional activity (McPherson et al. 2018a). Furthermore, individuals with severe motor impairments display increased structural integrity in ipsilateral reticulospinal tracts compared to mildly impaired individuals, and this increased integrity is correlated with worst impairment and synergy scores (Owen et al. 2017). Some have argued that this contralesional activity may reflect use of uncrossed ipsilateral corticospinal tract, but this is unlikely since these pathways do not

substantially innervate the more distal portions of the limb and do not show any changes in synaptic strength following a unilateral pyramidal tract lesion (Soteropoulos et al. 2011; Zaaimi et al. 2012). Additionally, recent evidence using high resolution DTI of both the brainstem and spinal cord, where these tracts can be better separated, showed that chronic stroke individuals showed higher white matter integrity only in ipsilateral reticulospinal tract, but not ipsilateral CST compared to age-matched controls (Karbasforoushan et al. (In Press)).

Hypertonicity

Subcortical and cortical lesions do not only disrupt CST in the lesioned hemispheres. Both CST and corticobulbar pathways originate in sensorimotor cortex and pass through the interior capsule, and consequently a lesion in any of these areas will impact both CST and other corticobulbar pathways in the lesioned hemisphere. These cortical inputs to the brainstem are thought to play a critical role in maintaining the inhibitory and excitatory levels of the brainstem and its descending projections (Brown 1994; Li et al. 2019; Li and Francisco 2015). Following damage to these ipsilesional corticobulbar tracts, the brainstem, and specifically the reticulospinal tract, become hyperexcitable. In humans, this hyperexcitability of the reticulospinal tract can be measured via the acoustic startle reflex (ASR). A consistent finding is that individuals with stroke and spastic muscles show a greater ASR in the paretic limb compared to controls and their nonparetic limb (Honeycutt and Perreault 2014; Jankelowitz and Colebatch 2004), which falls in line with expectations of RST hyperexcitability. In particular, the metabotropic component of the RST is thought to be enhanced following a stroke due to the loss of cortical input. This increased metabotropic input and higher levels of monoamines, such as serotonin and norepinephrine, serve as a means of increasing the gain of ionotropic output through compensatory indirect motor

pathways following a stroke (McPherson et al. 2018b; Wei et al. 2014). However, although these monoamines can amplify motor output from the brainstem, which is normally weak, it comes at the cost of both a tonic neuromodulatory drive to motoneuron pools innervating the paretic arm (McPherson et al. 2008) and also an amplified reflex response due to amplified 1a afferent feedback (Johnson and Heckman 2014). Consequently, individuals have difficulty relaxing the muscles of the arm, especially wrist flexors, and display a constant background activity that leads to hyperexcitable reflexes.

Behavioral Recovery Following a Stroke

Behavioral recovery following a stroke can be quite variable. However, typically the majority of spontaneous recovery from motor impairments is expected to take place in the first 3 months (Bonita and Beaglehole 1988). For instance, Duncan and colleagues assessed upper extremity Fugl Meyer assessments (UEFMA), a clinical assessment of motor impairment, at 4 hours, as well as 5, 30, 90, and 180 days after admission and found that the UEFMA at 30 days explained 86 percent of variance at 6 months, with moderate and severe patients continuing to experience some recovery for 30-90 days (Duncan et al. 1992). Meanwhile, activities of daily living (ADLs), which can be improved through compensatory strategies in addition to true motor recovery, can still show spontaneous improvement up to 6 months following a stroke (Duncan et al. 1992; Jorgensen et al. 1995).

In addition to this often-observed time-constrained clinical recovery, the severity of initial diagnosis is a strong predictor of subsequent recovery. Individuals who present initially with mild to moderate hemiparesis consistently show substantial recovery on clinical assessments of

impairment, such as the UEFMA. Meanwhile, individuals who initially present with moderate to severe impairments show more variable recovery. In fact, one of the most consistent findings in stroke recovery is the ‘proportional recovery rule’, in which individuals with mild to moderate impairments will show roughly 70% recovery of their initial capacity of improvement (based on the Fugl Meyer Assessment). Meanwhile, only half of patients with severe impairments will show this proportional recovery, while the other half will show minimal spontaneous recovery (Prabhakaran et al. 2008; Winters et al. 2015). Although the exact importance of the value ‘70%’ has been debated (Hawe et al. 2018; Hope et al. 2019), it is clear that individuals initially presenting with mild to moderate impairments will show significant spontaneous recovery, while only a portion of patients with severe impairments will. Consequently, an initial severe neural injury is likely to result in motor compensation rather than recovery in the early phase following a stroke, which in turn may cause persistence of ‘learned nonuse’.

The reason that the majority of recovery is observed in the first 3 months following a stroke is thought to be due to the heightened state of plasticity following a stroke, termed the ‘critical period’. During this critical period, a host of molecular changes occur that encourage structural and synaptical changes that may be beneficial for recovery (Starkey and Schwab 2014). Although there is no direct evidence for this ‘critical period’ in humans due to technical limitations in quantifying it, rodent lesion studies have supported this notion of a limited time window in which the brain is increasingly responsive to training. For instance, training initiated within 48 hours following a caudal forelimb area infarct (analogous to the primary motor cortex) led to full recovery of pre-infarct performance on a prehension task in mice, whereas only small gains were observed if the training was delayed a week (Ng et al. 2015). Similarly, inducing a second stroke

after only partial recovery from a first stroke can reopen this critical period and lead to heightened responsiveness to training and subsequent full recovery (Zeiler et al. 2015). These results suggest that there is something about the ischemia itself that leads to a plastic state. The current goals of rehabilitation are to figure out 1. How to augment spontaneous recovery during this critical period immediately following stroke; and 2. How to create meaningful behavioral gains outside this short window of recovery in individuals who have seemingly plateaued.

Evidence from monkey lesion studies supports the ability for training to improve recovery. For instance, in two different studies, Nudo and colleagues showed that monkeys receiving a M1 infarct showed faster recovery (roughly 1 month until recovery versus 2 months until recovery) if they were trained on a skilled pellet-grasping compared to monkeys receiving no training and instead relying purely on spontaneous recovery (Nudo and Milliken 1996; Nudo et al. 1996b). Similarly, monkeys given more extensive M1 lesions that completely wiped out the digit representations only regained precision grip to pre-infarct levels if they received highly intensive training, whereas those who did not receive training did not ever reach pre-lesion levels (Murata et al. 2008). These findings are not only limited to the hand, as spontaneous recovery of reaching ability following extensive lesions to the elbow/shoulder region of M1 also does not reach pre-lesion levels, but instead requires further reaching training to fully recover (Herbert et al. 2015). Together, these results in monkeys indicate that intensive training of the hand and arm has the capability to improve recovery on top of any spontaneous recovery.

Currently, the gold standard therapy in the clinic for improving upper extremity function is task-specific or task-oriented training (Winstein et al. 2016a). Task-specific training is based on the

premise that practice of an action results in improved performance of that action and is focused on learning or relearning a motor skill (Bayona et al. 2005; Hubbard et al. 2009). These involve repeated, challenging practice of functional, goal-oriented activities. Constraint Induced Movement Therapy (CIMT), one version of task-specific training in which the good limb is constrained and the individual executes everyday tasks with the paretic limb that progressively increases in difficulty, is effective in individuals greater than 3 months following a stroke (Wolf et al. 2006). Similarly, an intense intervention involving practicing activities of daily living in over 200 chronic stroke patients found significant improvements in behavior after 6 months of treatment (Ward et al. 2019). However, it is worth noting that gains following CIMT are often associated with compensatory strategies, rather than true motor recovery (Kitago et al. 2013). Although individuals display increases in the clinical Action Research Arm Test (ARAT), which tests performance of activities of daily living, they showed no improvements in the impairment Fugl Meyer test or kinematic measures of reaching. Additionally, task-specific training does not seem to further improve spontaneous motor recovery in the first 3 months following a stroke since a Phase 3 multi-site trial of over 350 participants showed no difference between task-specific training, dose equivalent occupational therapy, or even standard non-dose equivalent therapy (Winstein et al. 2016b). Unfortunately, although CIMT and task-specific training has shown efficacy in the chronic stage of stroke, participation is limited to those with high level functionality due to the prerequisite of needing sufficient paretic hand function to carry out the task. For instance, CIMT usually requires greater than 10° voluntary finger extension ability as a common inclusion criterion (Kwakkel et al. 2015). Unfortunately, many individuals do not meet this requirement and are consequently excluded from these types of studies and left with minimal viable options for improving upper extremity function, especially for the hand.

The lack of viable options for individuals with more severe impairments has led to an influx of device-assisted interventions in which robotic, mechanical, or electrical stimulator devices are used to enable these individuals to participate in therapy. For instance, Lo and colleagues involved individuals with moderate to severe chronic stroke in the first multi-site clinical trial using an upper extremity robotic device (Lo et al. 2010). Although they observed improvements in motor impairments, they did not find significantly better results compared to standard therapy. Similarly, functional electrical stimulation (FES) has been shown to improve upper extremity function, but not significantly more than robotics or motor learning (Kwakkel et al. 2016; McCabe et al. 2015). These mixed results have resulted in devices with more complex functionality, including new characteristics such as EMG and dynamic control (Bundy et al. 2017; Fujiwara et al. 2017; Hu et al. 2009; Hu et al. 2015). Although the results of such approaches are promising, they have yet to be included in larger scale multi-site clinical trials and the quality of evidence is low (Mehrholz et al. 2015).

Neural Mechanisms of Recovery

Recovery is defined as the return to a pre-injury state at the functional (e.g., task-completion), performance (e.g., kinematics), and neuronal level (Levin et al. 2009). As mentioned in the prior section, about half of all individuals following a stroke will show significant spontaneous recovery at the impairment-level, while the other half will show minimal or no gains. Currently, the strongest neural predictor for whether an individual will show significant behavioral recovery is whether they have a Motor Evoked Potential (MEP) in the paretic hand/arm following transcranial magnetic stimulation (TMS) of the ipsilesional primary motor cortex within 2 weeks following

their stroke (Byblow et al. 2015). The size of the MEP is thought to be a reliable marker of the integrity of CST. Therefore, these findings implicate the ipsilesional CST as a major key to spontaneous recovery following a stroke. Importantly, this recovery occurs regardless of initial impairment as long as a MEP is present. In patients who do not have MEPs in the first 2 weeks following a stroke, asymmetry of the integrity of CST as measured by fractional anisotropy (FA) using diffusion tensor imaging (DTI) can then further predict those who may recover to a greater extent compared to those who will show minimal spontaneous recovery (Byblow et al. 2015). Meanwhile, at the cortical level, a meta-analysis of over 250 patients found that greater activity in the ipsilesional primary motor cortex, as measured by fMRI during various sensorimotor tasks, was associated with better recovery (Favre et al. 2014). Presumably, this ipsilesional M1 activity reflects use of residual ipsilesional CST, thus falling in line with the TMS and DTI findings linking recovery to CST integrity. This agrees with longitudinal studies that show that over-activation of the contralesional hemisphere typically returns to normal levels after 6-12 months in patients who recover well (Calautti et al. 2001; Loubinoux et al. 2003; Ward et al. 2003).

Changes at the cortical level during spontaneous recovery are not limited to only changes in activity within isolated regions. Another common observation is a change in connectivity between regions that progressively changes as individuals improve (Rehme and Grefkes 2013). The two most common findings are a stroke-induced asymmetry in connectivity between ipsilesional and contralesional M1 and altered connectivity between ipsilesional secondary motor regions and ipsilesional M1, which are found both at rest (Carter et al. 2010; Golestani et al. 2013; Park et al. 2011; Wang et al. 2010) and during movement (Grefkes et al. 2008b; Sharma et al. 2009) that improve alongside behavior in well-recovered individuals. Similar findings have also been found

in rats, in which initial losses in connectivity between ipsilesional and contralesional primary sensorimotor cortex accompany behavioral deficits, but then show a gradual restoration as behavior improves over the coming weeks (van Meer et al. 2010). These findings show that lesions following a stroke not only alter descending motor output, but also impact cortico-cortico communication that is relevant for motor control. However, it is worth noting that CST integrity has been shown to be a better predictor of recovery compared to functional connectivity (Lin et al. 2018).

In addition to spontaneous recovery, a crucial question is what neural mechanisms may underlie training-induced behavioral recovery. Extensive work in animal models of stroke show that behavioral recovery is accompanied by neural changes within the perilesional cortex. For instance, Nudo and colleagues found that monkeys trained on a skilled pellet retrieval task displayed remapping of the perilesional cortex specific to the distal portion (i.e., the trained portion) of the limb (Nudo et al. 1996b). Similar results have also been found in the mouse following a photothrombotic stroke of motor cortex and subsequent skilled reaching training (Clarkson et al. 2013). Importantly, this kind of remapping requires skilled motor training, rather than simple repetitive or unskilled movements (Pagnussat et al. 2012; Plautz et al. 2000) or just exercise (Maldonado et al. 2008). This suggests that movement-itself is not an adequate means for significant recovery, but rather impairment-targeted training that evokes the greatest behavioral gains.

In addition to training-induced remapping of the perilesional cortex, changes in gray and white matter often occur. For instance, white matter reorganization (Po et al. 2012), dendritic growth

(Biernaskie and Corbett 2001), and synaptogenesis (Tamakoshi et al. 2014) have all been found following motor skill training in animals. This has been thought to be due to the fact that neuronal activity promotes structural changes (Fields 2015; Gibson et al. 2014). Such changes are crucial since a combination of lack of paretic arm use (Allred et al. 2014), increased reliance on the unaffected limb (Kim et al. 2015), and compensation strategies (Jones 2017) all lead to aberrant plastic changes in the nonlesioned cortex that diminish performance improvements.

Similar to results from animal models of stroke, effective interventions in humans are often associated with increased reliance on the ipsilesional sensorimotor cortex. For instance, behavioral improvements following CIMT were accompanied by an expansion of the motor map related to the paretic hand within the ipsilesional hemisphere as measured by TMS (Sawaki et al. 2008). This parallels the initial findings of Nudo and colleagues looking at changes in intracortical microstimulation maps following rehabilitative training discussed earlier. In addition to this motor map expansion within the ipsilesional sensorimotor cortex following CIMT, individuals also have increased gray matter density (Gauthier et al. 2008), which is thought to reflect increased synaptogenesis. These cortical changes are not limited to CIMT, however. Both effective robotic training and bilateral arm training that improved behavioral performance cause increased activity within the ipsilesional sensorimotor cortex related to the hand as measured by fMRI (McCombe Waller et al. 2014; Takahashi et al. 2008). Additionally, intervention-induced improvements are also associated with restoration of connectivity between motor regions (Bajaj et al. 2015; Biasucci et al. 2018; Fan et al. 2015b) in addition to cortical remapping, suggesting that these cortico-cortico interactions may also be important avenues for behavioral improvements. Unfortunately, to this point, most of these studies have focused exclusively on individuals with mild to moderate

impairments. Whether individuals with more severe impairments can experience similar changes is still unclear.

Summary

The present background review overviewed the current state of the field's understanding of the healthy motor system, as well as the neural mechanisms underlying stroke-induced motor impairments and subsequent recovery. To this point, most human stroke studies have focused primarily on the neural mechanisms underlying weakness following a stroke, which is largely attributed to damage to CST. Meanwhile, the neural mechanisms underlying the loss of independent joint control, particularly at the level of the hand, are only beginning to be uncovered in humans. Evidence from monkeys implicates increased reliance on the ipsilateral cortico-reticulospinal tract following damage to CST as a possible mechanism for the observed loss of independent joint control. However, whether this is true at the level of the hand remains unclear.

Subsequent motor recovery, whether spontaneous or following training, seems to rely on reengaging residual ipsilesional resources, at least in individuals with mild impairments. However, it is not known whether individuals with more severe impairments are capable of experiencing similar changes due to a lack of involvement in traditional rehabilitation strategies. Assistive devices such as robotics, mechanical devices, and electrical stimulation offer a means with which to finally include this often-excluded population in hand and arm interventions and have promising behavioral results. Whether this population will show similar neural mechanisms of recovery, including reengaging residual ipsilesional resources, remains unclear.

3. Neural Effects of Lifting on Hand Opening in Healthy Individuals

An edited version of this chapter has been posted as a preprint and is currently under review:
Wilkins K.B. & Yao J. (2019). Coordination of multiple joints increases bilateral connectivity with ipsilateral sensorimotor cortices. bioRxiv DOI: <https://doi.org/10.1101/656819>.

Abstract

Although most activities of daily life require simultaneous coordination of both proximal and distal joints, motor preparation and execution during such movements has not been well studied in humans. Simple hand/finger movements evoke activity primarily in the contralateral motor cortices. However, increasing the complexity of the finger movements, such as a sequential finger-pressing task, leads to additional recruitment of ipsilateral resources. It has been suggested that this involvement of the ipsilateral hemisphere is critical for temporal coordination of distal joints. The goal of the current study was to examine whether increasing simultaneous coordination of multiple joints (both proximal and distal) leads to a similar increase in coupling or cortical activity with ipsilateral sensorimotor cortices during motor preparation and execution compared to a simple distal movement such as hand opening. To test this possibility, 12 healthy individuals participated in a high-density EEG experiment in which they performed either hand opening or hand opening while lifting at the shoulder on a robotic device. We quantified within- and cross-frequency cortical coupling across the sensorimotor cortex during motor preparation for the two tasks using dynamic causal modeling, as well as cortical activity in isolated cortical regions related to movement execution. Both hand opening and hand opening while lifting elicited coupling from secondary motor areas to primary motor cortex within the contralateral hemisphere exclusively in the beta band, as well as from ipsilateral primary motor cortex to contralateral primary motor cortex. However, lifting at the shoulder also led to an increase in coupling within the ipsilateral

hemisphere as well as interhemispheric coupling between hemispheres that expanded to theta, mu, and gamma frequencies. Meanwhile, there were no observed changes in cortical activity near the time of movement execution. Thus, increasing the demand of joint coordination between proximal and distal joints leads to increases in communication with the ipsilateral hemisphere during motor preparation as previously observed in distal sequential finger tasks but does not change the regions involved at motor execution.

Introduction

The majority of neuroimaging studies in humans focus on simple single-joint tasks due to practical constraints within the MRI scanner. It is clear from these studies that movements, particularly more distal ones, require communication between secondary motor regions and primary motor cortex contralateral to the moving limb (Grefkes et al. 2008a). Interestingly though, movements requiring greater sequential control, such as sequential finger tapping tasks, lead to increased activity in the ipsilateral sensorimotor cortex during motor preparation and execution, which appears important for temporal coordination (Chen et al. 1997; Tanji et al. 1988; Verstynen et al. 2005). However, task complexity can also be altered by changing the number of joints controlled. Considering that most activities of daily life require simultaneous coordination of multiple joints, both proximal and distal, it is important to understand how increasing the number of controlled joints may affect reliance on the ipsilateral hemisphere.

For single-joint tasks, connectivity or coupling between motor regions has been well studied. For instance, Grefkes et al., found a facilitation of cortical activity from contralateral secondary motor areas to contralateral primary motor cortex (M1) and inhibition of ipsilateral motor areas during a

simple fist closing task as measured by fMRI (Grefkes et al. 2008a). Similar results have been found using EEG in the form of positive coupling from supplementary motor area (SMA) to contralateral motor cortices (Bonstrup et al. 2015; Herz et al. 2012), which matched previous findings showing activation of SMA preceding contralateral M1 (Huang et al. 2004). This evidence corroborates results from single-cell recordings in monkeys showing increased prevalence of preparation-related neurons in secondary motor areas compared to M1 (Riehle and Requin 1989) and suggests a cascade-like communication from secondary motor areas to M1 constrained within the contralateral hemisphere.

Although most single-joint movements are typically associated with activity in contralateral sensorimotor cortices during movement preparation and execution, the ipsilateral sensorimotor cortices seem to play a functional role as well. For instance, it is possible to decode 3D movement kinematics solely from the ipsilateral hemisphere in both monkeys (Ganguly et al. 2009) and humans (Bundy et al. 2018; Hotson et al. 2014), suggesting a robust role for ipsilateral sensorimotor cortices in movement preparation/execution. Meanwhile, lesioning ipsilateral M1 in monkeys leads to a brief behavioral deficit in the ipsilesional hand due to deficits in postural hand control (Bashir et al. 2012). Similarly in humans, perturbation to ipsilateral M1 via TMS leads to an increase in timing errors in tasks (Avanzino et al. 2008; Chen et al. 1997), which is attributed to improper temporal recruitment of muscles (Davare et al. 2007). Although the specific neural mechanism behind the role of the ipsilateral sensorimotor cortices in movement is still up for debate, one of the most common findings is that it plays a demand-dependent role, since increasing the ‘complexity’ of the task leads to increased activity in the ipsilateral cortex (Buetefisch et al. 2014; Hummel et al. 2003; Seidler et al. 2004).

Task complexity is often manipulated by having participants execute increasingly difficult sequence finger tapping tasks. However, similar results have also been found for non-sequence related tasks of increased complexity such as executing a ‘chord’ involving coordination of multiple fingers (Verstynen et al. 2005). Thus, it seems that ipsilateral motor cortex is involved during preparation not only of sequential complex tasks, but also during movements that require multiple joint coordination. However, previous tasks have been limited to distal hand/finger movements or bimanual distal tasks. The question remains whether coordination of two joints within the same limb will lead to increased communication with the ipsilateral hemisphere.

We sought to test the hypothesis that increasing coordination from a 1-joint distal task to a 2-joint distal-proximal task would increase the involvement of ipsilateral sensorimotor cortices. To investigate this hypothesis, we measured high-density EEG while participants performed either hand opening or hand opening while simultaneously lifting at the shoulder. We quantified the connectivity within bilateral sensorimotor cortices during motor preparation using dynamic causal modeling for induced responses and cortical activity related to movement execution. This allowed us to not only establish the regions involved in each task, but also disentangle the roles of different frequency coupling between tasks. We found that although both tasks displayed the expected coupling from contralateral secondary motor areas to contralateral primary motor cortex restricted to beta band, the simultaneous lifting and opening task also elicited increased coupling within the ipsilateral hemisphere towards iM1 and between contralateral PM and ipsilateral M1 that spread to theta, mu, and gamma frequencies. However, by movement execution, there was no difference in cortical activity in any sensorimotor region between the two tasks. These results suggest that

the coordination between distal and proximal joints leads to additional bilateral communication and communication within ipsilateral sensorimotor cortices compared to a simple distal movement but does not alter the regions involved in the final motor command.

Materials and Methods

Participants

Twelve healthy right-handed participants (mean age: 59.8 ± 7.7 yrs.; age range: 45-74; 7 males, 5 females) took part in this study. All participants had no prior history of neurological or psychiatric disease. This study was approved by the Northwestern institutional review board and all participants gave written informed consent.

Experimental Design

Experimental setup

Participants sat in a Biodex chair (Biodex Medical Systems, Shirley, NY), with straps crossing the chest and abdomen to restrain the trunk. The participant's right arm was placed in a forearm-hand orthosis attached to the end effector of an admittance controlled robotic device (ACT^{3D}) instrumented with a six degree of freedom (DOF) load cell (JR³ Inc., Woodland, CA). The robot was set to the position with the height to provide a haptic table to the subject with shoulder at 85° abduction and allows the subject to move the right arm freely on the table.

At the beginning of each trial, participants moved their hand to a home position, with the shoulder at 85° abduction, 40° flexion, and the elbow at 90° flexion angle. Participants then received an auditory cue. Following the cue, participants relaxed at the home position for 5-7 s and then self-initiated either 1) hand opening (HO) with the arm resting on the haptic table, or 2) hand opening

while simultaneously lifting (HOL) the arm above the haptic table against 50% of subject's maximum shoulder abduction (SABD) torque. Importantly, the HOL task requires simultaneous activation of the shoulder abductors and finger extensor muscles and is not a sequential task. Participants were instructed to avoid eye movements by focusing on a point and avoid movements of other body parts during the performance of each trial, which was visually confirmed by the experimenter. Participants performed 60-70 trials of each task, broken into random blocks (one block consisted of 20-30 trials for a particular task). Rest periods varied between 15 to 60 seconds between trials and 10 minutes between blocks.

EEG Data Acquisition

Scalp recordings were made with a 160-channel High-Density EEG system using active electrodes (Biosemi, Inc, Active II, Amsterdam, The Netherlands) mounted on a stretchable fabric cap based on a 10/20 system with reflective markers on each of the electrode holders. All data were sampled at 2048 Hz. The impedance of the EEG signal was kept below 50 k Ω for the duration of the experiment. The positions of EEG electrodes on the participant's scalp were recorded with respect to a coordinate system defined by the nasion and pre-auricular notches using a Polaris Krios handheld scanner (NDI, Ontario, Canada). This allowed for coregistration of EEG electrodes with each participant's anatomical MRI data. Simultaneously, EMGs were recorded from the extensor digitorum communis (EDC), flexor carpi radialis (FCR), and intermediate deltoid (IDL) of the tested arm.

Structural Imaging of the Brain

On a different day, individuals participated in MRI scans at Northwestern University's Center for Translation Imaging on a 3 Tesla Siemens Prisma scanner with a 64-channel head coil. Structural T1-weighted scans were acquired using an MP-RAGE sequence (TR=2.3s, TE=2.94ms, FOV 256x256mm²) producing an isotropic voxel resolution of 1x1x1 mm. Visual inspection of acquired images was performed immediately following the data acquisition to guarantee no artifacts and stable head position.

Data Analysis

Dynamic causal modeling for induced responses

We used dynamic causal modeling for induced responses (DCM-IR) (Chen et al. 2008) to model the task-related time-varying changes in power both within and across a range of frequencies by estimating the coupling parameters within and between sources in a network. This approach has been used in previous hand movement tasks to elucidate the dynamic frequency interactions within a motor network (Bonstrup et al. 2015; Chen et al. 2010).

Definition of model space

Our network model consisted of 5 regions of interest, including contralateral primary motor cortex (cM1), ipsilateral primary motor cortex (iM1), contralateral premotor cortex (cPM), ipsilateral premotor cortex (iPM), and supplementary motor area (SMA). Locations of each of these regions were adapted from the Human Motor Area Template (Mayka et al. 2006) and are shown in Table 3.1. Bilateral SMAs were treated as a single source due to their mesial position on the cortices. SMA also served as the input to the modelled network. It was chosen due to its critical role in movement preparation during self-initiated motor tasks (Jahanshahi et al. 1995; Jenkins et al. 2000)

and has previously been found to be an appropriate input for self-initiated motor tasks using DCM-IR (Bonstrup et al. 2015; Chen et al. 2010; Loehrer et al. 2016).

Different within- and cross-frequency connections between these 5 sources were used to create 12 models, as shown in Figure 3.1., which have successfully been used before in a grip task (Chen et al. 2010). These 12 models were separated into 2 groups. Group 1 (models 1 to 6) allowed nonlinear and linear extrinsic (between region), but only linear intrinsic (within region) connections. Group 2 (models 7 to 12) allowed both nonlinear and linear connections for both extrinsic and intrinsic connections. Within each group, the 6 models consisted of 1 fully connected model, and the other 5 models missing 1 or 2 connections that were from one premotor area (PM) to either the other PM or to M1. The within- and cross-frequency connections between each region from the best fit model were then used for analyzing task-related differences.

Table 3.1. Coordinates for Motor Network

Sources	MNI-Coordinates (X,Y,Z)
Left M1	(-37, -26, 60)
Right M1	(37, -26, 60)
Left PM	(-35, -4, 60)
Right PM	(35, -4, 60)
SMA	(-2, -7, 60)

Note: Coordinates were adapted from Mayka et al., 2006

DCM Preprocessing

EEG data were preprocessed using SPM12 (SPM12, Wellcome Trust Centre for Neuroimaging, www.fil.ion.ucl.ac.uk/spm/). Data were first band-pass filtered between 1 and 50 Hz, segmented into single trials (-2200 to 500 ms with 0 ms indicating EMG onset), and baseline-corrected. Trials were visually inspected and removed if they displayed an artifact (e.g., blinks). Artifact free trials were projected from channel space to the sources using the generalized inverse of the lead-field matrix with an equivalent current dipole for our chosen sources using a subject-specific boundary element method (BEM) based on the subject's anatomical MRI (Chen et al. 2008). The

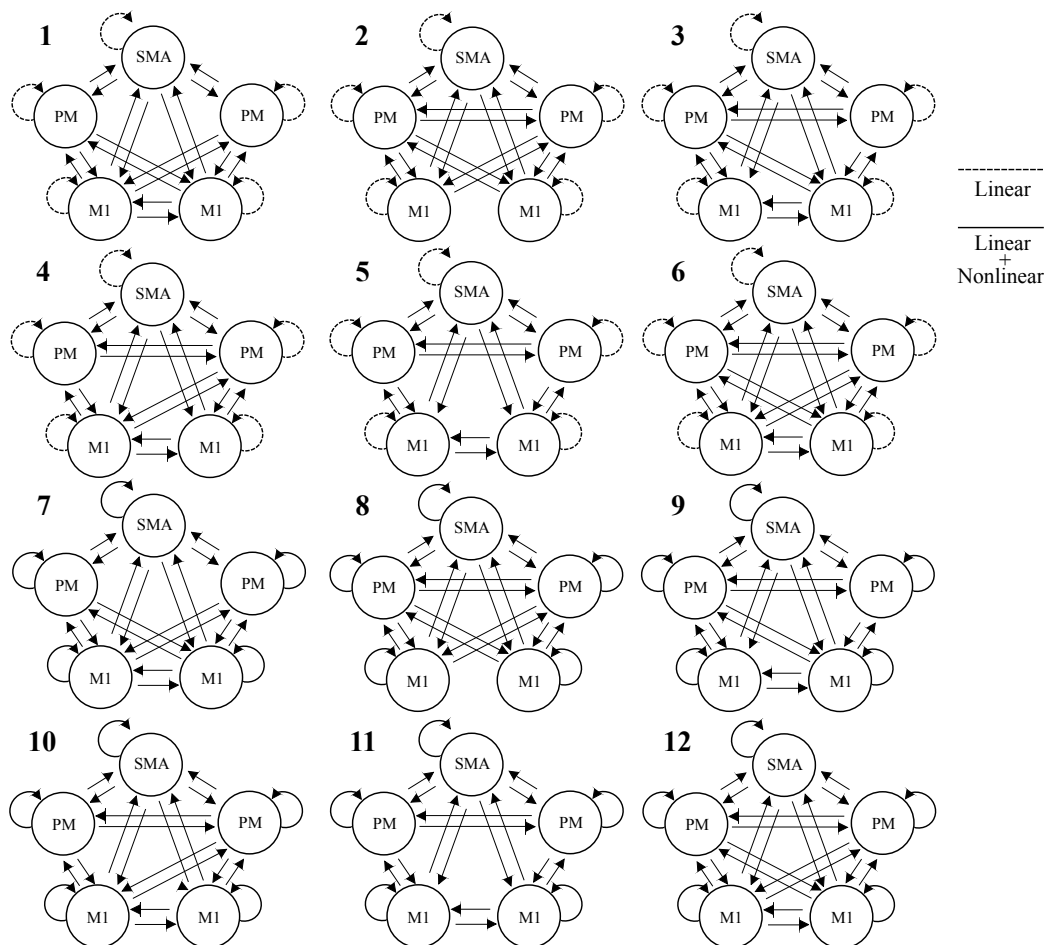


Figure 3.1

Models tested for DCM analysis. Models 1-6 allow only linear intrinsic (i.e., within-region) connections and both nonlinear and linear extrinsic (i.e., between-region) connections, while Models 7-12 allow both nonlinear and linear intrinsic and extrinsic connections. Individual models differ in interhemispheric connections allowed between M1 and PM regions. Dashed lines indicate only linear connections allowed, while solid lines indicate both linear and nonlinear connections allowed. The left side is the contralateral side.

spectrogram of each segmented trial from 4 to 48 Hz at each source was computed using a Morlet wavelet transform. This range includes theta (4-7 Hz), mu (8-12 Hz), beta (13-35 Hz), and gamma (36-48 Hz) frequencies. The spectrogram (frequency x time x source) was then averaged over all trials, cropped between -1000 to 0 ms, and then baseline-corrected by subtracting the mean of the frequency-specific instantaneous power during the time window -1000 to -833 ms.

The dimensionality of the averaged spectrogram was then reduced to four modes (i.e., mode x time x source) using singular value decomposition (SVD). Note, after SVD we project the 45 frequencies to 4 modes. We then reshape the spectrogram to obtain the instantaneous power vector $g_{20 \times 1}$ at each of the sampled times, with the first 4 elements as the instantaneous power on the 1st region from modes 1 to 4, and the 5th-8th elements as the instantaneous power on the 2nd region from modes 1-4, and so on. This dimensionality reduction both reduced the computational demand of the model inversion and denoised the data.

Calculation of coupling parameters

We simulated dynamics of the instantaneous power using the following equation:

$$\tau \dot{g}(t) = \tau \begin{bmatrix} \dot{g}_1 \\ \vdots \\ \dot{g}_J \end{bmatrix} = \begin{bmatrix} A_{11} & \dots & A_{1J} \\ \vdots & \ddots & \vdots \\ A_{J1} & \dots & A_{JJ} \end{bmatrix} g(t) + \begin{bmatrix} C_1 \\ \vdots \\ C_J \end{bmatrix} u(t),$$

Where the vector \dot{g} represents the first derivative of instantaneous power g . The sub-matrix A_{ij} is a 4 by 4 matrix containing the coupling parameters within and across different modes between the i^{th} and j^{th} regions ($J = 5$). The vector u represents the extrinsic input, which, in this study, is modeled as a gamma function with a peak at 400 ms prior to EMG onset with a dispersion of 400 ms from SMA to the whole network. These values were chosen in order to capture the peak of the

bereitschaftspotential during a self-initiated movement (Shibasaki and Hallett 2006). The C matrix contains the weights of the extrinsic input u from SMA. τ is a scaling factor and t represents time.

The model simulation was restricted to the time leading up to EMG onset (-1000 to 0 ms) to capture purely the motor preparation and command rather than any potential sensory feedback related to the task. We optimized the A and C matrices to minimize the error between the measured and simulated spectrogram. The quality of a model and the estimated A and C matrices was quantified by the variance accounted for from the simulated spectrogram. The resulting coupling parameters in the A matrix refers to the influence of power at a specific frequency in one motor region on the power at another frequency in another region (column to row). Positive (i.e., excitatory) or negative (i.e., inhibitory) coupling suggests changes in power in the first frequency and region are associated with the same or opposite directional change, respectively, in power in the second frequency and region.

Bayesian model selection

We performed Bayesian model selection (BMS) with random effects to assess which model best explained the observed data, while taking into account the complexity of the model (Penny et al. 2004; Stephan et al. 2009). We first used a family level inference with random effects to assess the overall importance of nonlinear coupling in intrinsic (i.e., within-region) connections. This involved comparing models 1-6 (Linear intrinsic connections) with models 7-12 (Linear and Nonlinear intrinsic connections). Following evaluation at the family level, we used BMS on the 6 models from the winning family to see which model best explained the observed data. The winning model, which was then used for further analysis on task-related differences in coupling, was

chosen based on the highest posterior exceedance probability (i.e., the probability that a given model is more likely than any of the other models tested). This process was performed for both tasks separately.

Inference on coupling parameters

Simulated spectrograms and A matrices from the four modes were projected back to the frequency domain allowing for characterization of the coupling parameters as a function of frequency for the winning model. The coupling matrices for each intrinsic and extrinsic connections in the winning model for each participant were further smoothed with a Gaussian kernel (full-width half-maximum of 8 Hz) for each condition. These matrices include the frequency-to-frequency (both within- and cross-frequency) coupling values for each connection.

Cortical activity related to movement execution

EEG data were low pass filtered at 50 Hz, aligned to the earliest EMG onset of the 3 muscles, and segmented from -2200 to +200 ms (with EMG onset at 0 ms) using Brain Vision Analyzer 2 software (Brain Products, Gilching, Germany). Data were then visually inspected for the presence of artifacts. Trials exhibiting artifacts (e.g., eye blinks) were eliminated from further analysis. The remaining EEG trials were baseline-corrected (from -2180 to -2050 ms) and ensemble-averaged. The averaged EEG signals were down-sampled to 256 Hz and imported into CURRY 6 (Compumedics Neuroscan Ltd., El Paso, TX). The cortical current density strength ($\mu\text{A}/\text{mm}^2$) in the time between 150 ms and 100 ms prior to EMG onset was computed using the standardized low resolution electromagnetic brain tomography (sLORETA) method ($L_p = 1$) based on a participant-specific boundary element method model with the regularization parameter automatically

adjusted to achieve more than 99% variance accounted for (Bradley et al. 2016; Yao and Dewald 2005). Possible sources were located on a cortical layer with 3 mm distance between each node. Although the inverse calculation was performed over the whole cortex, only the activity in bilateral sensorimotor cortices was further analyzed. Specific regions of interest (ROIs) included bilateral primary sensorimotor cortices (primary motor cortex (M1) + primary somatosensory cortex (S1)) and secondary motor cortices (supplementary motor area (SMA) + premotor area (PM)).

We quantified a cortical activity ratio $CAR = \frac{\sum_1^N s_n}{\sum_1^M s_m}$ for each of the 4 ROIs, where s_n represents the current density strength of the n^{th} node, and N and M represent the number of nodes in one of the ROIs and the whole sensorimotor cortices, respectively. The cortical activity ratio reflects the relative strength from one ROI as normalized by the total combined strength of the 4 ROIs.

Statistical Analysis

We ran a one-sample t -test for the coupling parameters for each connection to assess connections involved in the default network for each condition. We then ran a paired t -test on the coupling parameters on significant connections of the default network to assess task-related differences in coupling. Significance for specific coupling parameters was set at $p < 0.005$. To assess differences in cortical activity related to movement execution, we conducted a 2 (task) x 4 (region) repeated measures ANOVA. A p value of 0.05 or less was considered significant.

Results

Behavioral Results

We first sought to confirm that participants were simultaneously activating the hand and shoulder during the HOL task. We found that participants were reliably able to activate both muscles simultaneously, showing an absolute difference of EMG activation between muscles of 75.7 ± 54.6 ms (median = 57.6 ms; min = 36.5 ms; max = 161.0 ms) on average. Results are depicted in Figure 3.2.

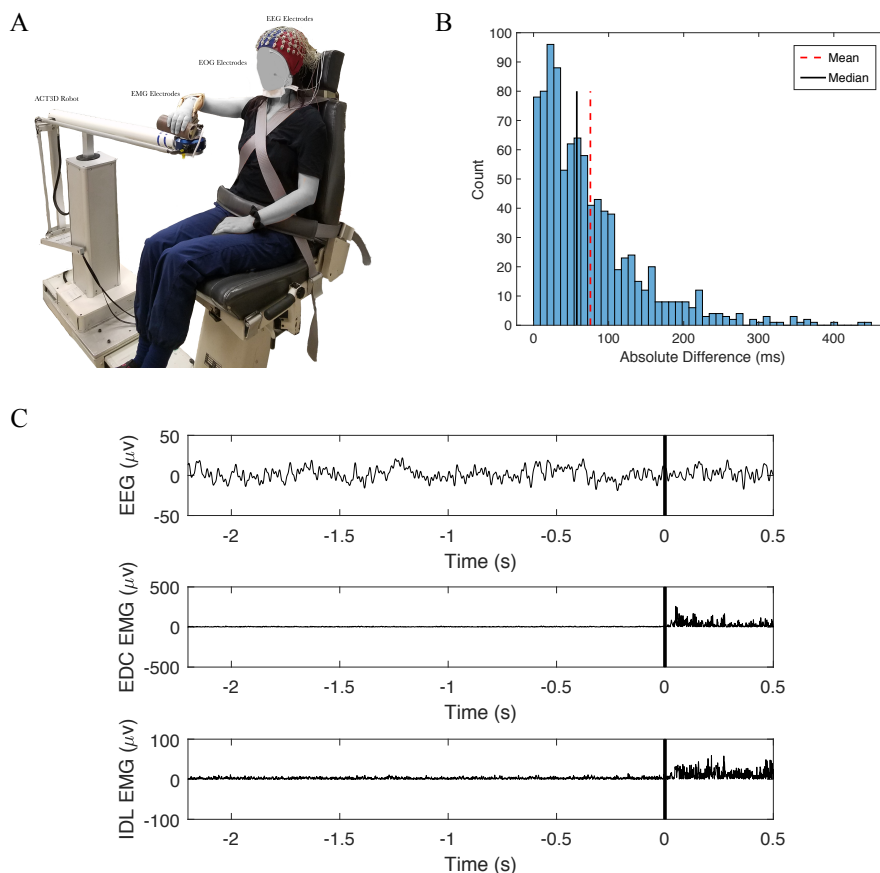


Figure 3.2

(A) EEG setup on the ACT3D robot. (B) Histogram of the absolute difference in onset between the extensor digitorum communis (EDC) and the deltoid (IDL) across all trials and participants. The mean absolute difference is represented by the red dashed vertical line and the median is represented by the solid black vertical line. (C) Example from one trial of EEG data (top) and extensor (middle) and deltoid (bottom) rectified EMG signal. Black vertical line at 0 s represents EMG onset across all 3 signals.

coupling for intrinsic (i.e., within-region) and extrinsic (i.e., between-region) connections (Exceedance probabilities for HO = 0.9999 and HOL: 0.9998; Table 3.2) When comparing the six models from the Nonlinear family (models 7-12 in Figure 3.1) BMS favored Model 12, which

Bayesian model selection and model fit

Results of BMS were consistent across the two tasks. Family-level inference showed the strongest evidence for the Nonlinear family, which allowed both within- and cross-frequency

contained full connections between the 5 regions of interest (Exceedance probabilities for HO: 0.9994 and HOL: 0.9981; Table 3.3).

Figure 3.3 depicts both the observed and simulated spectrograms for each of the 5 motor regions using the winning model for one participant during HO. Comparison of these two spectrograms shows the overall similarity between the measured and the model-based simulated data. Overall, this model explained ~80% of the original spectral variance for each condition (HO: 82.0%; HOL: 79.3%). Additionally, the four modes from the SVD preserved >95% of the data variance on average (HO: 95.3%; HOL: 95.7%).

Table 3.2. Exceedance probabilities for each family

Model Family	Open	Lift + Open
Linear	0.0001	0.0002
Nonlinear	0.9999	0.9998

Table 3.3. Exceedance probabilities for each model

Models	Open	Lift + Open
7	0.0001	0.0008
8	0.0001	0.0001
9	0.0003	0.0003
10	0.0000	0.0005
11	0.0001	0.0002
12	0.9994	0.9981

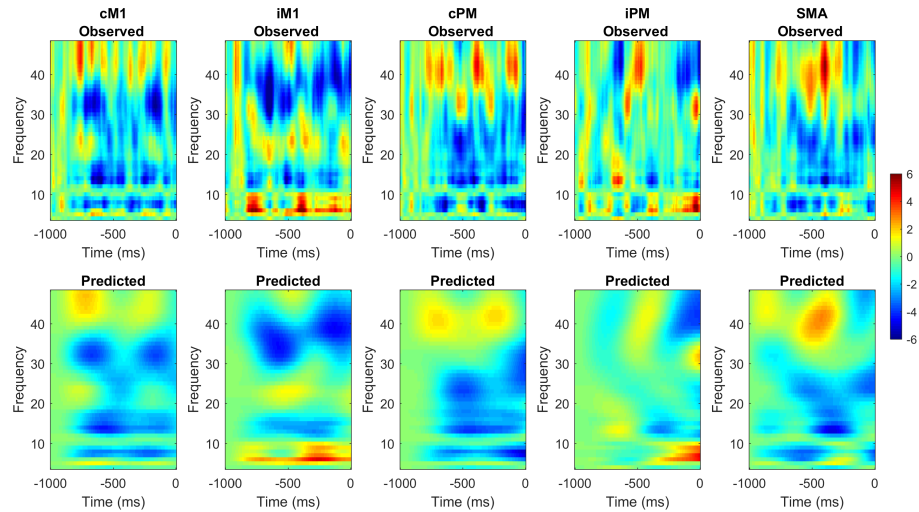


Figure 3.3

The observed (top) and model-predicted (bottom) time-frequency plot for each region for one participant using the winning model (Model 12). Red represents an increase in power compared to baseline and blue represents a decrease in power compared to baseline. 0 ms indicates movement onset. Overall, the model explained ~80% of the original spectral variance for each condition.

Figure 3.4 shows the

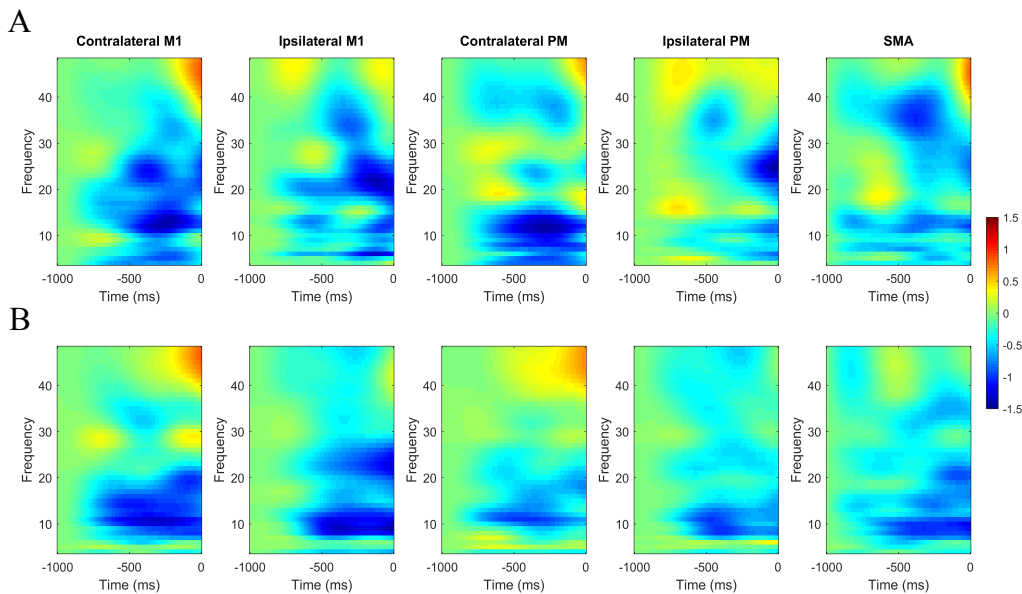


Figure 3.4

Average Time-Frequency plot for (A) Hand Opening (HO) and (B) Hand Opening while Lifting (HOL) for the 5 regions of interest. Blue depicts decreases in power relative to baseline and red depicts increases in power relative to baseline. 0 ms indicates EMG onset.

simulated spectrogram for each of the 5 motor regions using the winning model for both HO

(Figure 3.4A) and HOL (Figure 3.4B). A strong β band (13-35 Hz) desynchronization (i.e.,

decrease in power) is observed in the time leading up to movement onset, particularly in cM1, iM1, cPM, and SMA for both tasks. Additionally, cM1, cPM, and SMA show γ band (36-48 Hz) synchronization (i.e., increase in power) just before movement onset (starting ~100 ms before EMG onset).

Default motor networks for the two tasks

We then evaluated the default moto networks for the two tasks. The HO task had significant positive (i.e., excitatory) coupling from both SMA and contralateral premotor cortex to contralateral primary motor cortex. This included coupling from SMA to cM1, cPM to cM1, and SMA to cPM (See Figure 3.5A), all confined to the beta band (13-35 Hz). Additionally, individuals displayed positive interhemispheric coupling from iM1 to cM1 within the beta band.

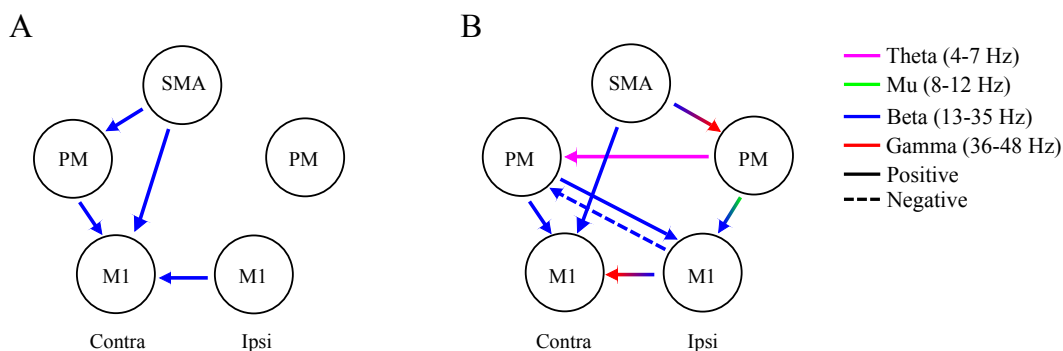


Figure 3.5

Default oscillatory coupling for (A) Hand Opening (HO) and (B) Hand Opening while Lifting (HOL). Arrows indicate directional connections showing significant coupling within the motor network. The color of the arrow indicates the frequency band involved. Arrows that change colors represent cross-frequency coupling. Solid lines indicate positive coupling while dashed lines indicate negative coupling. Contra = Contralateral hemisphere; Ipsi = Ipsilateral hemisphere relative to moving arm.

During the HOL task, individuals also had significant positive coupling from contralateral secondary motor areas to contralateral primary motor cortex. This included

coupling from SMA to cM1 and cPM to cM1 (see Figure 3.5B), again all confined to

beta band. However, in addition to this coupling,

individuals displayed ipsilateral and cross hemisphere coupling. This

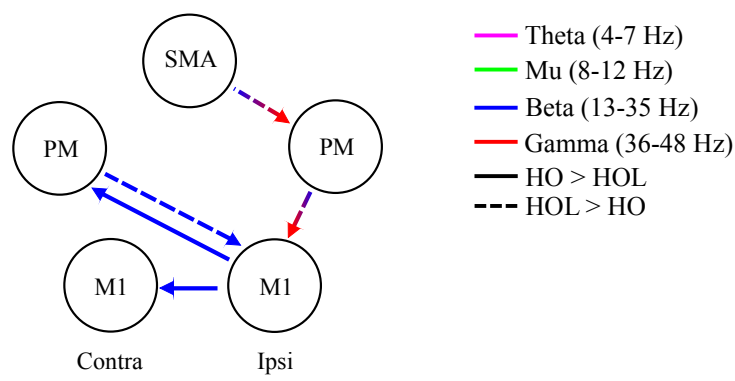


Figure 3.6 Differences in oscillatory coupling between the two tasks. Arrows indicate directional connections showing significant differences in coupling between tasks within the motor network. The color of the arrow indicates the frequency band involved. Arrows that change colors represent cross-frequency coupling. Solid lines indicate greater coupling for Hand Opening (HO) compared to Hand Opening while Lifting (HOL), while dashed lines indicate greater coupling for HOL compared to HO.

included positive interhemispheric coupling from iM1 to cM1 once again but involving beta and now gamma (36-48 Hz) oscillations. Additionally, HOL showed coupling (positive and negative) both within the ipsilateral hemisphere and across hemispheres (see Figure 3.5B). These connections spread across multiple frequency bands, including theta (4-7 Hz), alpha (8-12 Hz), beta and gamma frequencies (36-48 Hz). Table 3.4 contains the full characteristics of each significant connection for the two tasks.

Connection	Frequency Bands (peak [Hz])	# of Voxels	T-Value	Excitatory/Inhibitory
Condition: Open				
SMA → cM1	β → β (25 → 24)	14	2.7	+

cPM → cM1	$\beta \rightarrow \beta$ (27 → 20)	10	3.0	+
SMA → cPM	$\beta \rightarrow \beta$ (15 → 13)	60	4.0	+
iM1 → cM1	$\beta \rightarrow \beta$ (15 → 32)	15	3.6	+
Condition: Open while Lifting				
SMA → cM1	$\beta \rightarrow \beta$ (34 → 19)	11	3.5	+
cPM → cM1	$\beta \rightarrow \beta$ (26 → 23)	16	3.4	+
iM1 → cM1	$\beta \rightarrow \gamma$ (24 → 39)	34	3.4	+
cPM → iM1	$\beta \rightarrow \beta$ (30 → 17)	40	3.8	+
	$\mu \rightarrow \beta$ (12 → 35)	36	4.6	+
iM1 → cPM	$\beta \rightarrow \beta$ (33 → 25)	102	4.9	-
iPM → cPM	$\phi \rightarrow \phi$ (7 → 7)	14	3.8	+
SMA → iPM	$\beta \rightarrow \gamma$ (18 → 36)	8	3.4	+
iPM → iM1	$\mu \rightarrow \beta$ (11 → 14)	31	3.7	+
	$\beta \rightarrow \beta$ (32 → 13)	8	3.3	+

Notes: # of voxels refers to the spread of coupling around the peak frequency involved where each voxel represents coupling with 1 Hz resolution; Excitatory refers to positive coupling where a change in power in the 1st connection is associated with the same directional change in power in the 2nd connection; Inhibitory refers to negative coupling where a change in power in the 1st connection is associated with the opposite directional change in power in the 2nd connection; Highlighted rows reflect common connections in both tasks. M1 = Primary Motor Cortex; PM = Premotor Cortex; SMA = Supplementary Motor Area; c = contralateral; i = Ipsilateral

Table 3.4. Significant default frequency-to-frequency coupling

Task-related differences in coupling

We observed significant differences in coupling between the two tasks. Overall, the cortical network for preparing the HOL task was more complex than that for the HO task, as apparent from its increased involvement of additional network sources from ipsilateral motor cortices. This included from SMA to iPM and iPM to iM1 across multiple frequency bands (theta, beta, and gamma; see Figure 3.6) compared to HO. Additionally, the HOL task showed greater positive interhemispheric coupling from cPM to iM1 and more negative coupling from iM1 to cPM within the beta band compared to HO. The only significantly stronger link for the HO task is from iM1 to cM1 within the beta band compared to HOL. Table 3.5 contains the full characteristics of each significant connection for the two-task comparison.

Table 3.5. Significant differences in frequency-to-frequency coupling between tasks

Connection	Frequency Bands (peak [Hz])	# of Voxels	T-Value
Condition: Open > Open while Lifting			
iM1 → cM1	$\beta \rightarrow \beta$ (20 → 35)	113	5.9
iM1 → cPM	$\beta \rightarrow \beta$ (31 → 14)	37	5.2
Condition: Open While Lifting > Open			
SMA → iPM	$\beta \rightarrow \gamma$ (19 → 36)	53	3.9
	$\phi \rightarrow \gamma$ (4 → 41)	23	3.3
iPM → iM1	$\beta \rightarrow \gamma$ (19 → 38)	7	3.3
cPM → iM1	$\beta \rightarrow \beta$ (26 → 19)	71	4.4

Notes: # of voxels refers to the spread of coupling around the peak frequency involved where each voxel represents coupling with 1 Hz resolution; Excitatory refers to positive coupling where a change in power in the 1st connection is associated with the same directional change in power in the 2nd connection; Inhibitory refers to negative coupling where a change in power in the 1st connection is associated with the opposite directional change in power in the 2nd connection; M1 = Primary Motor Cortex; PM = Premotor Cortex; SMA = Supplementary Motor Area; c = contralateral; i = Ipsilateral

Cortical Activity Related to Movement Execution

After establishing the task-related differences in cortical coupling during motor preparation, we quantified the relative cortical activity strength using CAR in each sensorimotor ROI at motor execution for each task. We observed no interaction between region and task for CAR ($F(3,33) = 0.076, p = 0.97$). Results are depicted in Figure 3.7.

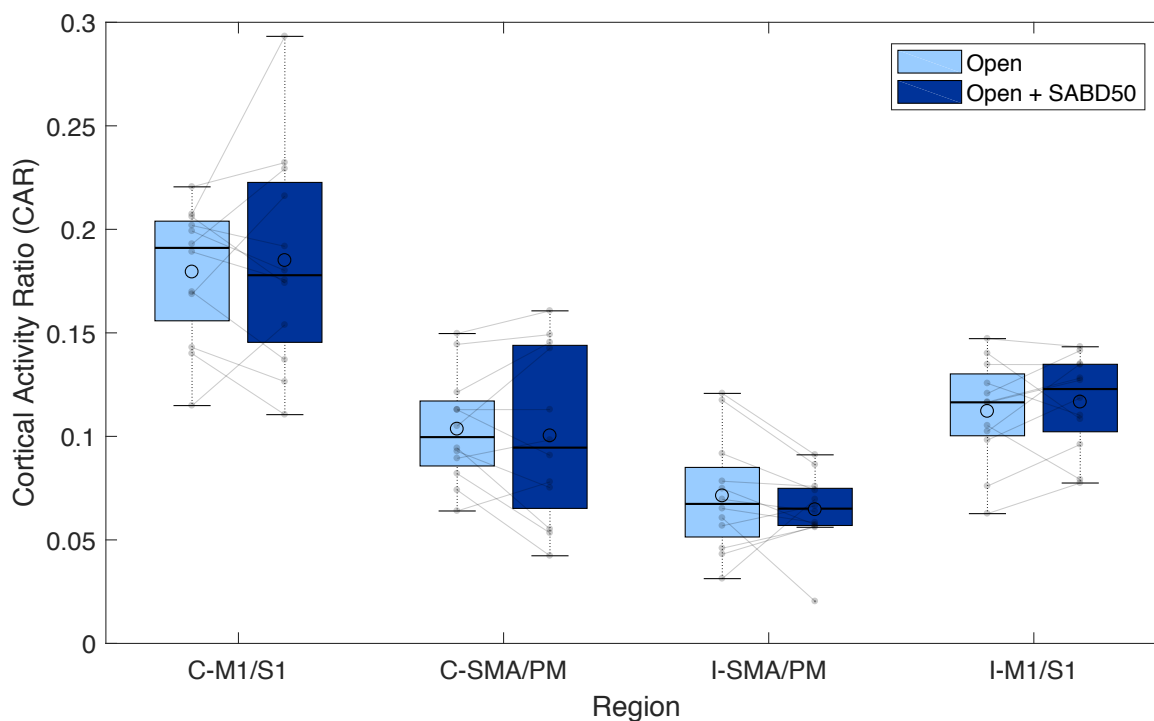


Figure 3.7

Cortical activity related to movement execution. Boxplots depict the cortical activity ratio (CAR) during hand opening (light blue) and hand opening while lifting (dark blue) across the 4 regions of interest. Individual data is overlaid. Individuals displayed no differences in CAR across any region between tasks. The median is shown by the horizontal black line and the mean is illustrated by the large open circle. C = contralateral, I = ipsilateral relative to the moving hand.

Discussion

This paper sought to investigate whether increasing coordination from a pure hand opening (HO) task to a simultaneous hand opening while lifting (HOL) task that requires coordination between the shoulder and hand would increase involvement of the ipsilateral hemisphere. For the first time,

we established the default network (i.e., cortical-cortical coupling at different frequencies) in the time leading up to movement execution for these two movements. Then we compared the difference between these default networks for the two tasks and showed that 1) contralateral beta-to-beta coupling between SMA/cPM and cM1 is commonly involved in both the HO and HOL tasks; and 2) increased bilateral connectivity and connectivity within the ipsilateral sensorimotor cortices across multiple frequency bands are involved in the HOL task, a task requiring coordination between the shoulder and hand, but not in the HO task. However, these changes in coupling during motor preparation did not ultimately lead to any changes in cortical activity related to movement execution.

Common Networks During Single- and Multi-Joint Movements

Common Network

Both tasks evoked a common excitatory coupling pattern from secondary motor cortices (SMA and cPM) to motor cortex (cM1) in the contralateral hemisphere in the beta frequency band (13-35 Hz). The involvement of secondary motor cortices falls in line with previous proposed roles for these regions: secondary motor areas feed into primary motor cortex during motor preparation and execution to shape motor output (Chen et al. 2019; Lara et al. 2018; Ohara et al. 2000; Sun et al. 2015; Weilke et al. 2001). Such increased preparatory activity from contralateral secondary motor areas was observed in both distal hand tasks (Okano and Tanji 1987) as well as multi-joint movements involving the shoulder, such as reaching (Picard and Strick 2003). In regard to the frequencies involved, the positive beta coupling reflects the common beta desynchronization seen across these regions in the time-frequency maps (see Figure 3.5), which is a feature of movement

preparation in both secondary and primary motor cortices. This beta band desynchronization is associated with the gradual release of inhibition in the motor cortex to initiate an action (Takemi et al. 2013; 2015), along with the descending motor command originating from layer V pyramidal cells (Lacey et al. 2014; Roopun et al. 2006). We posit that the presence of beta band coupling within secondary and primary motor areas in the contralateral hemisphere observed for the two tasks in this experiment reflects this common motor command for the two tasks.

Distinct Networks During Single- and Multi-Joint Movements

We provided evidence, for the first time, showing the increased involvement of the ipsilateral hemisphere during the preparation of the simultaneous hand opening and lifting (HOL) task, as compared to the pure hand opening (HO) task. Specifically, the HOL task elicited coupling within the ipsilateral hemisphere (SMA to iPM; iPM to iM1), as well as between the 2 hemispheres (i.e., bidirectional link between iM1 and cPM) during movement preparation.

Significant Differences between the 2 tasks

One of the significant between-task differences in the network was the presence of ipsilateral beta-to-gamma coupling both from SMA to iPM and from iPM to iM1 during HOL task. As beta oscillations are an index of inhibition (Picazio et al. 2014), beta ERD, as seen in SMA at -450 ms at 19 Hz and iPM around at -500 ms during HOL task in Figure 3.4, may suggest that the reduction of such inhibition facilitated the synchronization of targeted regions (i.e., iPM and iM1) at gamma band. Neural firing at gamma oscillations (30-80 Hz) on the superficial layers of the frontal cortex is believed to be generated by the loop of inhibition between fast spiking GABAergic interneurons

and pyramidal cells (Kopell et al. 2010). Therefore, the resulting gamma hyper-synchronization in iPM and iM1 may represent a shift in connectivity away from long-range interlaminar connectivity typically associated with slower frequencies such as beta towards more local circuits (Kopell et al. 2000). The computational results within the local circuits may further drive cells from deeper cortical layers since gamma oscillations can drive the connections to target cells in both superficial and deeper cortical layers (van Kerkoerle et al. 2014). This is different from the commonly involved beta-to-beta coupling at the contralateral side also from the secondary to the primary motor cortex, which may purely reflect the release of the prepared motor plan without the local computation that primarily occurs here in the ipsilateral motor cortices at higher frequencies.

The other significant distinct coupling for the HOL task is a bidirectional beta band coupling between iM1 and cPM, with cPM synchronization facilitating iM1 synchronization, whereas iM1 synchronization inhibits cPM synchronization. An anatomical link between iM1 and cPM has been reported via corpus callosum (Rouiller et al. 1994), although it is also possible this may reflect communication through hidden or additional nodes (either subcortical or cortical) not included in our motor network. In Figure 3.4 we observed increased synchronization in cPM around at 30 Hz, which was coupled with the increased synchronization in iM1 around at 19 Hz. This may reflect increased inhibition of iM1 activity initiated by cPM inhibition. On the other hand, the beta synchronization at high beta in iM1 increased and triggered beta desynchronization in cPM at low beta (~14 Hz) component, suggesting a release of inhibition to cPM activity. Overall, this loop may result in an increase in cortical activity at contralateral secondary motor cortices within the beta band, and an inhibition of activity in ipsilateral primary motor cortex.

The last significant difference in coupling between the 2 tasks was the shift of facilitation coupling from iM1 to cM1 in the beta band for HO task to a beta-to-gamma coupling still from iM1 to cM1 for HOL task. Ipsilateral M1 is known to communicate with cM1 via transcallosal connections starting during movement preparation through movement onset (Murase et al. 2004; Rouiller et al. 1994), and thus only the nature of this coupling (i.e., frequencies involved) seem to be changing based on the particular task. One possibility for the larger beta-beta coupling for the HO task is due to the distal-only nature of the task compared to the proximal-distal combination for the HOL task, as previous findings showed greater beta event-related desynchronization contralateral to the moving limb for distal finger movements compared to proximal shoulder movements (Stancak et al. 2000).

Other differences between the 2 tasks

When comparing the within and cross-frequency couplings between the two tasks listed in Table 3.5, there are several more couplings that were involved in HOL task, but not in the HO task, although further paired t-test did not report them as significant difference. One of them is the facilitative theta-to-theta coupling from iPM to cPM. Theta (4-7 Hz) oscillations have been implicated in long range integration and top-down processing for various tasks in the cognitive domain, showing higher power with increasing cognitive demand (Gevins et al. 1997; Jensen and Tesche 2002; von Stein and Sarnthein 2000). Considering that the simultaneous lifting and opening task did require increased coordination of multiple joints compared to the simple hand opening task, coupling between iPM and cPM in theta band might reflect the increased cognitive load for the HOL task as compared to HO task. The fact that theta coupling was prevalent only in the premotor areas rather than primary motor cortex further implies that this theta coupling may be

more indicative of cognitive processes rather than purely a motor command, as premotor areas are typically associated with more abstract and goal-directed representations of movement compared to M1 (Rizzolatti et al. 1988).

We also observed mu-to-beta coupling, uniquely in the HOL task, between cPM/iPM and iM1. Here, we have referred to this 8-12 Hz as the mu band rather than alpha due to its relation to movement. As shown in Figure 3.4, we observed a strong mu-wave suppression (at about -550 ms) in both iPM and cPM associated with beta suppression (at about -500 ms) in iM1 for HOL task but not HO task. Suppression of mu waves are commonly observed when one performs or visualizes performing a motor action. Oscillations at these lower frequencies may be more present in deeper cortical layers, which then innervate superficial cortical layers (Barbas 2015; Buffalo et al. 2011). The slower firing properties of deeper layers are more appropriate to synchronize cell assemblies over longer conduction delays (Kopell et al. 2000). Based on these previous results, it is possible that the observed mu to beta coupling from bilateral PMs to iM1 may indicate the use of deeper structures for the long-scale cross-hemisphere communication to iM1. This may be necessary for the higher level of coordination which is required for a multi-joint task like HOL. In line with this notion, previous findings showed that elderly individuals displayed greater spread of mu-suppression across primary and secondary motor areas during a self-paced thumb movement compared to younger individuals, probably due to having to put more effort into the task (Derambure et al. 1993). Another possibility is that this observed mu-beta coupling reflects use of descending motor pathways controlling the shoulder, as ipsilateral mu suppression has been linked with excitability of uncrossed pathways projecting to shoulder muscles (Hasegawa et al. 2017).

Potential Role of the Ipsilateral Hemisphere

Since increasingly difficult finger tasks elicit increased activity in the ipsilateral hemisphere (Tanji et al. 1988; Verstynen et al. 2005), we hypothesized and confirmed that the HOL task would similarly increase connectivity with the ipsilateral hemisphere compared to the HO task due to the increased complexity of simultaneously coordinating proximal and distal joints. However, the question remains what the overall potential role of the ipsilateral hemisphere involvement may be for the HOL task.

The observed ipsilateral connectivity for the HOL task may suggest that ipsilateral motor cortices are directly involved in the preparation and/or execution of the more complex movement. In line with this possibility, Horenstein and colleagues compared the amount of cortical activity in the ipsilateral sensorimotor cortex during a unimanual and bimanual complex finger tapping task (Horenstein et al. 2009). They found that the cortical activity maps in the ipsilateral hemisphere for each of the two tasks had substantial overlap. Since the activity in the ipsilateral hemisphere during movement of the ipsilateral hand overlapped with the activity during bimanual movement, they argued the overlapping activity was presumably due to the preparation and execution of the movement itself. This evidence fits well with previous decoding studies showing the ability to decode 3D movements purely from activity in the ipsilateral hemisphere (Bundy et al. 2018; Hotson et al. 2014) and that these ipsilateral representations seem to be related to active movement rather than sensory processes (as is likely the case here as well since analyses were restricted to the time leading up to EMG onset) (Berlot et al. 2019).

Considering the HOL task required simultaneous coordination of both the hand and the shoulder, it is also possible that the ipsilateral hemisphere plays a role in synchronizing the timing of recruitment of the muscles involved in the movement via transcallosal mechanisms. In support of this potential role, virtual lesions to ipsilateral M1 elicited by TMS have been shown to alter the timing of muscle recruitment and lead to significant motor deficits during a multi-joint grip-lift task (Davare et al. 2007). Similarly, inhibitory TMS over ipsilateral M1 led to temporal alterations in the sequence of finger tapping movements of increasing complexity, but without affecting the number of incorrect sequences of the movements (Avanzino et al. 2008). Therefore, it is possible that the increased coupling with the ipsilateral hemisphere observed here plays a significant role in coordinating the simultaneous activation of both proximal and distal joints. Gamma coupling may facilitate this due to its role in local computation and GABAergic inhibitory circuitry (Bartos et al. 2007; Kopell et al. 2000). Meanwhile, an alternative possibility that others have suggested is that this ipsilateral activity reflects inhibition of possible mirror movements of the ipsilateral hand rather than just an interhemispheric control mechanism (Verstynen and Ivry 2011).

No Change in Cortical Activity Related to Movement Execution

Although the addition of lifting led to an increase in coupling within the ipsilateral sensorimotor cortices and between hemispheres during motor preparation, no changes were observed in cortical activity in any of these regions related to movement execution. This suggests that the regions generating the actual motor command (predominantly contralateral primary sensorimotor cortex) for carrying out the movement were not significantly changing with the addition of lifting.

Limitations

We cannot fully rule out the possibility that the observed increase in ipsilateral connectivity during the multi-joint task indicates recruitment of descending uncrossed motor tracts from the ipsilateral hemisphere such as the ipsilateral corticospinal tract or cortico-reticulospinal tract. Although this is unlikely for the sequential finger tasks due a lack of innervation of these pathways to distal portions of the hand (Soteropoulos et al. 2011), it is potentially relevant for the task in this study as these pathways have been shown to have substantial connections to more proximal portions of the upper extremity, such as the deltoid that is involved in the lifting portion of the task (Baker 2011). Therefore, the observed increase in ipsilateral connectivity may reflect recruitment of ipsilateral descending motor tracts to drive the shoulder during the lifting task, with the contralateral hemisphere still providing the majority of the input for controlling the distal hand opening. However, this seems unlikely given that there is no increase in activity observed in ipsilateral sensorimotor cortices related to movement execution.

Furthermore, due to the lack of a lifting-only condition, i.e., a task only involving the shoulder joint, it is possible that a portion of the task-related changes in connectivity are solely related to the lifting component of the movement rather than the combination of simultaneously opening the hand and lifting at the shoulder. However, previous evidence has shown that activity during the motor preparation phase of a lifting-only single joint movement is primarily restricted to contralateral motor cortex and secondary motor areas with minimal ipsilateral involvement (Yao and Dewald 2018).

Other limitations of the presented study are associated with the use of the DCM-IR method. This method only takes into account the temporal changes in power of particular frequencies but does

not account for phase. Phase is known to play a critical role in cognitive and sensorimotor processes separate from power/amplitude (Fries 2015). Another limitation is that DCM-IR is limited in the number of sources that can be included in the model. However, we believe the tasks and ROIs chosen in this study are well-justified by previous work, and although they certainly do not characterize the entirety of the network involved in these tasks, we believe they carry enough information to make worthwhile conclusions about the impact of increasing task-complexity via simultaneous control of multiple joints on cortical communication.

Conclusion

The current study demonstrated that increasing task-complexity from controlling one joint (i.e., hand opening) to coordinating multiple joints simultaneously (i.e., hand opening while lifting) led to an increase in coupling within the ipsilateral sensorimotor cortex and between hemispheres. Different from the common beta-to-beta coupling in the contralateral hemisphere, ipsilateral coupling involves a wide range of within- and cross-frequency coupling including theta, mu, and gamma frequencies. However, this difference in coupling does not lead to any changes in regional activity at the time of movement execution. These results suggest that complexity-related reliance on the ipsilateral hemisphere holds true not just for complex sequential finger tasks, but also during combined distal-proximal multi-joint tasks more relevant to many activities of daily life.

4. Ipsilateral Secondary Motor Areas Drive the Negative Impact of Lifting on Hand Opening Ability Post-Stroke

Abstract

The corticospinal tract (CST) originating from the contralateral primary motor cortex is the primary means with which to control the hand and arm. In addition to this pathway, evidence from monkey studies shows the presence of connections to more proximal and even distal portions of the arm via uncrossed ipsilateral cortico-bulbospinal pathways, primarily originating from secondary motor areas. Reliance on these ipsilateral (i.e., contralesional) secondary motor areas and their projecting descending pathways may be increased following damage to CST as a compensatory means to control the paretic arm following a stroke, particularly during more demanding tasks. However, whether ipsilateral secondary motor areas and subsequent descending cortico-bulbospinal pathways can provide sufficient control of the hand in humans is still unclear. To address this issue, we combined magnetic resonance imaging (MRI), high density electroencephalography (EEG), and robotics in 17 individuals with chronic hemiparetic stroke and 12 healthy age-matched controls. We first tested for stroke-induced changes in the structural morphometry of the sensorimotor cortex and found that individuals with stroke had higher gray matter density in secondary motor areas and primary somatosensory cortex ipsilateral to the paretic arm compared to controls. We then measured cortical activity using EEG while participants attempted to generate hand opening either supported on a haptic table or while lifting against a shoulder abduction load. We found that the additional demand of shoulder abduction during attempted hand opening increased reliance on the ipsilateral secondary motor areas in stroke, but not controls. Furthermore, this increased use of ipsilateral secondary motor areas was associated

with decreased hand opening ability during lifting in stroke due to involuntary coupling between the shoulder and wrist/finger flexors. Together, this structural and functional evidence implicates a compensatory role for ipsilateral (i.e., contralesional) secondary motor areas following a stroke, but with limited capacity to support hand function.

Introduction

Hand function is often significantly impacted following a stroke, particularly in individuals with moderate to severe motor impairments. This is attributed to damage to the corticospinal tract (CST), which is the primary motor tract controlling the hand in healthy individuals (Lawrence and Kuypers 1968; Stinear et al. 2007). Following damage to the CST, individuals with stroke exhibit increased reliance on the ipsilateral (i.e., contralesional) sensorimotor cortices when attempting to move the paretic arm (Grefkes et al. 2008b; Ward et al. 2006). This may reflect recruitment of uncrossed indirect motor pathways originating from ipsilateral sensorimotor cortices to generate motor output (Baker et al. 2015). However, the question remains whether these alternate motor pathways originating from the ipsilateral sensorimotor cortex have the capacity to support hand function.

Uncrossed cortico-bulbospinal fibers originating from the cortex ipsilateral to the moving arm, such as the corticoreticulospinal tract (CRST), may serve as a compensatory backup system to control the paretic arm following damage to CST (Baker et al. 2015). One piece of evidence in support of this possibility comes from the finding that following a pyramidal CST lesion in monkeys, connections between the ipsilateral reticular formation and paretic wrist flexors and

intrinsic hand muscles are strengthened (Zaaimi et al. 2012). Importantly, these tracts primarily originate from secondary motor regions such as the supplementary motor area (SMA) and premotor cortex (PM) compared to CST which predominantly originates from primary motor cortex (M1) (Borra et al. 2010; Fregosi et al. 2017; Maier et al. 2002; Montgomery et al. 2013). Although the innervations from these tracts originating from secondary motor areas were thought to be limited to trunk and proximal muscles (Davidson and Buford 2006; Montgomery et al. 2013), more recent work found that they also innervate distal muscles such as the wrist and finger flexors (Riddle et al. 2009; Soteropoulos et al. 2012). This raises the possibility that they could be involved in subsequent hand recovery following stroke (Baker 2011). However, the reticulospinal tract branches more extensively at the spinal cord compared to the CST (Baker 2011; Matsuyama et al. 1999; Matsuyama et al. 1997; Peterson et al. 1975). Consequently, these pathways are not able to selectively activate individual muscles in the manner of CST and may not be sufficient for dexterous hand control (Herbert et al. 2015).

One of the main points of evidence for compensatory use of these uncrossed CRST following stroke in humans is the presence of abnormal coupling between the shoulder and the rest of the arm and hand. Lifting at the shoulder leads to abnormal coupling between shoulder abductors and elbow/forearm and finger flexor muscles that reduces reaching distance and hand opening ability, termed the flexion synergy (Dewald et al. 1995; Lan et al. 2017; Miller and Dewald 2012; Sukal et al. 2007). In fact, lifting at the shoulder can lead to involuntary closing during attempted opening in individuals with more severe impairments (Lan et al. 2017). Whereas the damage to CST accounts for the weakness, or inability to fully activate muscles (Schulz et al. 2012; Thickbroom et al. 2002), it does not address the presence of this abnormal coupling. Meanwhile, increased use

of ipsilateral cortico-bulbospinal pathways originating from secondary motor areas could account for this coupling due to its more extensive branching at the spinal cord. This extensive branching leads to activation of multiple muscle groups simultaneously. Additionally, these pathways innervate a greater proportion of flexor muscles compared to extensors preferentially elicits EMG activity in ipsilateral flexor muscles in monkeys (Davidson and Buford 2006; Hirschauer and Buford 2015). Therefore, attempting to drive movement of the arm via these compensatory ipsilateral pathways may allow control of more proximal portions of the arm, but at the detriment of distal hand function.

The goal of the current study was to investigate the potential compensatory role of ipsilateral secondary motor regions following a stroke and evaluate their capacity to support hand function following damage to CST. We hypothesized that individuals with a hemiparetic stroke would increasingly rely on ipsilateral secondary motor areas as compensation for damage to the lesioned hemisphere as the demand of the task increased, but that increased use of these areas would reduce hand opening ability due to the flexion synergy. To test this hypothesis, magnetic resonance imaging (MRI), high density electroencephalography (EEG), and robotics were combined. First any changes in structural morphometry in the ipsilateral sensorimotor cortex were examined as evidence for any systemic compensatory use of secondary motor areas post hemiparetic stroke.

Then cortical activity was measured in both primary and secondary motor regions during two tasks: 1. Hand opening in isolation and 2. Hand opening in conjunction with shoulder abduction (i.e., lifting). Cortical activity was compared with hand performance during these two conditions. We specifically examined grasping pressure during these two tasks as an indicator for hand opening ability since individuals with severe motor impairment cannot open their hand and instead

generate involuntary grasping forces when attempting to open (Lan et al. 2017). We found that i) individuals with stroke had increased gray matter density within secondary motor areas ipsilateral to the paretic arm (i.e., contralesional sensorimotor cortex) compared to controls; ii) the addition of shoulder abduction during attempted hand opening increased reliance on ipsilateral secondary motor areas in stroke, but not controls; iii) increased use of the ipsilateral secondary motor areas was associated with greater involuntary grasping (i.e., reduced hand opening ability) due to the flexion synergy. Together, these results implicate an increased reliance on ipsilateral secondary motor areas and presumably ipsilateral cortico-bulbospinal tracts as a compensatory means to generate more shoulder abduction torque in the paretic arm following a stroke, but with limited capacity to support distal hand opening.

Materials and Methods

Participants

Seventeen individuals with chronic hemiparetic stroke (mean age: 58.9 ± 7.6 yrs.) and moderate to severe impairment (Upper Extremity Fugl Meyer Assessment [UEFMA]: 10-38; mean = 20.8 ± 8.4) and twelve age-matched controls (mean age: 59.8 ± 7.7 yrs.) participated in this study. Demographic information for each participant is provided in Table 4.1 and lesion locations in Figure 4.1. All individuals with stroke were screened for inclusion by a licensed physical therapist. Inclusion criteria included being at least one-year following a stroke, an UEFMA no greater than 40 out of 66, MRI compatibility, and subcortical lesions not extending into sensorimotor cortices.

This study was approved by the Northwestern institutional review board and all participants gave written informed consent.

Table 4.1. Participant Demographics

Controls				Stroke					
Participant	Age	Sex	Dominant Arm	Participant	Age	Sex	UEFMA	Years post stroke	Lesioned Hemisphere
P1	60	M	R	P1	62	F	23	7	L
P2	59	M	R	P2	49	M	11	18	L
P3	45	F	R	P3	60	M	11	6	R
P4	74	M	R	P4	60	M	10	19	R
P5	68	F	R	P5	60	M	19	9	R
P6	61	M	R	P6	63	M	22	9	L
P7	61	M	R	P7	68	M	13	21	L
P8	48	F	R	P8	57	M	24	5	L
P9	60	F	R	P9	60	F	24	12	R
P10	54	F	R	P10	66	M	17	9	R
P11	61	M	R	P11	71	M	15	13	R
P12	66	M	R	P12	47	M	38	7	R
				P13	65	F	16	31	L
				P14	47	M	16	10	R
				P15	44	M	38	4	L
				P16	64	M	30	7	L
				P17	58	M	26	3	L
Average	59.8				58.9		20.8	11.2	
\pm Std	\pm 7.7				\pm 7.6		\pm 8.4	\pm 7.1	

UEFMA: Upper extremity Fugl-Meyer Assessment; Std: Standard Deviation

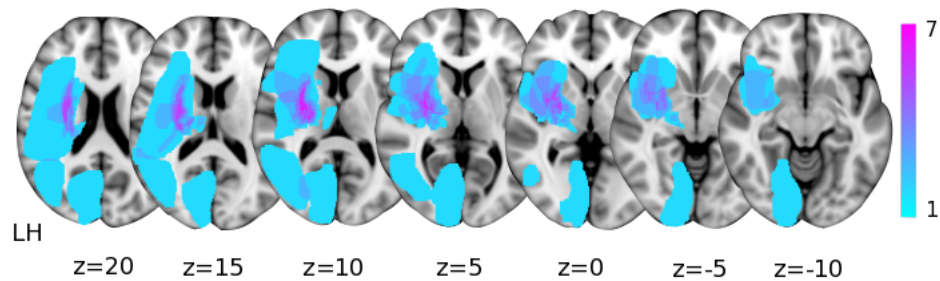


Figure 4.1

Subcortical lesion locations for the seventeen individuals with stroke overlaid on axial Montreal Neurological Institute T1 slices. The color bar indicates the number of participants with lesioned tissue in a particular voxel. LH indicates the lesioned hemisphere.

Experimental Protocols

Structural Imaging of the Brain

Individuals participated in MRI scans at Northwestern University's Center for Translation Imaging on a 3 Tesla Siemens Prisma scanner with a 64-channel head coil. Structural T1-weighted scans were acquired using an MP-RAGE sequence (TR=2.3s, TE=2.94ms, FOV 256x256mm²) producing an isotropic voxel resolution of 1x1x1 mm. Visual inspection of acquired images was performed immediately following the data acquisition to check the quality of the collected images and confirm stable head position.

Functional Imaging related to hand and arm

In a separate experiment, functional imaging related to hand opening with or without arm lifting was examined using EEG. During the EEG experiment, participants sat in a Biodex chair (Biodex Medical Systems, Shirley, NY), which restrained the trunk with straps crossing the chest and abdomen. The participant's paretic arm for individuals with stroke or dominant arm for healthy individuals was placed in a forearm-hand orthosis attached to the end effector of an admittance controlled robotic device (ACT^{3D}) instrumented with a six degree of freedom (DOF) load cell (JR³ Inc., Woodland, CA).

At the beginning of each trial, participants moved their hand to a home position, with the shoulder at 85° abduction, 40° flexion, and the elbow at 90° flexion angle. The participant then received an auditory cue. Following the cue, participants relaxed at the home position for 5-7 s and then self-initiated either 1) a maximum attempted hand opening with the arm resting on a haptic table, or 2)

a maximum attempted hand opening while lifting against 50% of maximum shoulder abduction torque (SABD50). Participants were instructed to avoid eye movements by focusing on a point and avoid movements of other body parts during the performance of each trial, which was visually confirmed by the experimenter. Participants performed 60-70 trials of each task, broken into blocks (one block consisted of 20-30 trials for a particular task). Rest periods varied between 15 to 60 seconds between trials and 10 minutes between blocks.

Scalp recordings were made with a 160-channel High-Density EEG system using active electrodes (Biosemi, Inc, Active II, Amsterdam, The Netherlands) mounted on a stretchable fabric cap based on a 10/20 system. The centers of all the electrode holders were attached with reflective markers. Simultaneously, EMGs were recorded from the extensor carpi radialis, flexor carpi radialis, and intermediate deltoid of the tested arm to assess timing of movement onset. All data were sampled at 2048 Hz. The impedance was kept below 50 k Ω for the duration of the experiment. The positions of EEG electrodes on the participant's scalp were recorded with respect to a coordinate system defined by the nasion and pre-auricular notches using a Polaris Krios handheld scanner (NDI, Ontario, Canada). This allowed for coregistration of EEG electrodes with each participant's anatomical MRI data. Additionally, for individuals with a stroke, involuntary grasping pressure during the two tasks was measured by a custom pressure sensor mat (Pressure Profile System Inc., CA) that was wrapped around a cylinder where the participant's fingers/palm were placed around (see Figure 4.3). Although participants were instructed to open their hand, individuals with severe chronic stroke display involuntary grasping due to the combination of weakness of finger extensor muscles and involuntary coactivation of finger flexor muscles (Lan et al. 2017). Therefore, instead of directly measuring hand opening ability, grasping pressure was measured and used as a marker

for hand opening ability, with increased involuntary grasping pressure reflecting reduced hand opening ability. At the start of the experiment, maximum grasping forces were measured for the paretic hand, which were used for normalization purposes in the data analysis.

Data Analysis

Structural Changes in Gray Matter Density

Anatomical T1 data were analyzed with FSL voxel-based morphometry (VBM) 1.1 (<https://fsl.fmrib.ox.ac.uk/fsl/fslwiki/FSLVBM>; Oxford University, Oxford, United Kingdom) (Douaud et al. 2007) using FSL tools (Smith et al. 2004). T1 images for individuals with right hemisphere lesions were flipped so that the lesions of all stroke participants were in the left hemisphere. The T1 images were then brain-extracted using the Brain Extraction Tool and segmented into gray matter using FAST4. The resulting gray matter partial volume images were aligned to Montreal Neurological Institute (MNI) 152 standard space using the affine registration tool FLIRT and averaged to create a study-specific gray matter template. Subsequently, individual gray matter partial volume images in native space were non-linearly registered to this template using FNIRT, modulated to correct for local expansion or contraction due to the non-linear component of the spatial transformation, and then smoothed with an isotropic Gaussian kernel with a sigma of 3 mm. These gray matter images were masked to only include the ipsilateral sensorimotor cortex including primary motor cortex, supplementary motor area, premotor cortex, and primary somatosensory cortex from the Human Motor Area Template (Mayka et al. 2006).

Involuntary Grasping Pressure

The grasping pressure was calculated as the sum of max pressure generated by the I-IV digits during a given trial (Lan et al. 2017) (see an example of the pressure generated in Figure 4.3B). Ensemble-averaged grasping pressure for each condition was then normalized by the maximum grasping pressure, which was calculated as the average of the largest 3 total grasping pressures during the max closing trials. Grasping pressure is thus referred to as the percent of pressure during a specific task compared to the individual's max closing pressure.

Cortical activity related to hand opening and hand opening while lifting against load

EEG data were low pass filtered at 50 Hz, aligned to the earliest EMG onset of the 3 muscles, and segmented from -2200 to +200 ms (with EMG onset at 0 ms) using Brain Vision Analyzer 2 software (Brain Products, Gilching, Germany). Data were then visually inspected for the presence of artifacts. Trials exhibiting artifacts (e.g., eye blinks) were eliminated from further analysis. The remaining EEG trials were baseline-corrected (from -2180 to -2050 ms) and ensemble-averaged. The averaged EEG signals were down-sampled to 256 Hz and imported into CURRY 6 (Compumedics Neuroscan Ltd., El Paso, TX). The cortical current density strength ($\mu\text{A}/\text{mm}^2$) in the time between 150 ms and 100 ms prior to EMG onset was computed using the standardized low resolution electromagnetic brain tomography (sLORETA) method ($L_p = 1$) based on a participant-specific boundary element method model with the regularization parameter automatically adjusted to achieve more than 99% variance accounted (Bradley et al. 2016; Yao and Dewald 2005). Possible sources were located on a cortical layer with 3 mm distance between each node.

Although the inverse calculation was performed over the whole cortex, only the activity in bilateral sensorimotor cortices was further analyzed. Specific regions of interest (ROIs) included bilateral primary sensorimotor cortices (primary motor cortex (M1) + primary somatosensory cortex (S1)) and secondary motor cortices (supplementary motor area (SMA) + premotor area (PM)).

We used the estimated current density strengths to calculate a Laterality Index ($LI = (C-I)/(C+I)$), where C and I are the current density strengths from the contralateral and ipsilateral sensorimotor cortices (i.e., combined primary sensorimotor and secondary motor cortices), respectively. LI reflects the relative contributions of contralateral versus ipsilateral sensorimotor cortices to the source activity, with a value close to +1 for a contralateral source distribution and -1 for an ipsilateral source distribution.

Additionally, we quantified a cortical activity ratio $CAR = \frac{\sum_1^N s_n}{\sum_1^M s_m}$ for each of the 4 ROIs, where S_n represents the current density strength of the n^{th} node, and N and M represent the number of nodes in one of the ROIs and the whole sensorimotor cortices, respectively. The cortical activity ratio reflects the relative strength from one ROI as normalized by the total combined strength of the 4 ROIs. When a significant effect of task in CAR was found, we further examined between-task difference in the sum of absolute amplitude activity in each ROI. This is to justify the possible interdependencies between regions (e.g., one region increasing in CAR can lead to a decrease in CAR in another even if the absolute activity does not change in the second region). However, measure of absolute activity can only be used for within-subject comparisons, due to the between subject variance in signal to noise ratio, scalp conductance, electrode impedance, etc.

Lastly, we assessed cortico-cortico coupling during movement preparation using dynamic causal modeling for induced responses (DCM-IR). Our network model consisted of 5 regions of interest, including contralateral primary motor cortex (cM1), ipsilateral primary motor cortex (iM1), contralateral premotor cortex (cPM), ipsilateral premotor cortex (iPM), and supplementary motor area (SMA). SMA served as the input to the modelled network. EEG data were preprocessed using SPM12 (SPM12, Wellcome Trust Centre for Neuroimaging, www.fil.ion.ucl.ac.uk/spm/). Data were first band-pass filtered between 1 and 50 Hz, segmented into single trials (-2200 to 500 ms with 0 ms indicating EMG onset), and baseline-corrected. Trials were visually inspected and removed if they displayed an artifact (e.g., blinks). Artifact free trials were projected from channel space to the sources using the generalized inverse of the lead-field matrix with an equivalent current dipole for our chosen sources using a subject-specific boundary element method (BEM) based on the subject's anatomical MRI (Chen et al. 2008). The spectrogram of each segmented trial from 4 to 48 Hz at each source was computed using a Morlet wavelet transform. This range includes theta (4-7 Hz), alpha (8-12 Hz), beta (13-35 Hz), and gamma (36-48 Hz) frequencies. The spectrogram (frequency x time x source) was then averaged over all trials, cropped between -1000 to 0 ms, and then baseline-corrected by subtracting the mean of the frequency-specific instantaneous power during the time window -1000 to -833 ms. After reducing the data to four modes using singular value decomposition (SVD), we estimated the DCM parameters of the A matrix using Bayesian inversion (as described in Chapter 3).

Statistical Analysis

Statistics for the GM density were computed within FSL. A voxel-wise Generalized Linear Model was applied with a Threshold-Free Cluster Enhancement (Winkler et al. 2014) to detect differences in gray matter density between individuals with stroke and controls. A voxel-based threshold of changes in gray matter density was set at $p < 0.05$ (Family-Wise Error Corrected; FWE). Statistics for the behavior and EEG were performed using SPSS (IBM, V23). A paired t-test was performed to assess any impact on task on the normalized grasping pressure in individuals with stroke. A 2 (group) x 2 (task) ANOVA was performed on LI for the EEG analysis. A 2 (group) x 2 (task) x 4 (region) ANOVA was performed on CAR for the EEG analysis. We performed post-hoc paired t-tests for any significant within-subject effect in ANOVA interactions. Pearson correlations were performed between significant cortical activity findings and grasping pressure. A p value of 0.05 or less was considered significant. Statistics for DCM were performed in SPM. Having already established the default coupling network for the two tasks in controls in Chapter 3, we ran a one-sample t -test for the coupling for each connection to assess connections involved in the default network for each condition in the stroke group. Significance for specific coupling parameters was set at $p < 0.005$.

Results

Differences in Gray Matter Density in Ipsilateral Sensorimotor Cortex

Structural differences in gray matter (GM) density within sensorimotor cortices were compared between individuals with stroke and healthy controls. Individuals with stroke had significantly greater GM density compared to controls in two ipsilateral clusters: 1) in premotor cortex (peak

voxel: $x = 46$, $y = 6$, $z = 50$, t -value = 5.17, $p < 0.05$ FWE corrected; Figure 4.2A), and 2) in primary somatosensory cortex (peak voxel: $x = 48$, $y = -26$, $z = 58$, t -value = 5.55, $p < 0.05$ FWE corrected; Figure 4.2B). Meanwhile, there were no regions of significantly greater GM density in controls compared to individuals with stroke within the ipsilateral sensorimotor cortex.

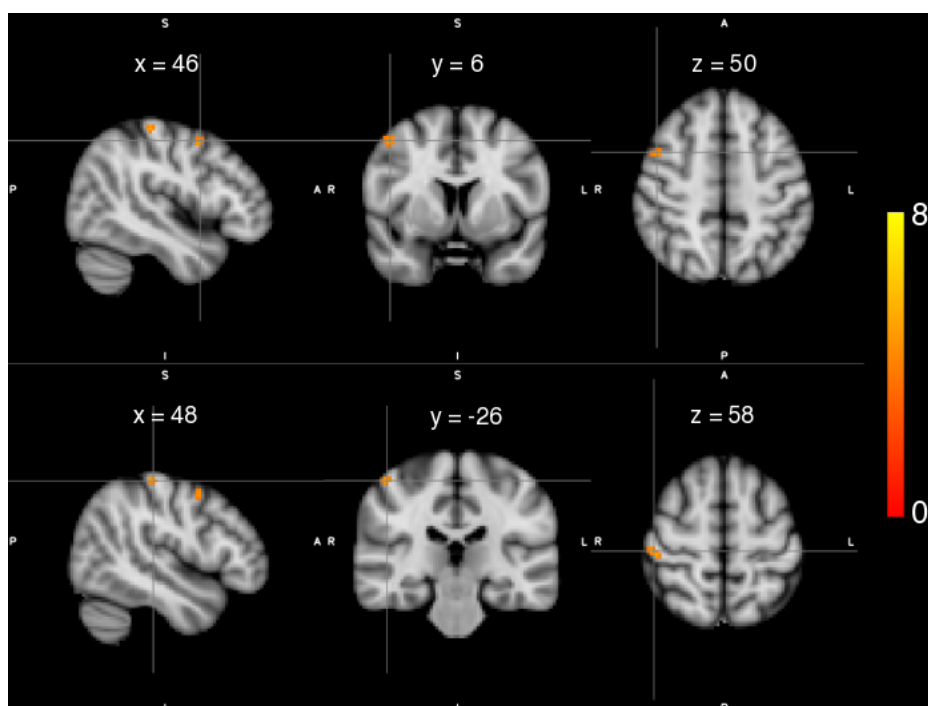


Figure 4.2

Statistical maps of gray matter (GM) density differences for individuals with stroke compared to healthy controls. Significantly higher GM density was observed in ipsilateral premotor cortex (Top) and ipsilateral primary somatosensory cortex (Bottom) in individuals with stroke compared to controls. Color maps indicate the thresholded t values at each voxel. A statistical threshold was set equivalent to $p < 0.05$ FWE.

Impact of Shoulder Abduction on Hand Opening Ability Post Stroke

Since the cohort of this study was primarily severely impaired and could not open their paretic hand, we measured grasping pressure as an indicator of the hand opening attempt. We found that twelve of the seventeen individuals with chronic stroke could not open their hand off the cylinder and therefore included them in the grasping pressure analysis. An example for one individual's grasping pressure during the two conditions is depicted in Figure 4.3C. Overall, these individuals

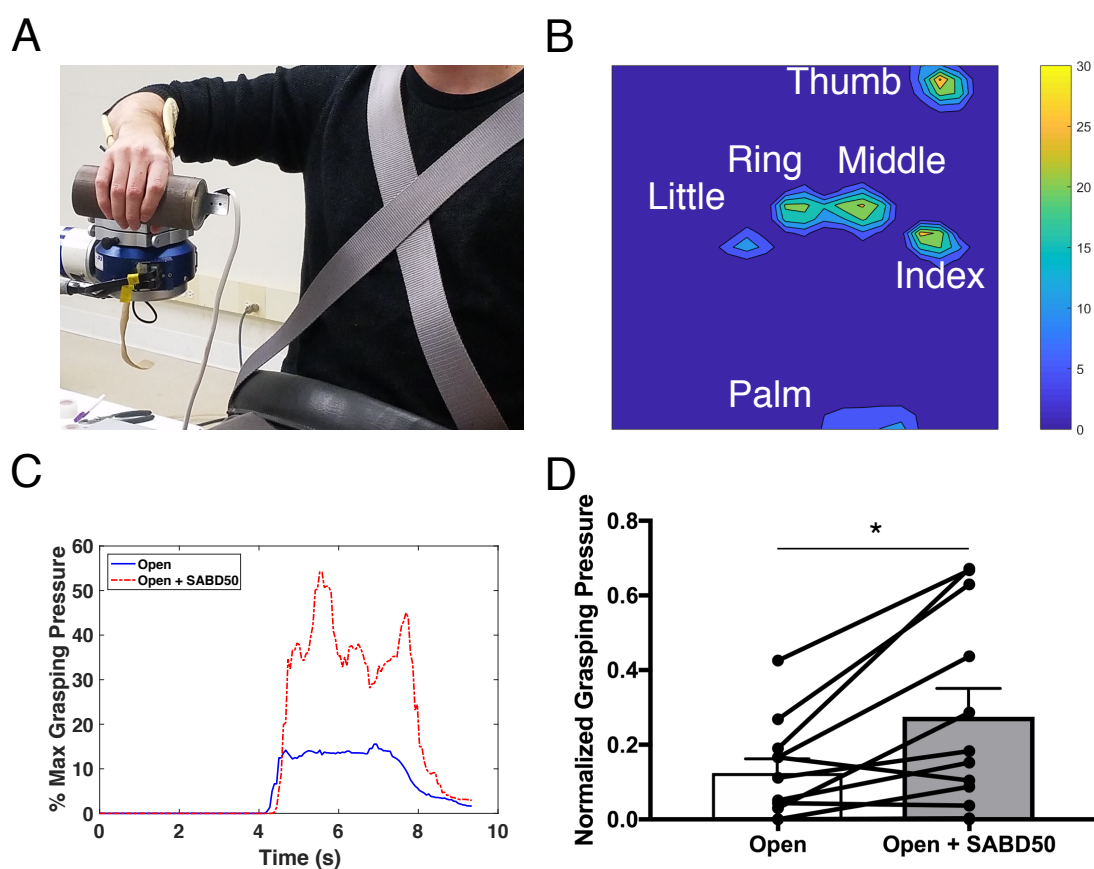


Figure 4.3

Shoulder abduction reduces hand opening ability in individuals with stroke. (A) The ACT-3D system with the attached forearm-hand orthosis equipped with a TactArray sensor mat to measure grasping pressure. (B) An example of grasping pressure measured by the TactArray sensor mat. (C) An example from one individual of grasping pressure over time for attempted hand opening on the table (solid Blue) and attempted hand opening while lifting against 50% max shoulder abduction (broken Red) depicted as the percentage of max grasping pressure. (D) Group averages with individual data overlaid of normalized grasping pressure for opening on the table vs. opening while lifting against 50% max shoulder abduction. Error bars depict SEM. * $p < 0.05$.

had a significant increase in involuntary grasping pressure (reduced hand opening ability) with the

addition of the SABD load compared to attempted hand opening on the table ($t(11) = 3.16, p = 0.009$; Figure 4.3D). Controls were not analyzed since they do not produce any involuntary grasping pressure during either condition, and a 50% max SABD load does not reduce hand opening ability (Lan et al. 2017).

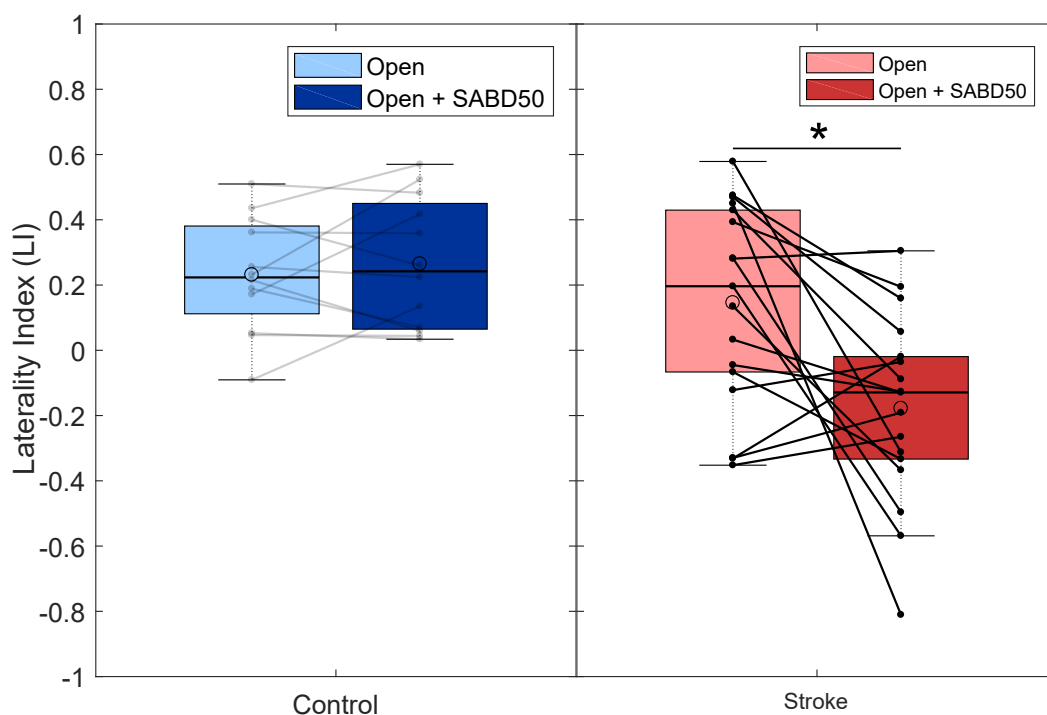


Figure 4.4

Shoulder abduction increases reliance on the ipsilateral hemisphere in stroke but not controls. Boxplots with individual data overlaid showing laterality index (LI) for controls (left; blue) and stroke (right; red) for hand opening on the table (light) and hand opening while lifting against 50% max shoulder abduction (dark). Controls show no difference between conditions, while the addition of SABD increases reliance on the ipsilateral hemisphere in individuals with stroke (i.e., negative LI). * $p < 0.05$.

Impact of Shoulder Abduction on Cortical Activity

A 2 (group) x 2 (task) ANOVA was conducted to examine the effect of group and task on the laterality index (LI). There was a statistically significant interaction between the effects of group

and task on LI ($F(1,54) = 6.62, p = 0.013$; Figure 4.4). Post hoc paired t-tests showed that LI was significantly lower (more ipsilateral) during the Open + SABD50 condition compared to opening on the table for individuals with stroke ($t(16) = 3.16, p = 0.006$). Meanwhile, controls showed no difference in LI between the two tasks.

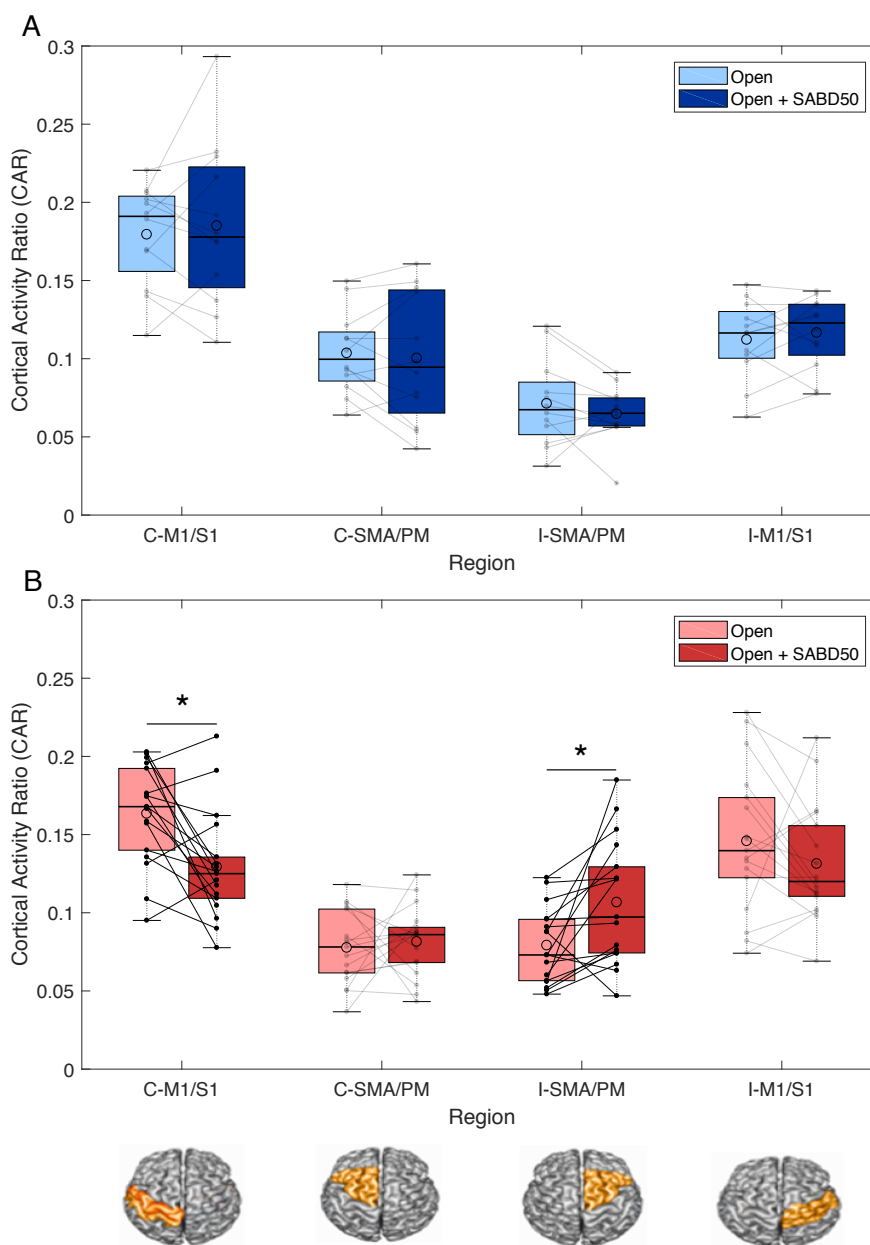


Figure 4.5

Cortical regions driving SABD-dependent reliance on the ipsilateral hemisphere. (A) Boxplots with individual data overlaid depicting cortical activity ratio (CAR) during hand opening (light blue) and hand opening while lifting against 50% max shoulder abduction (dark blue) across the 4 regions of interest in healthy controls. No changes in CAR are observed in any of the regions between the two tasks. (B) Boxplots with individual data overlaid depicting CAR during hand opening (light red) and hand opening while lifting against 50% max shoulder abduction (dark red) across the 4 regions of interest in individuals with stroke. Individuals demonstrated a decrease in activity in contralateral (ipsilesional) primary sensorimotor cortex (M1/S1) and an increase in ipsilateral (contralesional) secondary motor areas (SMA/PM) with the addition of SABD. ROIs are depicted below the figure. The median is shown by the horizontal black line and the mean is illustrated by the large open circle. C = contralateral, I = ipsilateral. * $p < 0.05$.

A 2 (group) x 2 (task)
x 4 (region) ANOVA
was conducted to

examine the effect of group, task, and region on CAR. There was a statistically significant three-way interaction between the effects of group, task, and region on CAR ($F(3,216) = 3.01, p = 0.03$; Figure 4.5). Post hoc paired t-tests showed that in individuals with stroke, the addition of lifting to opening caused significantly increased CAR in ipsilateral secondary motor areas (i-SMA/PM, $t(16)=3.01, p=0.008$) and decreased CAR in contralateral primary sensorimotor cortices (c-M1/S1, $t(16)=2.73, p=0.015$). In controls, there were no differences between any of the regions during the two tasks.

We further compared the between-task difference in the sum of absolute amplitude in i-SMA/PM and c-M1/S1, the 2 significant areas for CAR measure in individuals with stroke. Data were log transformed to normalize the data. Due to between-task differences in signal to noise ratio greater than 2 standard deviations from the mean difference thus making the comparison of absolute amplitude between conditions invalid, 2 participants were removed. Paired t-tests showed that the absolute amplitude of activity was increased in ipsilateral secondary motor areas with the addition

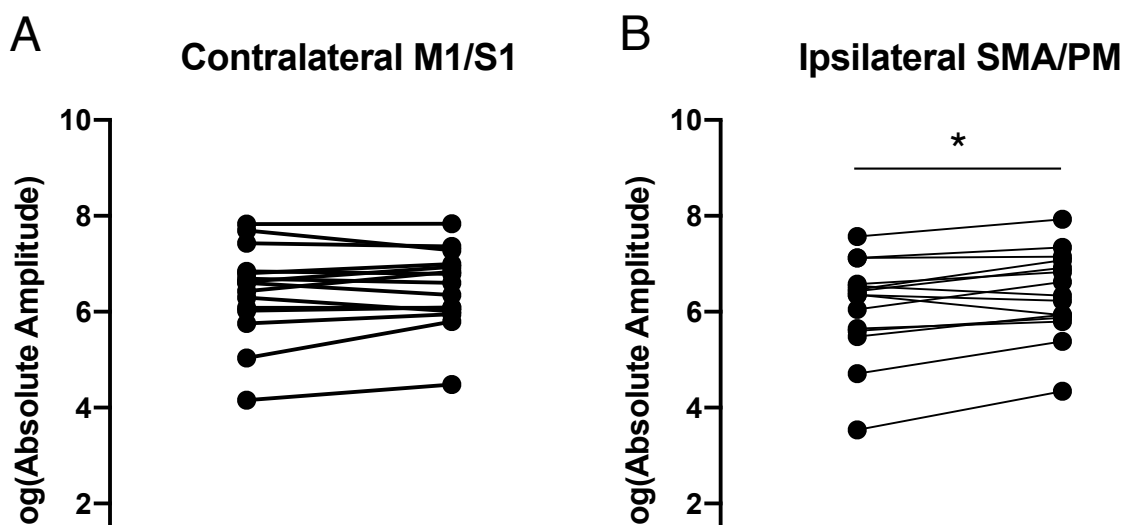


Figure 4.6

Absolute amplitude during the Open vs. Open + SABD50. (A) Individual data depicting the log transformed amplitude during hand opening versus hand opening while lifting against 50% max shoulder abduction in contralateral primary sensorimotor cortex (M1/S1). (B) Individual data depicting the log transformed amplitude for the two conditions for ipsilateral secondary motor areas (SMA/PM). * $p < 0.05$.

of SABD ($t(14) = 3.08, p = 0.008$), but there was no difference between conditions for contralateral primary sensorimotor cortices (see Figure 4.6).

Relationship Between Cortical Activity and Hand Opening Ability

Linear regression reported a positive correlation between involuntary grasping pressure and the CAR measure from i-SMA/PM during the Open + SABD50 condition ($R = 0.65, p = 0.022$; Figure 4.7A). Thus, individuals who showed more involuntary grasping forces when attempting to open during the SABD condition tended to show greater activity in ipsilateral secondary motor areas during that task. Meanwhile, there was no association between involuntary grasping pressure and activity in c-M1/S1 during this condition ($R = -0.20, p = 0.53$; Figure 4.7B).

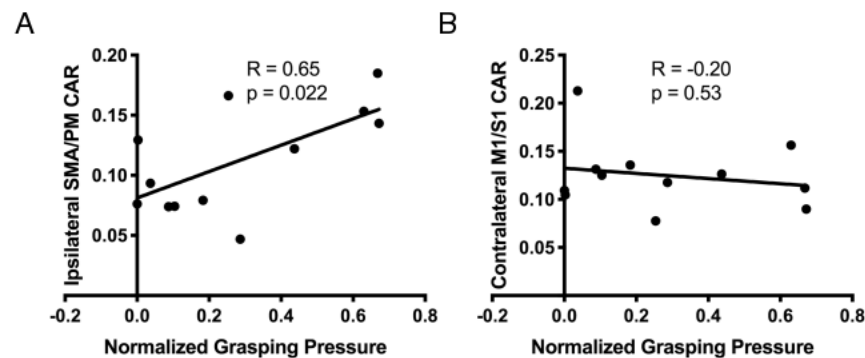


Figure 4.7

Association between cortical activity and hand opening ability in individuals with stroke. (A) Comparison of normalized grasping pressure during the hand opening + SABD50 condition and cortical activity ratio (CAR) in ipsilateral secondary motor areas (SMA/PM) during that task. Greater involuntary grasping pressure (i.e., reduced hand opening ability) is associated with greater activity in ipsilateral secondary motor areas in individuals with stroke. (B) Comparison of normalized grasping pressure during the hand opening + SABD50 condition and CAR in contralateral primary sensorimotor cortex (M1/S1) during that task. There is no association between activity in contralateral primary sensorimotor cortex and grasping pressure.

Relationship Between Cortical Activity and Cortical Structure

We found significant negative correlations between the Laterality Index (LI) during Open + SABD50 and gray matter density in the ipsilateral sensorimotor cortex in individuals with stroke

(see Figure 4.8). Thus, individuals who relied more on the ipsilateral hemisphere during Open + SABD50 also tended to show higher gray matter density in that hemisphere. This spanned across

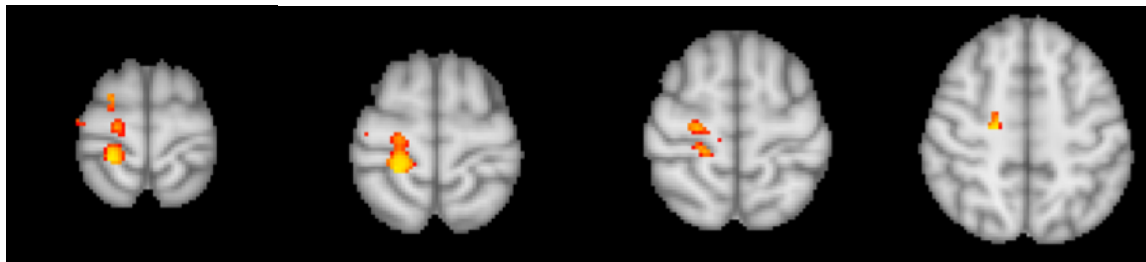


Figure 4.8

Clusters with significant negative correlations between LI during Open + SAB50 and GM density in the ipsilateral sensorimotor cortex, including clusters in M1, S1, PM, and SMA. However, no significant correlation was found between CAR in i-SMA/PM and gray matter density.

Cortico-Cortico Coupling

Finally, we evaluated the cortico-cortico oscillatory coupling during the motor preparation phase for the two tasks in individuals with stroke. Both tasks evoked significant coupling between all

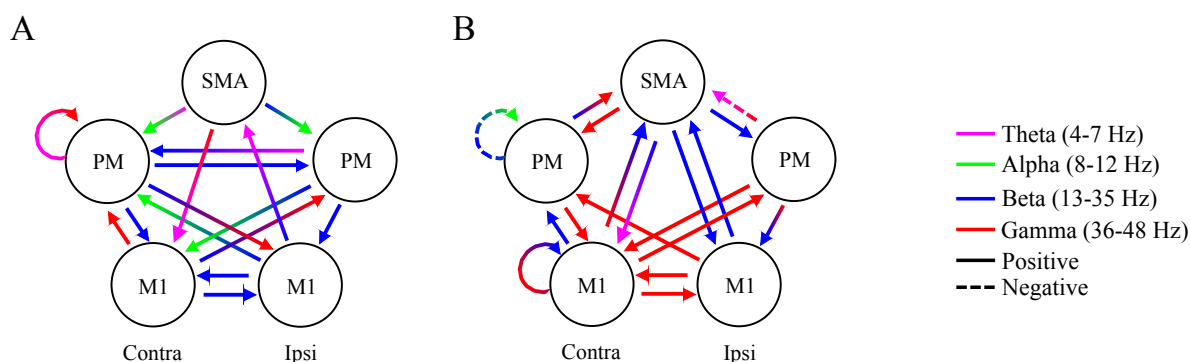


Figure 4.9

Default cortico-cortico oscillatory coupling for (A) Hand Opening and (B) Hand Opening while lifting against 50% max shoulder abduction for the stroke group. Arrows indicate directional connections showing significant coupling within the motor network. The color of the arrow indicates the frequency band involved. Arrows that change colors represent cross-frequency coupling. Solid lines indicate positive coupling while dashed lines indicate negative coupling. Contra = contralateral hemisphere; Ipsi = Ipsilateral hemisphere

ROIs across a range of frequency bands (see Figure 4.9), but with minimal differences between tasks. A complete list of all significant connections and the frequencies involved is listed in

Table 4.2.

Table 4.2. Significant default frequency-to-frequency coupling

Connection	Frequency Bands (peak [Hz])	# of Voxels	Excitatory/Inhibitory
Condition: Open			
iM1 → cM1	$\beta \rightarrow \beta$ (25 → 16)	159	+
cPM → cM1	$\beta \rightarrow \beta$ (16 → 25)	16	+
iPM → cM1	$\beta \rightarrow \alpha$ (24 → 12)	28	+
SMA → cM1	$\gamma \rightarrow \phi$ (47 → 5)	7	+
cM1 → iM1	$\beta \rightarrow \beta$ (26 → 35)	77	+
cPM → iM1	$\beta \rightarrow \gamma$ (35 → 39)	35	+
iPM → iM1	$\beta \rightarrow \beta$ (23 → 30)	36	+
cM1 → cPM	$\gamma \rightarrow \gamma$ (39 → 37)	242	+
iM1 → cPM	$\beta \rightarrow \alpha$ (15 → 8)	26	+
cPM → cPM	$\phi \rightarrow \gamma$ (5 → 36)	21	+
iPM → cPM	$\phi \rightarrow \beta$ (4 → 33)	28	+
SMA → cPM	$\beta \rightarrow \alpha$ (6 → 8)	82	+
iM1 → iPM	$\beta \rightarrow \gamma$ (27 → 43)	214	+
cPM → iPM	$\beta \rightarrow \beta$ (24 → 32)	191	+
SMA → iPM	$\beta \rightarrow \alpha$ (16 → 10)	29	+
iM1 → SMA	$\beta \rightarrow \phi$ (35 → 4)	13	+
Condition: Open while Lifting			
cM1 → cM1	$\gamma \rightarrow \beta$ (42 → 27)	59	-
iM1 → cM1	$\gamma \rightarrow \gamma$ (44 → 45)	385	+
cPM → cM1	$\gamma \rightarrow \gamma$ (46 → 44)	271	+
iPM → cM1	$\gamma \rightarrow \gamma$ (39 → 38)	45	+
SMA → cM1	$\beta \rightarrow \phi$ (15 → 7)	140	-
cM1 → iM1	$\gamma \rightarrow \gamma$ (37 → 48)	31	+
iPM → iM1	$\gamma \rightarrow \beta$ (43 → 19)	68	+
SMA → iM1	$\beta \rightarrow \beta$ (29 → 29)	16	+
cM1 → cPM	$\beta \rightarrow \beta$ (19 → 15)	153	+
iM1 → cPM	$\gamma \rightarrow \gamma$ (39 → 39)	73	+
cPM → cPM	$\beta \rightarrow \beta$ (16 → 12)	22	-

SMA → cPM	$\gamma \rightarrow \gamma$ (43 → 43)	156	+
cM1 → iPM	$\gamma \rightarrow \gamma$ (38 → 48)	62	+
SMA → iPM	$\beta \rightarrow \beta$ (34 → 31)	35	+
cM1 → SMA	$\gamma \rightarrow \beta$ (36 → 13)	124	+
iM1 → SMA	$\beta \rightarrow \beta$ (23 → 27)	9	+
cPM → SMA	$\beta \rightarrow \gamma$ (27 → 48)	44	+
iPM → SMA	$\gamma \rightarrow \phi$ (40 → 7)	20	-

Notes: # of voxels refers to the spread of coupling around the peak frequency involved where each voxel represents coupling with 1 Hz resolution; Excitatory refers to positive coupling where a change in power in the 1st connection is associated with the same directional change in power in the 2nd connection; Inhibitory refers to negative coupling where a change in power in the 1st connection is associated with the opposite directional change in power in the 2nd connection; Highlighted rows reflect common connections in both tasks. M1 = Primary Motor Cortex; PM = Premotor Cortex; SMA = Supplementary Motor Area; c = contralateral; i = Ipsilateral

Discussion

We sought to evaluate the potential compensatory role of ipsilateral (i.e., contralesional) secondary motor regions following a stroke and their capacity to support hand function as compensation for damage to corticospinal tract. We found that individuals with stroke showed systematic changes in structural morphometry within ipsilateral secondary motor regions relative to the paretic arm in the form of increased gray matter density. Furthermore, when looking at cortical activity related to the hand, we found that the increased demand of SABD during attempted hand opening increased reliance on the i-SMA/PM in individuals with stroke, but not controls. Crucially, this reliance on ipsilateral secondary motor areas was associated with SABD-induced impairments in hand opening ability due to the flexion synergy. The combination of this structural and functional evidence points to increased compensatory reliance on ipsilateral secondary motor areas post moderate to severe stroke, but with limited capacity to support proper hand function.

If individuals with stroke are indeed relying more on ipsilateral secondary motor areas as compensation for CST damage, we would expect to see systematic changes in structural

morphometry in these regions. This expectation is based on the known relationship between functional activity and both synaptogenesis and dendritic growth commonly seen in animal training models (Murphy and Corbett 2009; Zatorre et al. 2012). In line with these expectations, we saw increased GM density within ipsilateral secondary motor areas, specifically in the premotor cortex, in individuals with stroke compared to controls. Increases in GM density have been proposed to indicate potential synaptogenesis, dendritic growth, or gliogenesis within these regions (Zatorre et al. 2012). The observed changes may reflect a combination of a greater reliance on the non-paretic limb, associated with a high prevalence of learned non-use (Baker et al. 2015; Taub et al. 2014) and a compensatory increased reliance on the ipsilateral projecting, cortico-bulbospinal tracts controlling the paretic limb in this population with more severe impairments. Findings have found increased dendritic growth and synapse proliferation in the ipsilateral cortex, particularly in animals showing excessive disuse (Jones 1999; Jones and Schallert 1994). Additionally, the more severe impairments prevalent in these individuals tends to lead to a reliance on compensatory strategies in everyday life, which has also been hypothesized to lead to associated structural changes in the ipsilateral cortex (Jones 2017).

Having established that individuals with chronic stroke have long-term changes in structure in i-SMA/PM, possibly indicating increased overall reliance on these regions, we then examined their functional capacity to support hand function. To this point, the majority of research on hand function following a stroke has focused on the role of CST damage and impairment levels (Maraka et al. 2014; Zhu et al. 2010). Although damage to CST and accompanying corticobulbar tracts explains the presence of weakness following a stroke, it does not account for the loss of independent joint control such as the flexion synergy often observed in individuals with more

severe impairments. The flexion synergy arises during lifting and reaching movements and leads to abnormal involuntary coactivation with wrist and finger flexors (Dewald et al. 1995; Lan et al. 2017; Miller and Dewald 2012; Sukal et al. 2007). We hypothesize that this occurs because residual resources from remaining contralateral corticospinal and corticobulbar tracts become insufficient as the demand of the shoulder abduction increases, and consequently individuals rely more on uncrossed ipsilateral cortico-bulbospinal pathways, such as the corticoreticulospinal tract, in compensation to carry out the motor task (McPherson et al. 2018a). Unfortunately, although these ipsilateral pathways allow control of the shoulder, they reduce hand opening distally at the hand due to coactivation between shoulder abductors and wrist/finger flexors (Hirschauer and Buford 2015; Lan et al. 2017). Our findings here support this hypothesis, as individuals with stroke have increased reliance on the ipsilateral hemisphere with the addition of an SABD load, whereas healthy controls, who have intact contralateral CST and corticofugal tracts, showed no effect of SABD.

We found that the observed shift to the ipsilateral hemisphere during the SABD task in the stroke group was driven by increased activity in i-SMA/PM as measured by CAR. This was confirmed when examining the overall absolute amplitude of cortical activity between the 2 conditions, suggesting that as the demand of the task increased, individuals with stroke attempted to use additional cortical resources from the ipsilateral secondary motor areas to execute the task. Ipsilateral secondary motor areas have been widely implicated for their compensatory role following a stroke, particularly in more impaired individuals. For instance, individuals following a stroke who used their paretic arm less in daily life, as measured by accelerometers, also showed greater activity in secondary motor areas during a grip task (Kokotilo et al. 2010). Similarly,

increased secondary motor activity correlated with greater jerk in a reach to grasp movement, highlighting its compensatory role and inability to fully eliminate impairment (Buma et al. 2016).

Importantly, SMA and PM serve as the primary origin for cortico-bulbospinal tracts such as the corticoreticulospinal tract (Fregosi et al. 2017; Montgomery et al. 2013). These tracts have been widely implicated in the presence of the flexion synergy due to their extensive branching at the spinal cord and flexor bias in the ipsilateral arm (Baker 2011). Given that we see both increased activity in these areas and a correlation with reduced hand opening ability during the SABD task, we argue this reflects increased recruitment of these ipsilateral cortico-bulbospinal pathways. This argument is grounded in work done in monkeys where lesions lead to an increase in strength of the corticoreticular projections (Zaaimi et al. 2012), and stimulation of reticulospinal pathways elicits activation of shoulder abductor and arm/hand flexor muscles (Hirschauer and Buford 2015). Furthermore, pharmacological manipulations in chronic hemiparetic stroke participants aimed at decreasing monoamine levels in the brainstem and spinal cord, reduce the expression of flexion synergy behavior (McPherson et al. 2018b). This reduction in flexion synergy behavior is likely the result of reducing the effects of the ionotropic component of reticulospinal pathways. It is unlikely that the increased activity in secondary motor areas during the SABD task in our study reflects use of descending projections from ipsilateral CST since these primarily originate from ipsilateral primary motor cortex, not SMA or PM, and these pathways do not sufficiently innervate the distal portions of the arm (Soteropoulos et al. 2011; Zaaimi et al. 2012). It is also important to note that we do not see a correlation between reduced activity in contralateral primary sensorimotor cortex and reduced hand opening ability during the SABD task, which corroborates the role of

ipsilateral cortico-bulbospinal pathways originating primarily from secondary motor areas as the main initiator of the flexion synergy-related hand opening impairment.

The main difference observed here compared to monkey models of stroke is that dependence on ipsilateral (i.e., contralesional) secondary motor areas, and presumably ipsilateral corticobulbospinal tracts, does not appear to be sufficient for significant hand function recovery. Unlike humans, monkeys maintain the ability to use the hand following a pyramidal CST lesion, possibly due to a more viable rubrospinal tract innervating the hand (Lawrence and Kuypers 1968; Nathan and Smith 1955). In fact, recovery of reaching and hand function correlates with increased structural connectivity within cortico-reticulospinal tract projections in monkeys (Darling et al. 2018; Herbert et al. 2015). However, the ability for these tracts to allow dexterous hand control seems limited in humans based on the results here, as well as previous findings showing that individuals with more severe impairments show increased white matter integrity in ipsilateral reticular formation, which is correlated with worse synergy (Owen et al. 2017). This seems to contradict assertions that ipsilateral secondary motor areas may support recovery of hand function following a stroke (Bestmann et al. 2010; Johansen-Berg et al. 2002b), at least in the case for hand opening. Instead, the current results fit better within the recently proposed framework by Li and colleagues in which increased reliance on the ipsilateral SMA/PM cortico-reticulospinal tract accounts for the movement impairments seen following a stroke (Li et al. 2019).

Interestingly, we also observed increased GM density within ipsilateral primary somatosensory cortex in addition to premotor cortex. One possibility is that this reflects reorganization within the sensory system to provide sensory information to motor outputs being generated by ipsilateral

cortico-bulbospinal pathways. Indeed, preliminary evidence has shown that sensory information travels from the contralateral somatosensory cortex to the ipsilateral somatosensory cortex via the corpus callosum following a stroke (Filatova et al. 2018). Additionally, sensory recovery following a stroke has been associated with changes in both the contralateral and ipsilateral somatosensory cortex (Dechaumont-Palacin et al. 2008; Winship and Murphy 2008). However, the majority of research on neural plasticity following a stroke has focused on the motor component of recovery, and thus it is difficult to prescribe the underlying neural mechanism driving this result.

We previously found that for healthy individuals, the addition of lifting leads to an increase in cortico-cortico coupling during movement preparation both within the ipsilateral hemisphere and between hemispheres, without affecting cortical activation at movement execution (see Chapter 3). Here, we find that individuals with stroke show significantly greater involvement of additional motor regions during motor preparation compared to previous results in healthy controls. However, the addition of lifting does not lead to further additional cortico-cortico coupling since the default network for hand opening already involves almost every region. One must keep in mind that for the population studied here, individuals with moderate to severe impairments, even a simple hand opening task is often impossible to execute. Therefore, the significant coupling between almost every motor region may signify an attempt to recruit additional resources to carry out the task. This may explain why the addition of lifting does not lead to further cortico-cortico coupling since the network is already essentially ‘tapped out’ for just hand opening. It is also worth noting that this observed cortico-cortico coupling is not limited to motor-related bands as observed in healthy controls in Chapter 3, and instead spreads across all frequency bands tested. Previous results have shown that individuals following a stroke show problems with cortical activity during

movement preparation (Amengual et al. 2014), including overactivation of additional motor regions (Yao and Dewald 2018). The combination of these previous results, and the excessive coupling observed here across both motor and non-motor frequencies points towards an inefficiency in motor preparation that may be contributing to the observed changes in cortical activity at movement execution.

Clinical Implications

Our results in individual with moderate to severe chronic stroke imply that ipsilateral secondary motor cortices are not only insufficient, but actually detrimental, to hand opening. This finding points to the need to reengage the lesioned hemisphere in order to improve hand function. Although ipsilateral secondary motor areas allow sufficient control of the shoulder, they do not sufficiently innervate extensor muscles of the hand and instead lead to involuntary coactivation of flexor muscles. Therefore, they do not seem to offer a viable solution for basic hand function. Importantly, we have previously demonstrated the possibility for individuals even with severe motor impairments to reengage the lesioned hemisphere and improve hand function (Wilkins et al. 2017). Considering it is also possible to reduce the flexion synergy through progressive SABD training (Ellis et al. 2018; Ellis et al. 2009), future work targeting both the flexion synergy and finger/wrist extensor weakness may yield a solution towards improving both hand and upper extremity function via a reengagement of ipsilesional resources.

Limitations

One of the main limitations of this study is the inability to directly measure activity within the corticoreticulospinal tract. We are limited to the cortex when using EEG to look at cortical activity related to the task, and thus cannot directly measure use of specific pathways. However, previous work has shown structural changes in this pathway following a stroke, especially in individuals with more severe impairments (Owen et al. 2017), supporting the notion of potential increased compensatory reliance. EEG also allows us to look at cortical activity during tasks involving SABD, which would be impractical inside an MRI scanner.

It is also worth noting that this experiment only looked at the effect of SABD on hand opening. Findings may be different for hand closing. Ipsilateral corticoreticulospinal tract makes substantial innervations to the flexor muscles of the wrist and fingers, and thus may enable sufficient hand closing control, at least for power grasps (Baker and Perez 2017; Lawrence and Kuypers 1968). This could explain why extensor weakness of the fingers is usually a more significant problem than flexor weakness following a stroke (Conrad and Kamper 2012; Kamper et al. 2006; Miller and Dewald 2012).

5. Neural Plasticity in Moderate to Severe Chronic Stroke Following a Device-Assisted Task-Specific Arm/Hand Intervention

An edited version of this chapter has previously been published:

Wilkins K.B., Owen M., Ingo C., Carmona C., Dewald J.P.A., Yao J. (2017). Neural Plasticity in Moderate to Severe Chronic Stroke Following a Device-Assisted Task-Specific Arm/Hand Intervention. *Frontiers in Neurology*. 8:284. DOI: 10.3389/fneur.2017.00284.

Wilkins K.B., Dewald J.P.A., Yao J. (2019). Intervention-Induced Changes in Cortical Connectivity and Activity in Severe Chronic Hemiparetic Stroke. *bioRxiv* DOI: <https://doi.org/10.1101/547083>.

Abstract

Currently, hand rehabilitation following stroke tends to focus on individuals with mild impairments, partially due to the inability for individuals with severe impairments to sufficiently use the paretic hand. Device-assisted interventions offer a means to include individuals with more severe impairments and show promising behavioral results. However, the ability for this population to experience neural plasticity, a crucial factor in functional recovery following effective post-stroke interventions, remains unclear. This study aimed to investigate neural changes related to hand function induced by a device-assisted task-specific intervention in individuals with moderate to severe chronic stroke (upper extremity Fugl-Meyer < 30). We examined functional cortical reorganization related to the paretic hand/arm and gray matter structural changes using a multimodal imaging approach. We found that individuals exhibited a shift in cortical activity from the contralesional to the ipsilesional hemisphere related to both hand opening in isolation and hand opening while simultaneously lifting at the arm following the intervention. For hand opening, this was driven by decreased activity during motor execution in contralesional primary sensorimotor cortex and increased activity in ipsilesional secondary motor cortex. This intervention-induced decrease in contralesional primary sensorimotor cortex activity

during movement execution was accompanied by a reduction in coupling from ipsilesional M1 to contralesional M1 within gamma frequencies during movement preparation. Meanwhile, for hand opening while lifting, individuals had increased activity during motor execution in ipsilesional primary sensorimotor cortex following the intervention. This intervention-induced increase in ipsilesional sensorimotor cortex activity during movement execution was accompanied by a shift to inhibitory coupling within ipsilesional M1 from gamma to beta frequencies. Additionally, participants had increased gray matter density in ipsilesional primary sensorimotor cortex and decreased gray matter density in contralesional primary sensorimotor cortex. These findings suggest that despite moderate to severe chronic impairments, participants following a stroke maintain ability to experience cortical reorganization and gray matter structural changes following a device-assisted task-specific arm/hand intervention. These changes are similar to those reported in individuals with mild impairment, suggesting that residual neural plasticity in more severely impaired individuals may have the potential to support improved hand function.

Introduction

Nearly 800,000 people experience a new or recurrent stroke each year in the US (Mozaffarian et al. 2015). Popular therapies, such as constraint-induced movement therapy (CIMT), utilize intense task-specific practice of the affected limb to improve arm/hand function in acute and chronic stroke with mild impairments (Taub et al. 2002; Wolf et al. 2006). The effectiveness of these arm/hand interventions is partially attributed to cortical reorganization in the ipsilesional hemisphere following training in acute and mild chronic stroke (Favre et al. 2014). Unfortunately, CIMT requires certain remaining functionality in the paretic hand to execute the tasks, and only about 10% of screened patients are eligible (Kwakkel et al. 2015), thus disqualifying a large population

of individuals with moderate to severe impairments. Recently, studies using device-assisted task-specific interventions specifically targeted towards individuals with chronic moderate to severe impairments reported positive clinical results (Klamroth-Marganska et al. 2014; Page et al. 2016; Singer et al. 2013). However, these studies primarily focused on clinical measures, but it is widely accepted that neural plasticity is a key factor for determining outcome (Krakauer et al. 2012; Pekna et al. 2012; Starkey and Schwab 2014). Consequently, it remains unclear whether individuals with chronic moderate to severe impairments following a stroke [upper extremity Fugl-Meyer Assessment (UEFMA) < 30] maintain the ability to experience neural changes following an arm/hand intervention.

Neural changes induced by task-specific training have been investigated widely using animal models (Nudo 2013). For instance, monkeys or rodents trained on a skilled reach-to-grasp task express enlarged representation of the digits of the hand or forelimb in primary motor cortex (M1) following training as measured by intracortical microstimulation (Kleim et al. 1998; Nudo et al. 1996a). Rats also display altered functional connectivity between ipsilesional and contralesional primary sensorimotor cortex following a unilateral stroke, which is restored following behavior improvements (van Meer et al. 2010). Additionally, rapid local structural changes in the form of dendritic growth, axonal sprouting, myelination, and synaptogenesis occur (Biernaskie and Corbett 2001; Gibson et al. 2014; Kleim et al. 2002; Maier et al. 2008). Importantly, both cortical and structural reorganization accompany motor recovery following rehabilitative training in these animals (Nudo et al. 1996b; Tamakoshi et al. 2014).

The functional neural mechanisms underlying effective task-specific arm/hand interventions in acute and chronic stroke participants with mild impairments support those seen in the animal literature described above. Several variations of task-specific combined arm/hand interventions, including CIMT, bilateral task-specific training, and hand-specific robot-assisted practice, have led to cortical reorganization such as increased sensorimotor activity and enlarged motor maps in the ipsilesional hemisphere related to the paretic arm/hand (Boake et al. 2007; McCombe Waller et al. 2014; Sawaki et al. 2008; Takahashi et al. 2008). These results suggest increased recruitment of residual resources from the ipsilesional hemisphere and/or decreased recruitment of contralesional resources following training. Similarly, individuals who recover well following a stroke exhibit a rebalancing of interhemispheric M1-M1 and intrahemispheric connectivity as their deficits improve (Golestani et al. 2013; Wu et al. 2015), suggesting that changes on a larger network-wide scale also support improved behavior. Although the evidence for a pattern of intervention-driven structural changes remains unclear in humans, several groups have shown increases in gray matter (GM) density in sensorimotor cortices (Gauthier et al. 2008), along with increases in fractional anisotropy in ipsilesional corticospinal tract (CST) (Fan et al. 2015a) following task-specific training in acute and chronic stroke individuals with mild impairments.

The extensive nature of neural damage in moderate to severe chronic stroke may result in compensatory mechanisms, such as contralesional or secondary motor area recruitment (Hamzei et al. 2008). These individuals show increased contralesional activity when moving their paretic arm, which correlates with impairment (Ward 2011) and may be related to the extent of damage to the ipsilesional CST (Stinear et al. 2007). This suggests that more impaired individuals may increasingly rely on contralesional corticobulbar tracts such as the corticoreticulospinal tract to

activate the paretic limb (McPherson et al. 2018a). These tracts lack comparable resolution and innervation to the distal parts of the limb, thus sacrificing functionality at the paretic arm/hand (Baker et al. 2015). Since this population is largely ignored in current arm/hand interventions, it is unknown whether an arm/hand intervention for individuals with more severe impairments will increase recruitment of residual ipsilesional corticospinal resources. These ipsilesional CSTs maintain the primary control of hand and finger extensor muscles (Lawrence and Kuypers 1968) and are thus crucial for improved hand function. Task-specific training assisted by a device may reengage and strengthen residual ipsilesional corticospinal resources by training distal hand opening together with overall arm use.

The current study seeks to determine whether individuals with moderate to severe chronic stroke maintain the ability to undergo cortical reorganization and/or structural changes alongside behavioral improvement following a task-specific intervention. We hypothesize that following a device-assisted task-specific intervention, individuals with moderate to severe chronic stroke will experience functional and structural changes previously observed in individuals with more mild impairments, demonstrated by (i) a shift in cortical activity during movement execution related to the paretic hand/arm from the contralesional hemisphere toward the ipsilesional hemisphere, (ii) complementary changes in cortico-cortico interactions during movement preparation that shape changes in focal activity at movement execution, and (iii) an increase in GM density in sensorimotor cortices in the ipsilesional hemisphere. To test these hypotheses, we examined changes in cortical activity within isolated motor regions at movement execution, dynamic cortical connectivity between motor regions during movement preparation, and structural changes in gray matter following a device-assisted intervention in individuals with moderate to severe chronic

hemiparetic stroke. Through this combined approach, we could observe how the interactions between regions during movement preparation gave rise to any intervention-induced activity changes alongside any changes in gray matter structure. We applied a frequency-based connectivity approach, since regions that synchronize in phase or power at the same frequency (i.e., linear coupling) or across different frequencies (i.e., nonlinear coupling) are considered to be directly or indirectly connected (Fries 2015; Kilner et al. 2002). Additionally, the well-established physiological underpinnings of specific frequency bands within the motor system would provide insight into the underlying neural mechanisms that may be shaping cortical activity at movement execution (Buzsaki and Draguhn 2004; Buzsaki and Wang 2012; Khanna and Carmena 2017; van Wijk et al. 2012). Finally, we examined these changes in relation to both hand opening and hand opening while lifting the arm since effective UE interventions have shown improvements in both hand control and coordination between the shoulder and hand due to a reduced expression of the flexion synergy during functional tasks (Lan et al. 2017; Miller and Dewald 2012; Sukal et al. 2007).

Materials and Methods

Participants

Eight individuals with chronic hemiparetic stroke (age: 63.5 ± 4 yrs.) and moderate to severe impairment (UEFMA: 11–24) participated in this study. Clinical information for each participant is provided in Table 5.1 and lesion locations in Figure 5.1. All individuals were screened for inclusion by a licensed physical therapist. Inclusion criteria include a UEFMA of 30 or below out of 66, no cognitive or perceptual impairment, no botulinum toxin within the last 6 months, MRI compatibility, no lesion including sensorimotor cortices, the ability to elicit enough EMG activity

at wrist/finger extensors, and the ability for the FES to generate a hand opening of at least 4 cm between the thumb and the index finger. This study was approved by the Northwestern University institutional review board, and all participants gave informed consent.

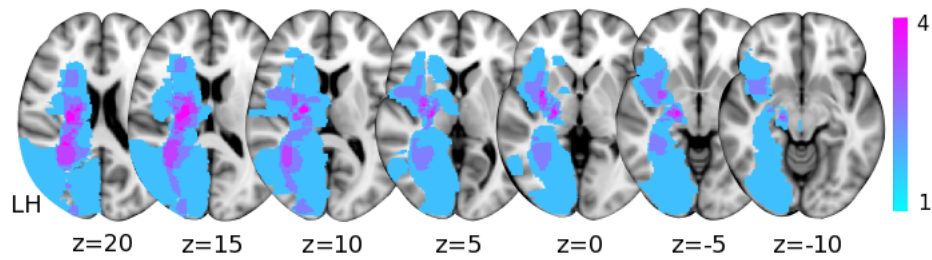


Figure 5.1
Lesion locations for the eight participants overlaid on axial Montreal Neurological Institute T1 slices. The color bar indicates the number of participants with lesioned tissue in a particular voxel.

Experimental Protocols

Intervention

Participants took part in a 7-week intervention consisting of three 2-h visits per week. During the visit, participants completed 20–30 trials of the following sequence of movements: (1) reaching out toward a jar, (2) driving the wrist/finger extensors to open the paretic hand, (3) grabbing the jar, (4) bringing the jar back toward themselves, and (5) releasing the jar. The weight, distance/height, and orientation of the jar relative to the participant were progressively altered to increase the challenge to each participant, as determined by the physical therapist. All participants started the motor task with the arm supported by the table. Depending on ability, participants were encouraged to progressively lift the paretic limb actively. During the task, a novel EMG-FES device, called ReIn-Hand, was used to assist paretic hand opening (see Figure 5.2). This device recorded EMG activities from eight muscles (deltoid, biceps brachii, triceps, extensor communis digitorum, extensor carpi radialis (ECR), flexor digitorum profundus, flexor carpi radialis (FCR), and abductor pollicis). While the user performed the functional reaching and opening, the ReIn-

Hand detected hand opening by extracting EMG features to trigger an Empi transcutaneous electrical neuro-stimulation device (Vista, CA, USA). The stimulation electrodes were applied to the wrist/finger extensors with the following settings: biphasic waveform, frequency = 50 Hz \pm 20%, pulse width = 300 μ s, amplitude = sufficient for maximal hand opening without discomfort (> 4 cm between thumb and index finger), and duration = 3 s. The novelty of this device is that even with the increased expression of the flexion synergy at the elbow (Sukal et al. 2007), wrist, and fingers (Lan et al. 2017; Miller and Dewald 2012) during reaching that is prevalent in this population, the device can still detect the attempted hand opening and drive the paretic hand open, thus allowing for a user-driven stimulation to support functional usage of the paretic hand and arm. All participants could successfully use the device to complete the described task (including opening, grasping, and releasing), although some participants experienced difficulty in sufficiently supinating the hand when releasing the jar to keep it upright on the table. Additionally, the physical therapist stretched the hand and arm at the beginning of the experiment and between trials to effectively elicit hand openings with the EMG-FES device.

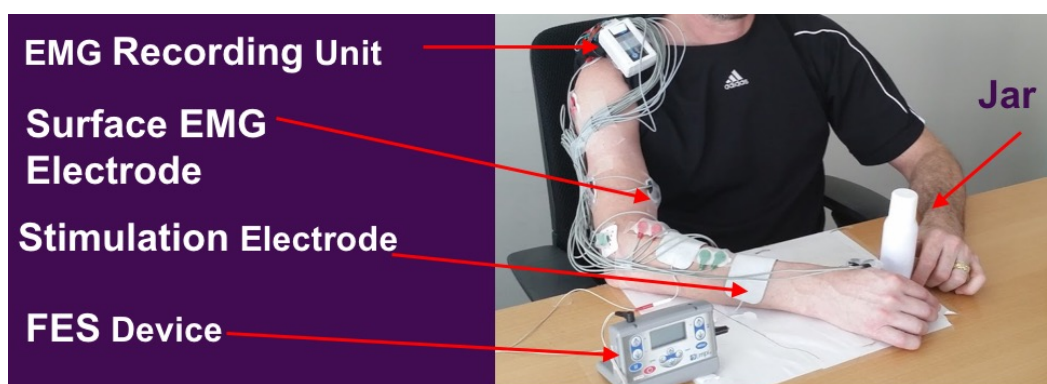


Figure 5.2
Depiction of ReIn-Hand device.

Pre- and Post-Intervention Tests

Clinical Assessments

For each participant, within 1 week prior to and following the intervention, a licensed physical therapist completed a set of clinical assessments, with the motor-related tests including UEFMA, Box and Blocks Test (BBT), and active range of motion (AROM) averaged over the II and V digit.

Structural Imaging of the Brain

Within 2 weeks prior to and following the intervention, participants took part in MRI scans at Northwestern University's Center for Translation Imaging on a 3 TS Prisma scanner with a 64-channel head coil. Structural T1-weighted scans were acquired using an MP-RAGE sequence (TR = 2.3 s, TE = 2.94 ms, FOV 256 mm × 256 mm) producing an isotropic voxel resolution of 1 mm × 1 mm × 1 mm. Visual inspection of acquired images was performed immediately following the data acquisition to guarantee no artifacts and stable head position.

Functional Imaging Related to Hand Opening

Participants took part in an EEG experiment within one week prior to and following the intervention. Participants sat in a Biodex chair (Biodex Medical Systems, Shirley, NY) with straps crossing the chest and abdomen to limit potential trunk movements. The participant's paretic arm was placed in a forearm-hand orthosis attached to the end effector of an admittance controlled robotic device (ACT^{3D}) instrumented with a six degree of freedom (DOF) load cell (JR³ Inc., Woodland, CA). At the beginning of each trial, participants moved their hand to a home position, with the shoulder at 85° abduction, 40° flexion, and the elbow at 90° flexion angle. The participant received an auditory cue once they reached the home position. Following the cue, the participant relaxed at the home position for 5-7 s and then self-initiated one of 2 movements: 1) maximum paretic hand opening with the arm resting on a haptic table, or 2) maximum paretic hand opening while lifting against 50% of their maximum shoulder abduction (SABD) torque. This shoulder

abduction level was used since it is roughly equivalent to the weight of the limb in this population, thus making it a functionally relevant shoulder abduction level for translation to many activities of daily living that require simultaneously using the hand while lifting the arm. Participants were instructed to avoid eye movements by focusing on a point and movements of other body parts during the performance of each trial, which was confirmed by electrooculogram (EOG) traces and visual inspection by the experimenter, respectively. Participants performed 60-70 trials of each condition, which were separated into blocks (one block consisted of 20-30 trials of a particular condition). Blocks were randomized to minimize any order effects. Rest periods varied between 15 to 60 seconds between trials and 10 minutes between blocks.

Scalp recordings were made with a 160-channel High Density EEG system using active electrodes (Biosemi, Inc., Active II, Amsterdam, The Netherlands) mounted on a stretchable fabric cap based on a 10/20 system. The impedance was kept below 50 k Ω for the duration of the experiment. Simultaneously, EMGs were recorded from the extensor carpi radialis, flexor carpi radialis, and deltoid of the paretic arm, which were used to detect movement onset for post-processing purposes. All data were sampled at 2048 Hz. Additionally, the positions of EEG electrodes on the participant's scalp were recorded with respect to a coordinate system defined by the nasion and pre-auricular notches using a Polaris Krios handheld scanner and reflective markers (NDI, Ontario, Canada). This allowed for coregistration of EEG electrodes with each participant's anatomical MRI data.

Data Analysis

Reorganization of Cortical Activity Related to Movement Execution

EEG data were aligned to the earliest EMG onset of the 3 muscles and segmented from -2200 to +200 ms (with EMG onset at 0 ms) using Brain Vision Analyzer 2 software (Brain Products, Gilching, Germany). Data were then visually inspected for the presence of artifacts. Trials exhibiting artifacts (e.g., eye blinks) were eliminated from further analysis. The remaining EEG trials were baseline-corrected (from -2180 to -2050 ms), low pass filtered at 70 Hz, and ensemble-averaged. The averaged EEG signals were down-sampled to 256 Hz and imported into CURRY 6 (Compumedics Neuroscan Ltd., El Paso, TX). The cortical current density strength ($\mu\text{A}/\text{mm}^2$) from 150 ms to 100 ms prior to EMG onset was computed using the standardized low-resolution electromagnetic brain tomography (sLORETA) method ($L_p = 1$) based on a subject-specific boundary element method model with the regulation parameter automatically adjusted to achieve more than 99% variance accounted for. Possible sources were located on a cortical layer with 3 mm distance between each node. Although the inverse calculation was performed over the whole cortex, only the activity in the specific regions of interest (ROIs) was further analyzed. These ROIs included bilateral primary sensorimotor cortices (primary motor cortex (M1) + primary somatosensory cortex (S1)) and secondary motor cortices (supplementary motor area (SMA) + premotor area (PM)).

To investigate the shift of cortical activity related to hand opening, we used the estimated current density strengths to calculate a laterality index [$LI = (I - C)/(I + C)$], where I and C are the current density strengths from the ipsilesional and contralesional sensorimotor cortices, respectively (i.e., combined primary sensorimotor and secondary motor cortices). LI reflects the relative contributions of each cerebral hemisphere to the source activity, with a value close to +1 for an ipsilesional source distribution and -1 for a contralesional source distribution.

Additionally, we quantified a cortical activation ratio $CAR = \frac{\sum_1^N s_n}{\sum_1^M s_m}$ for each of the 4 ROIs, where s_n represents the current density strength of the n^{th} node, and N and M are the number of nodes in a specific ROI and the whole sensorimotor cortices, respectively. The cortical activity ratio reflects the relative strength from one ROI as normalized by the total combined strength of the 4 ROIs.

Dynamic causal modeling for induced responses

We used dynamic causal modeling for induced responses (DCM-IR) (Chen et al. 2008) to model the task-related time-varying changes in power both within and across a range of frequencies by estimating the coupling parameters within and between sources in a network. This approach has been used in previous hand movement tasks to elucidate the dynamic interactions within a motor network (Bonstrup et al. 2015; Chen et al. 2010; Loehrer et al. 2016).

Definition of model space

Our motor network model consisted of 5 ROIs, including bilateral primary motor cortex (M1), bilateral premotor cortex (PM), and supplementary motor area (SMA). Locations of each of these regions were adapted from the Human Motor Area Template (HMAT) (Mayka et al. 2006) and are shown in Table 5.2. Bilateral primary somatosensory cortices were not included to reduce the computational demand and complexity of the model. Bilateral SMAs were treated as a single source due to their mesial position on the cortices. SMA also served as the input to the modelled network. It was chosen due to its critical role in movement preparation during self-initiated motor tasks (Jahanshahi et al. 1995; Jenkins et al. 2000), and has previously been found to be an appropriate input for self-initiated motor tasks using DCM-IR (Bonstrup et al. 2015; Chen et al. 2010; Loehrer et al. 2016).

Different within- and cross-frequency connections between these 5 sources were used to create 12 models as shown in Figure 5.3 which have successfully been used before in a similar motor task in healthy controls (Chen et al. 2010). These 12 models were separated into 2 groups. Group 1 (models 1 to 6) allowed nonlinear and linear extrinsic (between region), but only linear intrinsic (within region) connections. Group 2 (models 7 to 12) allowed both nonlinear and linear connections for both extrinsic and intrinsic connections. Within each group, the 6 models consisted of 1 fully connected model, and the other 5 models missing 1 or 2 connections that were from one premotor area (PM) to either the other PM or to M1. Using this model, we tested the importance of nonlinear frequency interactions within regions as well as the importance of various connections to premotor regions.

Table 5.1. Participant Demographics and Clinical Characteristics

Subject	Age Range	Time Since Stroke (yrs.)	Lesioned Hemi	Lesion Location	UE FMA	Pre BBT	Post BBT	Pre AROM (°)	Post AROM (°)
S01	60-65	9	L	IC	23	0	6	-20	11
S02	60-65	8	R	IC, BG	12	1	3	0	5
S03	65-70	3	R	Par, Occ, IC	17	0	1	0	0
S04	60-65	22	R	IC, BG, Thal	11	0	1	0	17.5
S05	60-65	13	R	Occ, IC	24	0	0	0	2.5
S06	70-75	20	L	IC, BG, Thal	13	0	0	0	1.5
S07	55-60	6	L	IC, BG	24	0	3	0	5
S08	60-65	9	L	IC, Thal	22	11	13	38.5	55

Note: AROM=Active Range of Motion, BBT=Blocks and Box Test, BG=basal ganglia, FMA=Fugl-Meyer Assessment, IC=Internal Capsule, Occ=Occipital Lobe, Par=Parietal Lobe, Thal=Thalamus, UE=Upper Extremity.

Table 5.2. Coordinates of Motor Network

Sources	MNI-Coordinates (X,Y,Z)
Left M1	-37 -26 60

Right M1	37 -26 60
Left PM	-35 -4 60
Right PM	35 -4 60
SMA	-2 -7 60

Note: Coordinates were adapted from Mayka et al., 2006

DCM Preprocessing

EEG data were preprocessed using SPM12 (SPM12, Wellcome Trust Centre for Neuroimaging, www.fil.ion.ucl.ac.uk/spm/) in the same manner, as described in section 2.5, up until trial averaging. Artifact free trials were projected from channel space to the sources using the generalized inverse of the lead-field matrix using an equivalent current dipole for our chosen sources (see below) (Chen et al. 2008). The spectrogram from 4 to 48 Hz at each source was computed using a Morlet wavelet transform (wavelet number: 7). This range includes theta (4-7 Hz), mu (8-12 Hz), beta (13-30 Hz), and gamma (31-48 Hz) frequencies. The spectrogram was then averaged over all trials, cropped between -1000 to 0 ms, and then baseline-corrected by subtracting the frequency-specific power of the first 1/6 samples of the time window (-1000 to -833 ms). The input from SMA to the whole network was modelled as a gamma function with a peak at 400 ms prior to EMG onset with a dispersion of 400 ms. These values were chosen in order to capture the peak of the *bereitschaftspotential* during a self-initiated movement (Shibasaki and Hallett 2006). The model simulation was restricted to the time leading up to EMG onset (-1000 to 0 ms) to capture purely the motor preparation and command, rather than any potential sensory feedback related to the task. The dimensionality of the spectrogram was then reduced to four modes using singular value decomposition (SVD). The four modes preserved > 96% of the data variance

on average. This dimensionality reduction both reduced the computational demand of the model inversion and denoised the data.

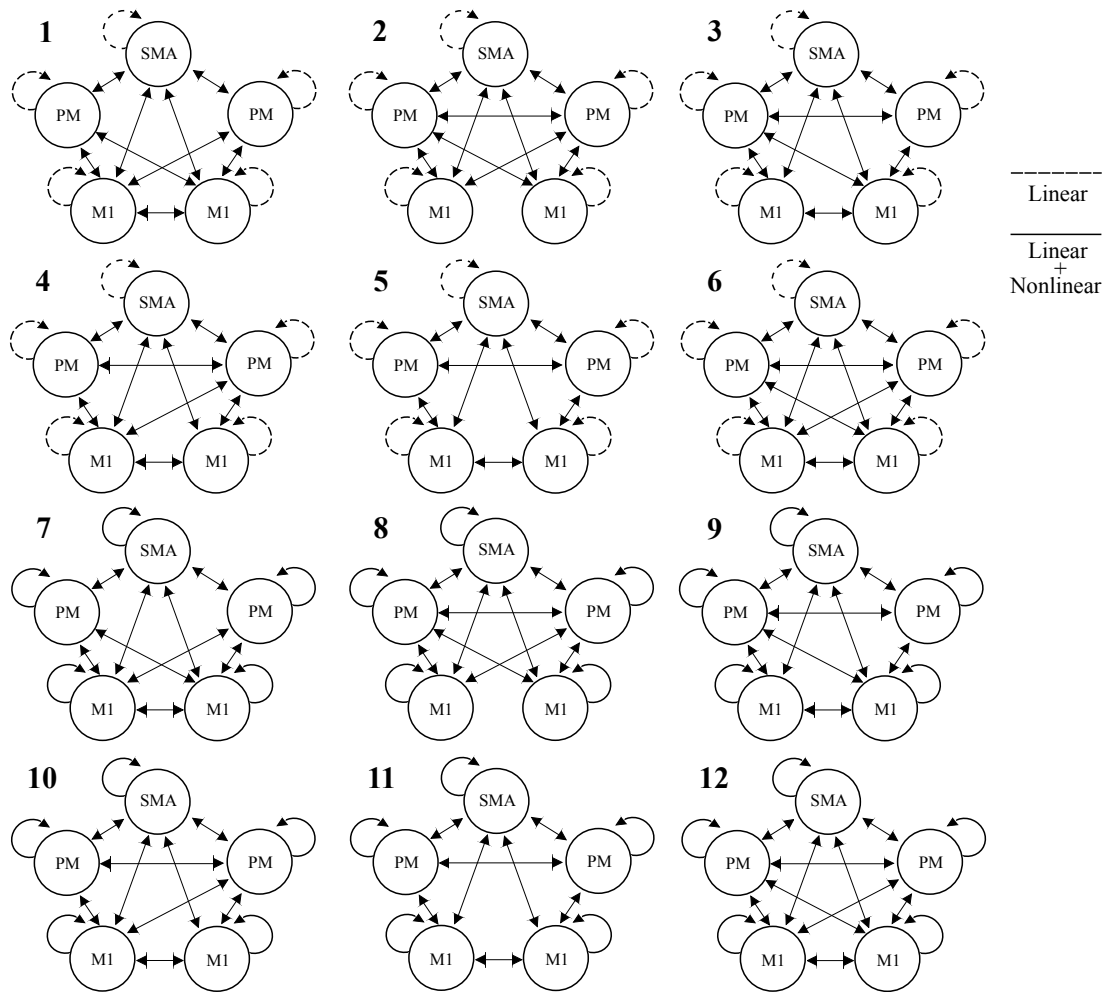


Figure 5.3

Models tested for DCM analysis. Models 1-6 allow only linear intrinsic connections and both nonlinear and linear extrinsic connections, while Models 7-12 allow both nonlinear and linear intrinsic and extrinsic connections. Individual models differ in interhemispheric connections allowed between M1 and PM regions. Dashed lines indicate only linear connections allowed, while solid lines indicate both linear and nonlinear connections allowed. The left side is the lesioned side.

Calculation of coupling parameters

For each of the models shown in Figure 5.3, the dynamics of the spectrogram were evaluated using the following equation for each model described above:

$$\tau \dot{g}(t) = \tau \begin{bmatrix} \dot{g}_1 \\ \vdots \\ \dot{g}_J \end{bmatrix} = \begin{bmatrix} A_{11} & \dots & A_{1J} \\ \vdots & \ddots & \vdots \\ A_{J1} & \dots & A_{JJ} \end{bmatrix} g(t) + \begin{bmatrix} C_1 \\ \vdots \\ C_J \end{bmatrix} u(t),$$

where vectors g and \dot{g} represent the instantaneous power and its first derivative at each of the modes (results of SVD) for each of the sources in the motor network. The A matrix contains the coupling parameters within and across different modes between any 2 regions within the $J=5$ regions, and the C matrix contains the weights of the extrinsic input u from SMA. Each of the elements in the coupling A matrix refers to the influence of power at a specific frequency in one motor region on the power at another frequency in another region. Positive (i.e. excitatory) or negative (i.e. inhibitory) coupling suggests changes in power in the first frequency and region are associated with the same directional or opposite change, respectively, in power in the second frequency and region. τ is a scaling factor and t represents time. Using the above equation and the output of the SVD, the DCM-IR method optimizes the A and C matrices to best describe the spectrogram of the measured data. The quality of a model and the estimated A and C matrices was quantified by the accounted variance from the predicted spectrogram.

Bayesian model selection

We performed Bayesian model selection (BMS) with random effects (Stephan et al. 2009) on the 12 models described above for both the hand opening and the simultaneous lifting and opening conditions using the data from all of the participants to assess which model best explained the observed data. BMS with random effects was chosen since it is better equipped to handle potential heterogeneity associated with the study of a diseased population such as stroke (Stephan et al. 2009), and it contains a complexity term that penalizes a model based on the number of parameters it uses. The winning model, which was then used for further analysis of intervention-induced

changes, was chosen based on the highest posterior exceedance probability (i.e. the probability that a given model is more likely than any of the other models tested).

Inference on coupling parameters

Predicted spectra and A matrices from the four modes were projected back to frequency domain allowing for characterization of the coupling parameters as a function of frequency for the winning model. The coupling matrices for each intrinsic and extrinsic connections in the winning model for each participant were further smoothed with a Gaussian kernel (full-width half-maximum of 8 Hz) for each condition. These matrices include the frequency-to-frequency (both within- and cross-frequency) coupling values for each connection.

Structural Changes in GM Density

Anatomical T1 data were analyzed with FSL-voxel-based morphometry (VBM) 1.1 (<https://fsl.fmrib.ox.ac.uk/fsl/fslwiki/FSLVBM>; Oxford University, Oxford, United Kingdom) (Douaud et al. 2007) using FSL tools (Smith et al. 2004). First, T1 images for participants who have left hemisphere lesions were flipped to ensure that the lesions of all participants were in the right hemisphere. The T1 images were then brain-extracted using the Brain Extraction Tool and segmented into GM using FAST4. The resulted GM partial volume images were aligned to Montreal Neurological Institute (MNI) 152 standard space using the affine registration tool FLIRT and averaged to create a study-specific GM template. Subsequently, individual GM partial volume images in native space were non-linearly registered to this template using FNIRT, modulated to correct for local expansion or contraction due to the non-linear component of the spatial transformation, and then smoothed with an isotropic Gaussian kernel with a sigma of 3 mm.

Statistical Analysis

Statistics were performed using a combination of SPSS (IBM, V24), MATLAB 2017b, and FSL. Clinical and neural measures were examined for normality using a Shapiro–Wilk test. A Wilcoxon signed rank test was used if assumptions of normality were not met. A paired t-test was performed on LI. A 2 (time) x 2 (task) x 4 (region) repeated measures ANOVA was performed on the cortical activity ratio after checking the data did not violate Mauchly’s sphericity test. We performed post-hoc paired t-tests when a main ANOVA effect or interaction was found. Significance was set a $p < .05$. Individual data are depicted for significant findings. To assess intervention-induced changes in coupling parameters, T-statistics were used to calculate statistical parametric maps separately for each connection and condition pre/post intervention. Significance for intervention-induced changes in specific coupling parameters was set at $p < 0.05$ with family wise error (FWE) correction. Finally, to detect intervention-induced changes in GM density, a voxel-wise General Linear Model was applied with Threshold-Free Cluster Enhancement (Winkler et al. 2014). Voxel-based threshold of changes in GM density was set at $p < 0.001$ uncorrected.

Results

Changes in arm/hand function following EMG-FES task-specific training

Table 5.1 shows BBT and AROM scores before and after the intervention. Notably, most participants initially scored a 0 on the pre-assessment BBT and had 0° of AROM due to the severity of their motor impairments at the arm/hand. The clinical data violated the assumptions of normality based on the Shapiro–Wilk test. Therefore, a Wilcoxon signed rank test was used and reported a significant increase in BBT following the intervention (average increase of 1.9 blocks per minute,

$p = 0.03$; Table 5.1) and AROM (average increase of 9.9° , $p = 0.03$; Table 5.1), indicating improvement of paretic arm/hand control, although FMA did not change.

Cortical reorganization related to the hand and arm

Figure 5.4A shows an example of ensemble-averaged EEG for the 160 channels for Participant 1. There is a stable baseline from roughly -2 to -1.5 s prior to EMG onset and then a slow increase in electrical potential when approaching EMG onset, consistent with the Bereitschaftspotential. The cortical activity for Participant 1 while performing hand opening on the table is depicted in Figure 5.4B before the intervention and in Figure 5.4C after the intervention. This participant had bilateral activity in sensorimotor cortex prior to the intervention as seen in Figure 5.4B and dominant ipsilesional activity following the intervention as seen in Figure 5.4C. We quantified the pre- and post-intervention LI in each of the participants (see results in Figure 5.5). Paired t-tests found a significant increase in LI following the intervention for both hand opening [$t(7) = 3.09$, $p = 0.02$] and lifting and opening [$t(7) = 4.85$, $p = 0.002$], signifying a post-intervention shift toward the ipsilesional hemisphere for both tasks.

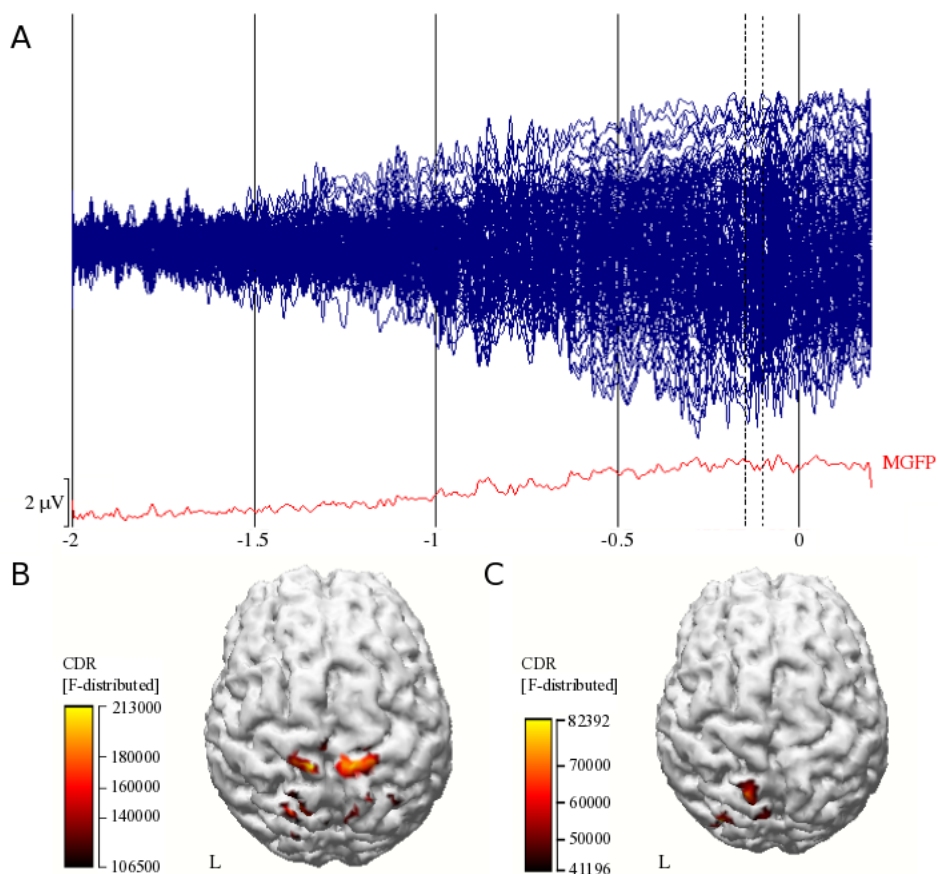


Figure 5.4

(A) Ensemble-averaged EEG of the 160 channels (blue butterfly plot) and Mean Global Field Power (MGFP; red line) from -2 s to +0.2 s (0 = EMG onset). Vertical dashed lines represent the start and end of the window of interest (-150 to -100 ms). A scale bar is included in the lower left; (B) reconstructed cortical activity between -150 and -100 ms prior to movement onset for Subject 1 during hand opening pre-intervention, and (C) post-intervention. Color bars indicate the current density reconstruction (CDR) statistic from sLORETA. Left hemisphere is the lesioned hemisphere.

To further investigate regions responsible for the post-intervention LI changes, we quantified the pre- and post-intervention cortical activity ratios for primary sensorimotor (M1/S1) and secondary motor cortices (SMA/PM) related to movement execution. A 2 (time) x 2 (task) x 4 (region) repeated measures ANOVA found a significant Time * Task ($F[1,7] = 8.03, p = 0.025$) and Time * Region ($F[3,21] = 4.64, p = 0.012$) interaction. Post hoc paired t-tests found that following the intervention there was a significant decrease in the cortical activation in contralesional M1/S1 ($p = 0.042$) during hand opening and a trending increase in activity in ipsilesional SMA/PM ($p =$

0.06; See Figure 5.6A). For the simultaneous lifting and opening condition, a significant increase in cortical activation in ipsilesional M1/S1 ($p = 0.025$) was observed (See Figure 5.6B).

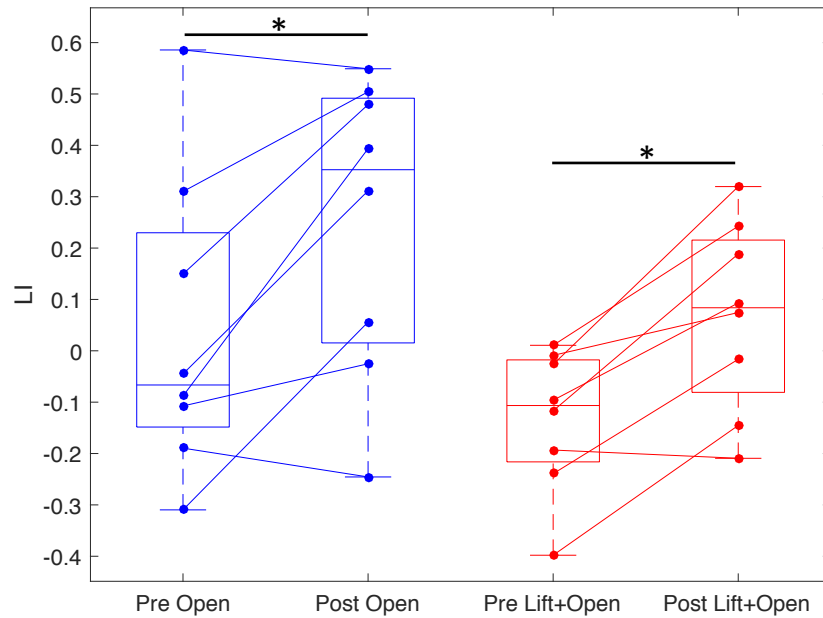


Figure 5.5

Box plots of laterality index (LI) prior to and following the intervention for paretic hand opening (blue; left) and paretic lifting and opening (red; right). Positive LI indicates predominantly ipsilesional activity. * indicates $p < 0.05$.

Bayesian model selection and model fit

In order to determine any intervention-induced changes in connectivity, we first had to evaluate which DCM model tested best explained the observed data. BMS with random effects clearly preferred model 12 for each condition (see Table 5.3), which had full connections between the 5 motor regions of interest and allowed both within- and cross-frequency interactions for intrinsic and extrinsic connections. Exceedance probabilities were .973 for the opening condition and .975 for the simultaneous lifting and opening condition. Figure 5.7 depicts both the observed and predicted spectrograms in each of the 5 motor regions using the winning model for one participant during the hand opening condition. Comparison of these two spectrograms shows the overall similarity between the observed data (i.e., power changes over time) and the model-predicted data.

Overall, this model explained ~85% of the original spectral variance for each condition, indicating that it was suitable for evaluating any intervention-induced changes.

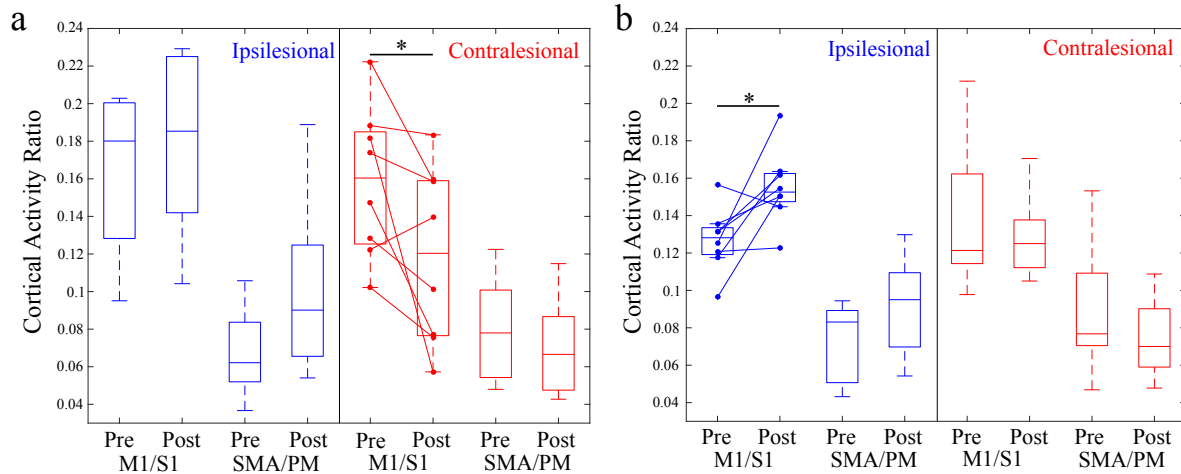


Figure 5.6

Box plots depicting cortical activity ratio Pre/Post Intervention for (A) hand opening on the table and (B) hand opening while lifting. Regions include combined primary motor cortex and primary somatosensory cortex (M1/S1) and combined supplementary motor area and premotor area (SMA/PM) for both the ipsilesional (Blue) and contralesional (Red) hemispheres. Participants demonstrated a decrease in contralesional primary sensorimotor cortex activity for hand opening following the intervention (left) and an increase in ipsilesional primary sensorimotor cortex activity for hand opening while lifting following the intervention (right). * indicates $p < 0.05$.

Table 5.3. Exceedance probabilities for each model

Models	Open	Lift + Open
1	0.0018	0.0022
2	0.002	0.0024
3	0.0028	0.0017
4	0.0023	0.0022
5	0.0021	0.0013
6	0.0022	0.002
7	0.0056	0.0029
8	0.0021	0.0037
9	0.0019	0.0026
10	0.0021	0.0024
11	0.0025	0.0018
12	0.9726	0.9748

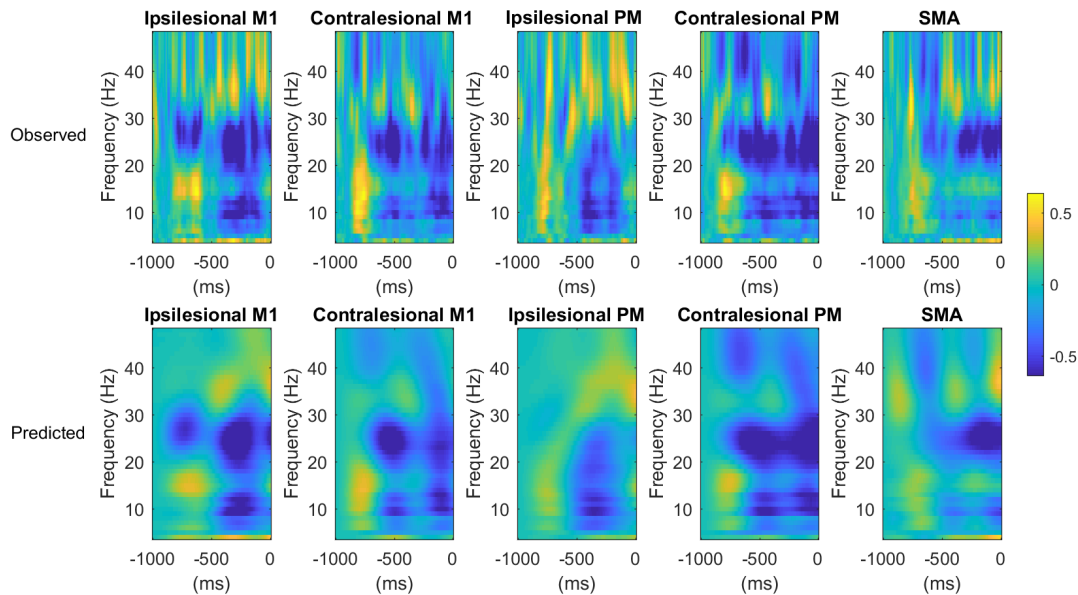


Figure 5.7

The observed (top) and model-predicted (bottom) time-frequency plots for each region for one participant using the winning model (Model 12). Yellow indicates an increase in power compared to baseline and blue indicates a decrease in power compared to baseline. 0 ms indicates movement onset. Overall, the model explained ~85% of the original spectral variance for each condition.

Intervention-induced changes in coupling parameters

Once we determined the model that best explained the observed data, we examined whether any intervention-induced changes in connectivity for any of the region-region connections occurred. We found that the intervention induced two significant changes in the coupling parameters, one for each motor task. After the intervention, participants had significantly less excitatory coupling from ipsilesional M1 to contralesional M1 in gamma frequencies (47 Hz \rightarrow 36 Hz) during hand opening (see Figure 5.8A). When looking at the individual coupling values for this particular regional coupling, we found that prior to the intervention, 6 out of 8 participants had positive coupling values, indicating that increases in gamma in ipsilesional M1 were associated with increases in gamma in contralesional M1 (see Figure 5.8B). However, following the intervention, 5 out of 8 participants showed zero or negative coupling, indicating that increases in gamma in

ipsilesional M1 no longer were associated increases in gamma in contralesional M1 (see Figure 5.8B).

For the task of simultaneous lifting and opening, the intervention induced significantly more negative or inhibitory coupling within ipsilesional M1 from gamma to beta (44 Hz → 25 Hz) (see Figure 5.8C). When looking at the individual coupling values for this particular regional coupling, we found that prior to the intervention, 6 out of 8 participants showed positive coupling values, indicating that increases in gamma power within ipsilesional M1 were associated with subsequent increases in beta power also within ipsilesional M1 (see Figure 5.8D). However, following the intervention, 7 out of 8 participants showed negative or inhibitory coupling, indicating that increases in gamma power within ipsilesional M1 were associated with subsequent decreases in beta power within ipsilesional M1 (see Figure 5.8D).

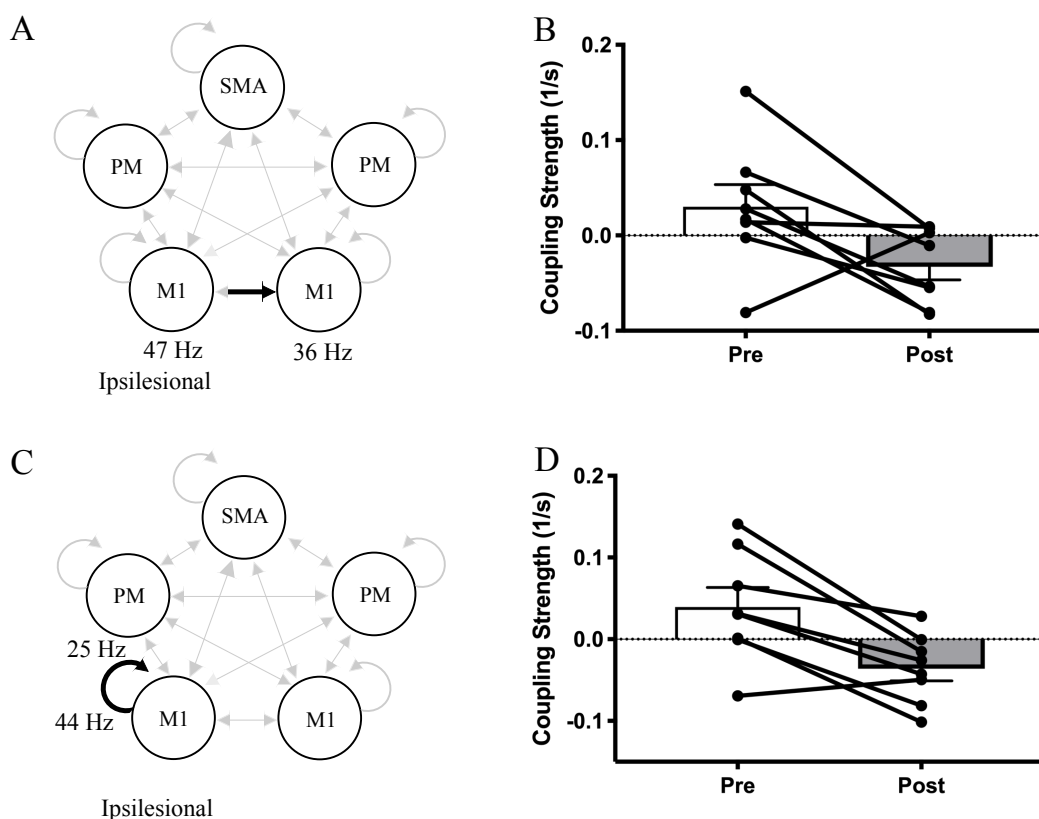


Figure 5.8

Intervention-Induced Motor Network Coupling Changes. (A) Schematic of significant decreases in coupling (black) from ipsilesional M1 (47 Hz) to contralesional M1 (36 Hz) within the motor network (light gray) following the intervention for Hand Opening. None of the other region interactions (light gray arrows) showed significant changes pre to post intervention. (B) Individual coupling strength data pre/post intervention for the connection depicted in A. 6 out of 8 subjects demonstrated a reduction in coupling strength for this M1-M1 connection within gamma frequencies. (C) Schematic of significant decreases in intrinsic coupling (black) in ipsilesional M1 (44 Hz to 25 Hz) within the motor network (light gray) following the intervention for Hand Opening while Lifting. None of the other region interactions (light gray arrows) showed significant changes pre to post intervention. (D) Individual coupling strength data pre/post intervention for the connection depicted in C. 7 out of 8 subjects demonstrate negative coupling within ipsilesional M1 from gamma to beta frequencies following the intervention. Positive values indicate excitatory coupling, while negative values indicate inhibitory coupling.

Intervention-induced changes in gray matter density

Following the intervention, we found that participants had significantly increased GM density in M1 and S1 in the lesioned hemisphere ($x = 52, y = -16, z = 30, t\text{-value} = 2.55, p < 0.001$) and decreased GM density in M1 and S1 in the non-lesioned hemisphere ($x = -46, y = -20, z = 60, t\text{-value} = 2.41, p < 0.001; x = -44, y = -18, z = 36, t\text{-value} = 2.79, p < 0.001$) as depicted in Figure 5.9A/B. Additionally, participants had increased GM density in the thalamus in the lesioned

hemisphere ($x = 2, y = -20, z = 10, t\text{-value} = 3.13, p < 0.001$) as shown in Figure 5.9C. A complete list of significant regions is provided in Table 5.4.

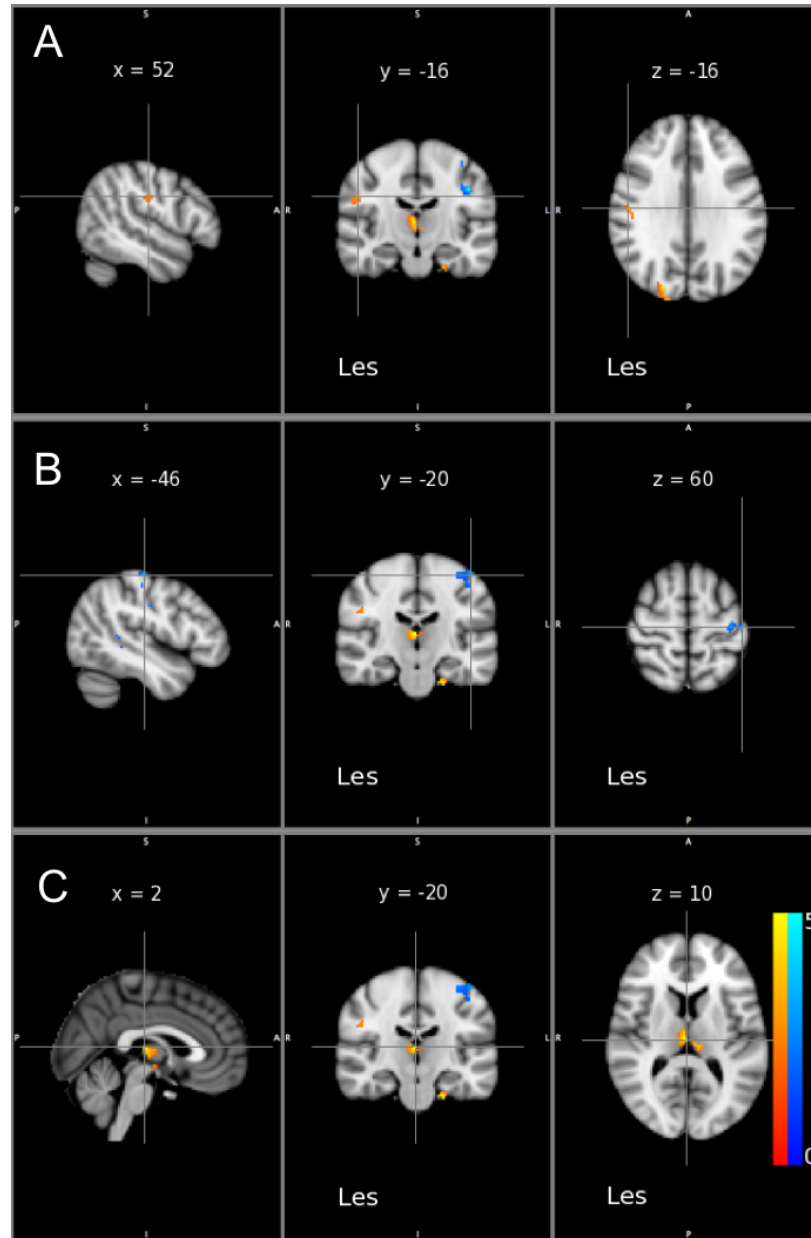


Figure 5.9

Statistical maps of gray matter (GM) density changes across all patients. Significant increases (red/yellow) and decreases (Blue) in GM density following the intervention are depicted on sagittal, coronal, and axial sections (left to right) on Montreal Neurological Institute T1 slices. Sections show the maximum effect on (A) ipsilesional M1/S1, (B) contralesional M1/S1, and (C) ipsilesional thalamus. Les indicates the side of the lesioned hemisphere. Color maps indicate the t values at every voxel. A statistical threshold was set at $p < 0.001$ uncorrected.

Table 5.4. Brain regions exhibiting changes in Gray Matter Density

	Brain Region	Peak Voxel MNI: x, y, z (mm)	<i>t</i>	Cluster Size (voxels)
Pre > Post	L Superior Parietal Lobule	24, -52, 44	3.02	115
	NL Postcentral Gyrus	-46, -20, 60	2.41	82
	NL Frontal Orbital Cortex	-22, 24, -24	3.61	63
	NL Precentral Gyrus	-44, -18, 36	2.79	52
Post > Pre	L Thalamus	2, -20, 10	3.13	249
	L Occipital Cortex	22, -84, 30	2.58	112
	L Temporal Pole	24, 12, -32	3.33	92
	NL Hippocampus	-22, -20, -32	3.02	70
	L Postcentral Gyrus	52, -16, 30	2.55	41

Note: L = Lesioned Hemisphere; NL = Non-Lesioned Hemisphere; t = t-value

Discussion

The present study investigated neural changes in individuals with moderate to severe stroke following an EMG-FES-assisted task-specific arm/hand intervention. Specifically, we found a shift of sensorimotor cortical activity related to both hand opening and hand opening while lifting from contralesional to ipsilesional cortex, along with structural changes in the form of increased ipsilesional M1/S1 and decreased contralesional M1/S1 GM density. Although similar device-assisted hand/arm training in this population has been investigated before to examine behavioral improvements (Klamroth-Marganska et al. 2014; Lo et al. 2010; Platz et al. 2009), this study provides evidence for corresponding neural changes even in this more severe chronic population.

Shift Toward Ipsilesional Hemisphere

As expected, before the intervention, participants showed cortical activity predominantly from the contralesional hemisphere related to both paretic hand opening in isolation and hand opening while simultaneously lifting at the shoulder, as reflected by the overall negative LI. The initial contralesional activity may suggest an increased reliance on low-resolution contralesional

corticobulbar pathways such as the corticoreticulospinal tract (Baker et al. 2015; Yao et al. 2009) for general paretic arm function. In fact, participants with more severe impairments actually tend to involuntarily close the hand and activate shoulder muscles when asked to open (Lan et al. 2017), which may reflect this increased reliance on ipsilateral corticobulbar pathways that innervate primarily flexor hand and proximal muscles compared to extensors (Zaaimi et al. 2012). These pathways lack sufficient innervation to extensor muscles of the hand to produce appropriate hand opening (Baker 2011) and are often associated with greater motor impairment (Baker et al. 2015; McPherson et al. 2018a).

Effective hand/arm interventions in individuals with mild impairments following a stroke have reported a post-intervention shift toward ipsilesional sensorimotor areas (Askim et al. 2009; Michielsen et al. 2011). This shift is thought to be a beneficial since it may indicate increased use of ipsilesional CSTs, which maintain the primary innervations to the extensor muscles of the hand (Lawrence and Kuypers 1968). Intervention-induced shifts toward the ipsilesional hemisphere have rarely been investigated in individuals with more severe impairments following a stroke, especially not for arm/hand training partially due to the lack of inclusion of these participants in arm/hand interventions. In this study, we found that a ReIn-Hand-assisted arm/hand intervention induced a positive change in LI for both hand opening in isolation and hand opening while simultaneously lifting at the shoulder. Our results suggest that even moderate to severe chronic stroke participants maintain the ability to show similar cortical reorganization back toward the ipsilesional hemisphere following task-specific training as seen in more mild participants. This ipsilesional shift may suggest decreased recruitment of contralesional corticobulbar pathways and increased reliance on ipsilesional CSTs during paretic hand opening, which may allow for greater

functionality at the hand as seen by the increase in BBT and AROM. Additionally, it could reflect increased ability to actually drive hand opening when instructed rather than involuntary closing and activating proximal muscles (Lan et al. 2017). It is worth noting that only six out of eight participants exhibited this intervention-induced shift despite all showing improvements on either BBT or AROM, possibly reflecting compensatory behavioral strategies following the intervention rather than recovery in these two participants.

Changes in Cortical Activity Driving LI Shift

We calculated the cortical activity ratio in each sensorimotor region to further elucidate which regions were contributing to the LI shift. Following the intervention, participants showed decreased activity in contralesional primary sensorimotor cortex (M1/S1) and a trending increase in ipsilesional secondary motor cortex (SMA/PM) for paretic hand opening.

Increased contralesional primary sensorimotor cortex activity is associated with greater impairment following stroke (Calautti et al. 2007; Ward et al. 2003) and greater damage to CST (Schaechter et al. 2008; Ward et al. 2006). Therefore, this decreased activity could reflect either decreased recruitment of contralesional descending motor pathways or changes in interhemispheric balance between primary sensorimotor cortices (Grefkes and Fink 2011) and thus allow for increased functional use of the affected hand.

Stroke patients tend to activate secondary motor areas more following greater CST damage (Ward et al. 2006) and there is a positive correlation between ipsilesional secondary motor area activation and recovery (Hubbard et al. 2015; Johansen-Berg et al. 2002a). The trend towards increased

recruitment of ipsilesional SMA/PM may be due to increased recruitment of direct projections to the spinal cord (Macpherson et al. 1982), although these connections are not as efficacious as connections from M1 to the spinal cord (Maier et al. 2002). Alternatively, plasticity within intrinsic cortico-cortico neuronal connections in M1 (Sanes and Donoghue 2000) may allow increased communication between SMA/PM and M1 following injury. Thus, ipsilesional secondary motor areas may serve as a potential avenue for functionally relevant cortical reorganization via either descending or intrinsic connections in addition to removal of contralesional cortical activity.

In addition to the observed intervention-induced decrease in activity in contralesional primary sensorimotor cortex during paretic hand opening, we further found that following the intervention, these individuals had a reduction in coupling from ipsilesional M1 to contralesional M1 within gamma frequencies.

In healthy controls, gamma band power increases in contralateral primary sensorimotor cortex just before the onset and during movement (Ball et al. 2008; Cheyne et al. 2008; Crone et al. 1998a; Igarashi et al. 2013; Szurhaj et al. 2006; Yanagisawa et al. 2012). This increase in gamma power has been shown to facilitate movement in studies using transcranial alternating current stimulation (tACS) to artificially increase gamma power over the contralateral primary sensorimotor cortex (Joundi et al. 2012; Moisa et al. 2016; Nowak et al. 2017). Typically, gamma is associated with local intracortical processing, particularly within GABAergic interneuronal circuits (Bartos et al. 2007; Kopell et al. 2000), with increases in gamma power related to movement associated with decreases in GABA_A (Nowak et al. 2017). However, gamma synchronization is usually confined to a small area in the contralateral primary sensorimotor cortex in controls (Ball et al. 2008; Cassim

et al. 2001; Cheyne et al. 2008), rather than bilateral increases in gamma during movement as observed here prior to the intervention.

Before the intervention, individuals with severe chronic stroke showed positive gamma coupling (as seen by the positive coupling shown in Figure 5.8B) from ipsilesional M1 to contralesional M1. This abnormal initial positive gamma coupling between ipsilesional and contralesional M1 may indicate abnormal intercortical communication between the two hemispheres (via callosal or subcortical means (Gerloff et al. 1998)) and may give rise to the initial increased contralesional activity in these individuals. This is supported by previous findings in stroke showing weaker GABAergic inhibition from the ipsilesional to the contralesional hemisphere following stroke (Butefisch et al. 2008; Liepert et al. 2000; Murase et al. 2004; Nair et al. 2007), and that this imbalance is associated with greater abnormal contralesional activity during paretic hand movements (Cunningham et al. 2015).

Following the intervention, we found that the abnormal interhemispheric gamma coupling decreased in 6 out of 8 participants (see Figure 5.8B), which may be connected to the intervention-induced reduction in contralesional activity in the primary sensorimotor cortex (see Figure 5.6A). The intervention-induced decrease in positive gamma coupling between ipsilesional and contralesional M1 may underlie the subsequent decrease in CAR in contralesional primary sensorimotor cortex and reflect a return to a more normal state as observed in healthy controls.

For the simultaneous lifting and opening task, we observed increased ipsilesional primary sensorimotor activity following the intervention. This focal activity change during the lifting and

opening task was supported by an altered coupling, in which the intervention induced a shift from positive to negative coupling between gamma and beta within ipsilesional M1 (see Figure 5.8D). This intervention-induced change in cross-frequency coupling is particularly relevant since gamma and beta power are typically inversely related in healthy controls during movement (van Wijk et al. 2012). Whereas gamma tends to increase in power prior to and during the onset of movement, beta decreases in power (Crone et al. 1998a; Crone et al. 1998b). This decrease in beta power during movement preparation in healthy controls has been linked with the reduction of inhibition in M1 just prior to movement to release the motor command (Takemi et al. 2013; 2015). Consequently, movements executed during elevated beta synchrony are slower (Gilbertson et al. 2005), and increasing beta power using tACS has been shown to impair movement in healthy controls (Joundi et al. 2012; Pogosyan et al. 2009). Importantly, stroke individuals show less decreases in beta during movement compared to controls (Rossiter et al. 2014), and persistence of inhibition in ipsilesional M1 during movement preparation (Hummel et al. 2009). Therefore, the shift from positive to negative coupling between gamma and beta in ipsilesional M1 following the intervention may reflect a return to a more typical pattern seen in healthy controls.

Prior to the intervention, we saw that increased gamma power was associated with increased beta power in ipsilesional M1 (as seen by positive coupling between gamma and beta power in 6/8 participants, see Figure 5.8D). This positive coupling shifted to negative after the intervention, where increases in gamma power were associated with decreases in beta power. Importantly, decreases in beta power are inversely related to BOLD activity in the sensorimotor cortex, suggesting some interplay or association between these two physiological processes (Ritter et al. 2009; Yuan et al. 2010). Given beta's role in descending layer V pyramidal neurons (Lacey et al.

2014; Roopun et al. 2006), the observed intervention-induced increase in CAR may reflect increased drive and use of remaining descending ipsilesional motor resources during the lifting and opening condition following the intervention, rather than purely an intracortical change. This is significant since reliance on descending tracts from the contralesional hemisphere has been linked with synergy-induced impairments (Davidson and Buford 2006; Owen et al. 2017), particularly during tasks involving lifting at the shoulder (McPherson et al. 2018a; Sukal et al. 2007), as examined here. Meanwhile, increased use of descending corticospinal tract from the ipsilesional hemisphere has been shown to be crucial for improved function following stroke (Rehme et al. 2012; Stinear et al. 2007; Ward et al. 2006), especially for independent control of multijoint movements of the upper extremity (Baker et al. 2015). Although contralesional corticobulbar pathways can support more proximal paretic arm movements such as reaching (Herbert et al. 2015), they do not offer sufficient control of independent joints during multijoint movements (Baker 2011; Riddle et al. 2009). Thus, the ability to maintain ipsilesional recruitment during combined shoulder-hand tasks is critical for potential functional improvement since ipsilesional corticospinal tract, unlike contralesional corticobulbar tracts, has more specific branching in the spinal cord that allows for independent control of the different parts of the arm (Baker 2011; Kuypers et al. 1962; Lemon 1993; Matsuyama et al. 1997).

Increased Gray Matter Density in Ipsilesional Sensorimotor Cortex

Previous work found significant decreases in GM volume in ipsilesional precentral gyrus following a subcortical stroke, which was associated with greater impairment (Cai et al. 2016). However, following task-specific training, mild chronic stroke participants showed increases in

GM density in ipsilesional sensorimotor cortex (Gauthier et al. 2008), and increases in perilesional GM density were associated with better recovery in acute stroke (Abela et al. 2015). Similarly, we found increased ipsilesional M1/S1 GM density following the intervention in our moderate to severe stroke population. Additionally, a significant positive correlation was found between changes in LI and changes in GM density in ipsilesional M1/S1 following the intervention ($r = 0.70$, $p < 0.05$), showing that activity shifting to the ipsilesional hemisphere was associated with increased ipsilesional M1/S1 GM density.

Increases in GM density may suggest potential synaptogenesis, dendritic growth, or gliogenesis at the cortex (Zatorre et al. 2012). Thus, these changes may be due to new synapse formation and dendritic growth commonly seen in animal training models (Murphy and Corbett 2009). Additionally, these participants likely experienced cortical atrophy prior to the intervention due to disuse of the paretic limb, which may have been partially remedied following the intervention due to increased use of the paretic arm/hand. Despite greater damage to ipsilesional descending motor tracts, these severely impaired individuals maintain the ability to reorganize ipsilesional primary sensorimotor cortices.

In these individuals with more severe impairments, we also found an intervention-induced decrease in contralesional M1/S1 GM density, which was not reported before in mildly impaired individuals. This decrease may be specific to more severe patients since following a stroke, increased use of the contralesional hemisphere occurs to a greater degree in severely impaired individuals compared with milder individuals (McPherson et al. 2018a). The decrease in GM density in contralesional M1/S1 may indicate a decrease in dendritic complexity or synapses in

these areas (Sowell et al. 2001). These structural changes may be a result of decreased activation in these areas due to decreased recruitment during movement or overall decreased use (Langer et al. 2012; Zito and Svoboda 2002). Alternatively, they may be due to decreased tonic activity in these contralesional sensorimotor areas, which is thought to be a contributor to hyperexcitability in the brainstem and subsequent increased tone in this population (Brown 1994; Li and Francisco 2015).

The increases in GM density seen in the thalamus in our results may be due to the repeated use of electrical stimulation throughout the intervention. Although we focused on the motor changes in this study, it is likely that these participants show sensory neural changes as well due to the augmented afferent feedback generated by the EMG-FES device. Therefore, it is not surprising to see changes in the thalamus due to its central role as a sensory relay station for both the cutaneous and proprioceptive sensory modalities (Kandel et al. 2013).

Limitations

The main limitation of the current study is the small sample size. Despite the relatively small *n*, we observed consistent patterns of functional and structural changes. These changes signify the importance of examining the potential neural mechanisms found here in a larger population of moderate to severe chronic stroke participants. Additionally, there was no control group in the present study. However, this study was aimed at investigating the feasibility of whether this population maintained the ability to experience neural changes following an intervention, rather than answering the question of what the optimal intervention for this population is. Another potential confounding factor from the task-specific intervention is the amount of stretching of the

arm and hand between trials. However, stretching on its own is unlikely to drive the functional and structural changes found in this study (Teasell et al. 2009), even though it may temporarily reduce the stretch reflex activation of wrist and finger flexors (Schmit et al. 2000). Additionally, reduced flexion synergy and subsequent decreased involuntary shoulder abduction/adduction force generation during hand opening (Miller and Dewald 2012) could contribute to intervention-induced changes in LI.

One of the primary long-term goals of the current study is to substantially increase the population included in task-specific therapy. Although the current ReIn-Hand device allowed our cohort of moderate to severe chronic stroke individuals to participate in task-specific training, it does require both detectable extensor EMGs to drive the device and responsiveness to FES to create sufficient hand opening. In our experience, limiting our inclusion criteria satisfied these requirements in most of initially screened participants (18 out of 20). However, due to the current sample size, it is difficult to accurately specify the portion of individuals who could utilize the ReIn-Hand device.

Conclusion

The present study shows the ability of even moderate to severe chronic stroke participants to experience cortical reorganization at both the functional and structural levels following a device-assisted task-specific intervention in a manner resembling that seen in mild chronic stroke participants. Importantly, the intervention led to complementary changes in coupling between motor regions during movement preparation in movement-related frequencies and focal cortical activity changes in isolated regions at movement execution related to both the hand and arm that were also accompanied by related structural changes. Despite the tendency to focus on acute or

mild chronic stroke patients in hand function rehabilitation, the current study encourages the continued push to use devices to involve moderate to severe chronic stroke participants in task-specific arm/hand rehabilitation.

6. Discussion

Thesis Summary

In Chapters 1 and 2, I provided an overview of two current problems facing the stroke rehabilitation field: 1. The negative impact of lifting on hand opening ability, and 2. The limited capacity for individuals with severe motor impairments to experience neural changes following an intervention. In Chapters 3 and 4, I presented work that aimed to elucidate the effect of adding on lifting to hand opening in both healthy individuals and individuals with chronic hemiparetic stroke. I first examined cortical activity and connectivity in healthy individuals during hand opening alone and while lifting at the shoulder using high-density EEG. I found that lifting led to an increase in cortical coupling with ipsilateral sensorimotor cortices during motor preparation but did not affect the predominantly contralateral primary motor cortex reliance at movement execution. In Chapter 4, I found that the same addition of lifting led to an increased reliance on the ipsilateral sensorimotor cortices (i.e., contralesional hemisphere), specifically in secondary motor areas (SMA/PM) at movement execution. Importantly, greater activity in these secondary motor areas during the lifting and opening task was associated with greater involuntary grasping pressure (i.e., reduced hand opening ability). Furthermore, individuals with stroke showed long-term structural changes in these ipsilateral secondary motor areas, characterized by increased gray matter density compared to controls.

Having established that the negative impact of lifting on hand opening ability following stroke is associated with increased reliance on the contralesional hemisphere, I then sought to see what neural changes may accompany behavioral improvements following a hand/arm intervention in Chapter 5. I found that following an 8-week device-assisted task-specific intervention, individuals

relied more on the ipsilesional hemisphere for both hand opening and hand opening while lifting. This was characterized by a decrease in activity in contralesional primary sensorimotor cortex and an increase in activity in ipsilesional primary sensorimotor cortex at movement execution. This change in cortical activity at movement execution was accompanied by complementary changes in cortical coupling during motor preparation, including a reduction in both interhemispheric M1-M1 coupling and changes in intrinsic coupling within ipsilesional M1. Furthermore, individuals showed intervention-induced structural changes in the form of increased gray matter density in ipsilesional primary sensorimotor cortex and decreased gray matter density in contralesional primary sensorimotor cortex.

Neural Mechanisms Underlying the Negative Impact of Lifting on Hand Opening Ability

To this point, the majority of neuroimaging studies involving motor tasks in healthy controls are limited to single-joint (often distal) tasks due to practical constraints for multi-joint movements within the MRI scanner. However, multi-joint movements such as the addition of lifting to a reach or hand opening attempt, further exacerbate impairments in individuals with stroke, while having no obvious negative behavioral effects in healthy individuals.

In Chapter 3, I showed that healthy individuals have an increase in coupling with the ipsilateral sensorimotor cortices during motor preparation with the addition of lifting to hand opening, but that it did not alter the predominantly contralateral cortical activity in primary sensorimotor cortex at movement execution. This may suggest that although the shift from a single-joint distal hand opening to a multi-joint distal-proximal lift and open changes the amount of cortical

communication that occurs in the time leading up to the movement, the actual descending motor command does not change drastically on a regional level. It is possible, if not likely, that the addition of lifting will lead to additional recruitment of corticobulbar tracts compared to the primarily CST-controlled hand opening. These pathways originate both from the contralateral and ipsilateral sensorimotor cortices. However, given that we observed no major changes in activity within our regions of interest (primary or secondary motor areas on either hemisphere) with the addition of lifting, it appears that healthy controls are primarily relying on motor tracts projecting from the contralateral sensorimotor cortex.

Although we do not see changes in cortical activity during motor execution, there is a clear difference in coupling between motor regions during the motor preparation for hand opening compared to hand opening with lifting. However, it is important to note that both tasks had coupling from secondary motor areas (SMA & cPM) to cM1 within the beta band. One possibility is that this reflects the common activity patterns in the contralateral motor areas seen near movement execution since beta band is most often implicated in the observed descending motor command, rather than just local cortical computation. Therefore, regardless of whether the participant is doing a simple distal hand opening movement or a multi-joint lifting and hand opening movement, we see this common beta coupling within the contralateral motor areas.

The addition of lifting led to an increase in coupling both within the ipsilateral hemisphere (SMA→iPM; iPM→iM1) and also between hemispheres (bidirectional iM1-cPM). These differences in coupling spanned multiple frequency bands, including theta, mu, and gamma. Importantly, these frequencies, particularly theta and gamma, are not traditionally associated with

motor commands. Rather, theta is typically implicated in more cognitively-demanding tasks and long-range synchronization of cortical regions, and gamma is thought to reflect more local computational processing. One possibility is that the increase in coupling within these frequencies in the ipsilateral hemisphere reflects the increased coordination required for simultaneously moving multiple joints. This would fit in line with why we do not see any changes in cortical activity in the ipsilateral hemisphere at movement execution during the lifting and opening task since this change in coupling may not reflect changes in descending commands, but only cortico-cortico communication.

Once we established how the addition of lifting to hand opening impacted cortical activity and coupling in healthy controls, we could then see how this may go awry in individuals with chronic hemiparetic stroke who display significant behavioral consequences during these types of movements (Chapter 4). Unlike healthy controls, the addition of lifting led to increased activity at movement execution in the ipsilateral (i.e., contralesional) sensorimotor cortices, specifically in secondary motor areas (SMA/PM). Crucially, greater activity in ipsilateral secondary motor areas during the lifting and opening movement was associated with reduced hand opening ability. This increased activity in ipsilateral secondary motor areas with the addition of lifting may reflect increased recruitment of uncrossed ipsilateral cortico-bulbospinal tracts. These ipsilaterally-projecting tracts primarily originate from SMA and PM, not M1, and may lead to the involuntary coactivation of finger/wrist flexor muscles during shoulder abduction due to their more diffuse projections at the spinal cord and preferential innervation of flexor muscles (Fregosi et al. 2017; Matsuyama et al. 1997; Montgomery et al. 2013).

Based on the present results and previous work from our lab showing that progressively increasing SABD load during reaching led to a progressive reliance on the ipsilateral hemisphere (McPherson et al. 2018a), we propose that there is a dynamic interplay between reliance on residual resources from the contralateral (i.e., ipsilesional) hemisphere during movement and compensatory reliance on the ipsilateral (i.e., contralesional) hemisphere. More specifically, when the demand of the task is low (e.g., minimal SABD torque required), individuals can still rely primarily on remaining resources from the contralateral hemisphere. However, as the demand of the task increases, residual resources become insufficient, and therefore ipsilaterally-projecting cortico-bulbospinal pathways, originating primarily from SMA and PM, are also recruited to help carry out the movement. Although these pathways help activate the shoulder abductors, their broadly branched projections lead to simultaneous involuntary coactivation of wrist/finger flexors which reduces hand opening ability.

The above findings raise interesting questions regarding recovery following stroke and the potential compensatory role for these ipsilateral cortico-bulbospinal tracts. On the one hand, it seems like these pathways may be important for maintaining the ability to drive the shoulder following a stroke. For instance, although the shoulder may be weaker following a stroke compared to healthy controls, its relative strength is still greater than the more distal muscles, especially at the level of the hand. Additionally, inhibiting the ipsilateral sensorimotor cortex with transcranial direct current stimulation (tDCS) in individuals with more severe impairments, worsened proximal control, further suggesting these tracts may be important for recovery of proximal movements (Bradnam et al. 2012). However, whereas some evidence from monkeys suggests that these pathways may even play a role for hand recovery following a CST lesion

(Darling et al. 2018), our results here and the commonly observed lack of residual hand function following a stroke suggest that these pathways cannot support recovery of the hand (at least for opening). Furthermore, they actually seem to have a detrimental effect since use of these pathways leads to coactivation of wrist/finger flexors which makes it even more difficult to open the hand. Therefore, there appears to be a complex relationship regarding these pathways in terms of their potential utility for more proximal musculature compared to their hindrance for distal function.

In addition to changes in cortical activity during movement execution, we also again examined how the addition of lifting altered cortico-cortico coupling during motor preparation in individuals with stroke. Initially, we hypothesized that individuals with stroke would have more extensive coupling, including the ipsilateral hemisphere, during hand opening compared to controls. The addition of lifting would then further increase the extensiveness of this coupling. Interestingly, we found that the addition of lifting did not significantly alter coupling during motor preparation; instead, there was already coupling between almost every motor region examined across both hemispheres during hand opening in isolation. It is worth noting that the individuals included all suffered from moderate to severe motor impairment and had significant difficulty opening their hand. Therefore, one possibility is that even during hand opening, a task that these individuals cannot execute properly, individuals recruit almost the whole motor network in an attempt to drive the hand. Consequently, we do not see much change in the motor preparation when we add on the lifting. This is a stark departure from what was observed in healthy controls, who had a relatively simple network for hand opening within the contralateral hemisphere. Additionally, whereas in healthy controls this coupling was limited to only beta band, the coupling in individuals following a stroke expands to theta, mu, and gamma frequency bands.

Interestingly, in addition to the observed changes in activity and cortico-coupling related to the hand and arm, individuals with stroke had structural changes in their ipsilateral sensorimotor cortex. Crucially, the same secondary motor regions implicated in the negative impact of lifting on hand opening also had structural increases in gray matter density compared to healthy controls. This increase in gray matter density is a proxy measure of synaptogenesis, dendritic complexity, and gliogenesis (Zatorre et al. 2012), compared to healthy age-matched controls. Since this is a structural change, we lose the ability to determine the potential cause of this change. For instance, one possibility is this change in gray matter may reflect the compensatory long-term reliance on ipsilateral projecting cortico-bulbospinal tracts. However, this change could also merely reflect a compensatory change in response to using the nonparetic limb more (and its associated descending tracts). Regardless of which of these may be contributing most to the observed change, the combination of both the functional and structural changes do indeed point to an overall increased reliance on the ipsilateral (i.e., nonlesioned) secondary motor areas, but clearly does not support recovery as these individuals display severely impaired motor abilities.

Neural Changes Following an Intervention

Prior research shows that effective interventions are associated with an increased reliance on the ipsilesional hemisphere, but these results are limited to the acute phase following a stroke or individuals with chronic mild impairments. However, individuals in the acute phase experience a heightened state of plasticity and therefore are more likely to experience significant neural changes following training and individuals with mild impairments may have more significant residual resources in the lesioned hemisphere to enable recovery. I looked to expand these results to

individuals with severe motor impairments, often excluded from traditional upper extremity therapies, to see if they still maintained the capacity to experience similar changes as previously found in these other populations.

In Chapter 5, I showed that even individuals with severe motor impairments maintain the ability to reengage the ipsilesional sensorimotor cortex following an arm/hand intervention. Importantly, the observed neural changes, characterized by an increased functional and structural reliance on the ipsilesional sensorimotor cortex, resemble previous findings in more mildly impaired individuals. The fact that these individuals who suffer from more significant damage to critical motor tracts still maintain the ability to reengage residual ipsilesional resources points to the need to include this population in upper extremity hand/arm interventions using assistive devices.

The ability to reengage ipsilesional resources following an intervention is critical since I showed in Chapter 4 that use of contralesional sensorimotor cortex, and presumably compensatory uncrossed cortico-bulbospinal tracts, is not sufficient for hand function recovery. In fact, use of these pathways has a detrimental effect on hand opening ability due to involuntary coactivation of finger flexor muscles. Therefore, if the goal of an intervention is to improve hand opening ability, it appears the primary means with which to achieve that goal is through use of remaining ipsilesional corticospinal tract, which provides the main innervations to the finger extensor muscles. However, if the goal of the intervention is to focus primarily on improving proximal control, then contralesional resources may be sufficient for improving function (Herbert et al. 2015).

Importantly, individuals experienced complementary changes in functional (both cortical activity at movement execution and cortical coupling between regions during movement preparation) and structural changes in cortical gray matter. This is perhaps not surprising since there is a known interplay between functional and structural changes in response to training and/or motor learning (Gibson et al. 2014; Kleim et al. 2002; Zito and Svoboda 2002). Given that the population studied was in the chronic phase (> 1-year following a stroke; avg: 11.25 years), it is unlikely that these changes would occur spontaneously since any critical period of heightened plasticity would be long closed.

Future Directions

The findings from this dissertation open up several interesting potential lines of inquiries from both a basic science and clinical perspective. One of the most obvious would be to quantify activity in brainstem nuclei using fMRI during movement and see how well it correlates with cortical activity in ipsilateral secondary motor areas in individuals following a stroke. Given the positive correlation found between activity in ipsilateral secondary motor areas and involuntary grasping pressure, we presume that this cortical activity reflects use of the diffusely projecting cortico-bulbospinal tracts. If we also saw that relevant brainstem nuclei, such as in the reticular formation, were active during these tasks and associated with cortical activity in secondary motor areas, this would provide further evidence for this assumption. Unfortunately, it is not feasible to implement movements with SABD in the MRI scanner. A possible solution could be to examine cortical and brainstem activity during max closing, as this is thought to be at least partially controlled by ipsilaterally projecting cortico-bulbospinal tracts (Baker et al. 2015).

Given the association between cortical activity in ipsilateral secondary motor areas and reduced hand opening ability, one way to causally test this potential relationship would be to see whether inhibitory rTMS over ipsilateral SMA/PM reduces the negative impact of the synergy. For instance, if the negative impact of lifting on hand opening ability is due to recruitment of these ipsilateral secondary motor regions and their descending projections, then inhibiting these regions via TMS should reduce the lifting-induced involuntary finger flexor coactivation. Previous work in our lab attempted a similar experiment using both excitatory and inhibitory tDCS and its effect on reaching ability (Yao et al. 2015). However, this experiment targeted primary motor cortex, not the secondary motor areas which are the primary origin of the cortico-reticulospinal tract. Additionally, it did not look at the SABD-induced effects at the hand. Recent improvements in electrical field modeling would allow for specific targeting of SMA and/or PM without major concern for field spread to other regions if using MRI-guided stimulation. For instance, ring-electrode tDCS configurations combined with finite element head models provides enhanced spatial focality compared to the diffuse current spread from traditional tDCS rectangular-pads (Datta et al. 2009). Similarly, pipelines now exist to combine TMS with MRI-based head models to model the expected electric field (Windhoff et al. 2013).

Another potential line of inquiry is to further investigate the mechanisms that allow for the progressive switch from reliance on ipsilesional to contralesional resources. The dynamic causal modeling results from this dissertation give us some insight into potential cortico-cortico communication during the motor preparation phase by providing both directional coupling and the frequencies involved in such coupling. A potential next step could be to take this information and try to causally manipulate specific regional coupling through some sort of cortical stimulation. For

instance, TMS could be used to perturb specific nodes within the motor network, based on the DCM results. Alternatively, transcranial alternating current stimulation (tACS), which has shown the ability to entrain cortical regions to particular frequency oscillations (Tavakoli and Yun 2017), could be used to target and enhance specific frequencies thought to be important during the motor preparation and execution in either healthy controls or stroke.

Clinically, the next step is to find an optimal hand/arm intervention for individuals with severe impairments. Although the intervention presented in Chapter 5 had promising behavioral results for improved hand function, it served primarily as a feasibility study, considering it lacked a control group. There is no evidence to suggest that this task-specific intervention using the ReIn-Hand EMG-FES device is the optimal path for improving hand function in individuals with severe impairments. The next step would be to test this intervention in a larger sample against another type of intervention. One possibility would be to test this against a group using the ReIn-Hand EMG-FES device, but without the task-specific component (e.g., participants practice hand opening with the device, but do not execute reach-to-grasp). This would allow us to tease out what improvements are specific to practicing hand opening using an EMG-driven FES device, and whether adding on a task component further improves behavior. Another possibility is to target the flexion synergy impairment. In the intervention in Chapter 5, the shoulder was not well controlled, and thus the flexion synergy was never specifically targeted. However, work from our lab has shown that if you train individuals with stroke on a reaching task with progressive increases in SABD-loading then you can see significant increases in work area and reaching distance. Therefore, one possibility is to combine that approach with the ReIn-Hand device and task used in Chapter 5. In this scenario, participants would still use the ReIn-Hand device to carry out task-

specific movements such as a reach-to-grasp. However, we would control the amount of SABD-torque required for the lifting component of the task using a robotic device such as the ACT-3D. Initially, the SABD-torque required would be lowered so that the participant receives assistance from the ACT-3D in the Z-direction during the task, thus minimizing the impact of the synergy. As the training progresses, the amount of SABD-torque required would be increased as the participant's loss of independent joint control improves. In this design, we would therefore be targeting both the flexion synergy, using the ACT-3D robot, and weakness, using the ReIn-Hand device, while combined with the known benefit of task-specific practice.

Alternatively, another possible clinical step could be to combine excitatory rTMS to ipsilesional primary motor cortex with inhibitory rTMS to contralesional secondary motor areas (SMA/PM). This would potentially augment any residual resources within ipsilesional primary motor cortex, the main output for CST, and inhibit use of contralesional secondary motor regions and their cortico-bulbospinal projections. Using TMS and tDCS has risen in popularity following stroke but has primarily focused on inhibiting contralesional primary motor cortex. Since secondary motor areas, not primary motor cortex, are where most cortico-bulbospinal projections originate from, it may make more sense to inhibit these regions instead. This may explain why a recent large multi-site clinical trial inhibiting contralesional primary motor cortex found no significant improvements (Harvey et al. 2018).

Regardless of the type of intervention, it is crucial that future interventions include high resolution kinematic measures to evaluate changes in movement performance. Clinical measures give some insight into how the intervention may change behavior on a broad scale, but lack the necessary

resolution to evaluate how an intervention may impact particular aspects of performance. For instance, many clinical measures evaluate task performance or goal completion (e.g., the Action Research Arm Test [ARAT]), and thus are prone to improvements merely through compensatory behavioral changes. Even clinical measurements of impairment, such as the Fugl Meyer assessment, only evaluate movements on a 1-3 ordinal scale based on the evaluator's observation. If we are to use scientifically-driven therapeutic options, we must also evaluate performance in a manner that allows dissection of how movements have changed following training in a quantitative and objective fashion. This will allow us to disentangle whether improvements seen are merely the result of compensatory change versus true motor recovery (i.e., a return to a normal movement pattern) and ideally produce more reproducible results across sites.

Conclusion

Hand function is often limited following stroke due to a combination of weakness and loss of independent joint control that makes it difficult to use the hand in many activities of daily life. Unfortunately, most individuals with severe motor impairments are excluded from traditional hand/arm therapies due to a lack of residual function. The work here provides insight into both the neural mechanisms underlying hand dysfunction following a stroke and subsequent intervention-induced improvements. Specifically, the exacerbated negative effect of lifting on hand opening in individuals with stroke is related to an increase in activity in contralesional secondary motor areas not seen in healthy controls; whereas intervention-induced behavioral improvements are accompanied by an increased functional and structural reliance on the ipsilesional primary sensorimotor cortex. Together these results implicate reliance on contralesional resources as not

only insufficient, but actually detrimental to hand function, and the need to reengage remaining ipsilesional resources to achieve hand function recovery.

References

- Abela E, Seiler A, Missimer JH, Federspiel A, Hess CW, Sturzenegger M, Weder BJ, and Wiest R.** Grey matter volumetric changes related to recovery from hand paresis after cortical sensorimotor stroke. *Brain Struct Funct* 220: 2533-2550, 2015.
- Allred RP, Kim SY, and Jones TA.** Use it and/or lose it-experience effects on brain remodeling across time after stroke. *Frontiers in human neuroscience* 8: 379, 2014.
- Amengual JL, Munte TF, Marco-Pallares J, Rojo N, Grau-Sanchez J, Rubio F, Duarte E, Grau C, and Rodriguez-Fornells A.** Overactivation of the supplementary motor area in chronic stroke patients. *Journal of neurophysiology* 112: 2251-2263, 2014.
- Archer DB, Patten C, and Coombes SA.** Free-water and free-water corrected fractional anisotropy in primary and premotor corticospinal tracts in chronic stroke. *Human brain mapping* 38: 4546-4562, 2017.
- Arikuni T, Watanabe K, and Kubota K.** Connections of area 8 with area 6 in the brain of the macaque monkey. *J Comp Neurol* 277: 21-40, 1988.
- Askim T, Indredavik B, Vangberg T, and Haberg A.** Motor network changes associated with successful motor skill relearning after acute ischemic stroke: a longitudinal functional magnetic resonance imaging study. *Neurorehabilitation and neural repair* 23: 295-304, 2009.
- Avanzino L, Bove M, Trompetto C, Tacchino A, Ogliaastro C, and Abbruzzese G.** 1-Hz repetitive TMS over ipsilateral motor cortex influences the performance of sequential finger movements of different complexity. *The European journal of neuroscience* 27: 1285-1291, 2008.
- Bajaj S, Butler AJ, Drake D, and Dhamala M.** Brain effective connectivity during motor-imagery and execution following stroke and rehabilitation. *NeuroImage Clinical* 8: 572-582, 2015.
- Baker SN.** The primate reticulospinal tract, hand function and functional recovery. *The Journal of physiology* 589: 5603-5612, 2011.
- Baker SN, and Perez MA.** Reticulospinal Contributions to Gross Hand Function after Human Spinal Cord Injury. *The Journal of neuroscience : the official journal of the Society for Neuroscience* 37: 9778-9784, 2017.
- Baker SN, Zaaimi B, Fisher KM, Edgley SA, and Soteropoulos DS.** Pathways mediating functional recovery. *Progress in brain research* 218: 389-412, 2015.
- Ball T, Demandt E, Mutschler I, Neitzel E, Mehring C, Vogt K, Aertsen A, and Schulze-Bonhage A.** Movement related activity in the high gamma range of the human EEG. *NeuroImage* 41: 302-310, 2008.
- Barbas H.** General cortical and special prefrontal connections: principles from structure to function. *Annual review of neuroscience* 38: 269-289, 2015.
- Barbas H, and Pandya DN.** Architecture and frontal cortical connections of the premotor cortex (area 6) in the rhesus monkey. *J Comp Neurol* 256: 211-228, 1987.
- Bartos M, Vida I, and Jonas P.** Synaptic mechanisms of synchronized gamma oscillations in inhibitory interneuron networks. *Nat Rev Neurosci* 8: 45-56, 2007.
- Bashir S, Kaeser M, Wyss A, Hamadjida A, Liu Y, Bloch J, Brunet JF, Belhaj-Saif A, and Rouiller EM.** Short-term effects of unilateral lesion of the primary motor cortex (M1) on ipsilesional hand dexterity in adult macaque monkeys. *Brain Struct Funct* 217: 63-79, 2012.
- Bayona NA, Bitensky J, Salter K, and Teasell R.** The role of task-specific training in rehabilitation therapies. *Topics in stroke rehabilitation* 12: 58-65, 2005.

- Beevor CE, and Horsley V.** A Record of the Results Obtained by Electrical Excitation of the So-Called Motor Cortex and Internal Capsule in an Orang-Outang (*Simia satyrus*). *Philosophical Transactions of the Royal Society of London* 181: 129-158, 1890.
- Berlot E, Prichard G, O'Reilly J, Ejaz N, and Diedrichsen J.** Ipsilateral finger representations in the sensorimotor cortex are driven by active movement processes, not passive sensory input. *Journal of neurophysiology* 121: 418-426, 2019.
- Bestmann S, Swayne O, Blankenburg F, Ruff CC, Teo J, Weiskopf N, Driver J, Rothwell JC, and Ward NS.** The role of contralesional dorsal premotor cortex after stroke as studied with concurrent TMS-fMRI. *The Journal of neuroscience : the official journal of the Society for Neuroscience* 30: 11926-11937, 2010.
- Biasiucci A, Leeb R, Iturrate I, Perdakis S, Al-Khodairy A, Corbet T, Schnider A, Schmidlin T, Zhang H, Bassolino M, Viceic D, Vuadens P, Guggisberg AG, and Millan JDR.** Brain-actuated functional electrical stimulation elicits lasting arm motor recovery after stroke. *Nature communications* 9: 2421, 2018.
- Biernaskie J, and Corbett D.** Enriched rehabilitative training promotes improved forelimb motor function and enhanced dendritic growth after focal ischemic injury. *The Journal of neuroscience : the official journal of the Society for Neuroscience* 21: 5272-5280, 2001.
- Boake C, Noser EA, Ro T, Baraniuk S, Gaber M, Johnson R, Salmeron ET, Tran TM, Lai JM, Taub E, Moyer LA, Grotta JC, and Levin HS.** Constraint-induced movement therapy during early stroke rehabilitation. *Neurorehabilitation and neural repair* 21: 14-24, 2007.
- Bohannon RW, and Smith MB.** Interrater reliability of a modified Ashworth scale of muscle spasticity. *Phys Ther* 67: 206-207, 1987.
- Bonita R, and Beaglehole R.** Recovery of motor function after stroke. *Stroke; a journal of cerebral circulation* 19: 1497-1500, 1988.
- Bonstrup M, Schulz R, Feldheim J, Hummel FC, and Gerloff C.** Dynamic causal modelling of EEG and fMRI to characterize network architectures in a simple motor task. *NeuroImage* 124: 498-508, 2015.
- Borra E, Belmalih A, Gerbella M, Rozzi S, and Luppino G.** Projections of the hand field of the macaque ventral premotor area F5 to the brainstem and spinal cord. *J Comp Neurol* 518: 2570-2591, 2010.
- Bouton CE, Shaikhouni A, Annetta NV, Bockbrader MA, Friedenberg DA, Nielson DM, Sharma G, Sederberg PB, Glenn BC, Mysiw WJ, Morgan AG, Deogaonkar M, and Rezai AR.** Restoring cortical control of functional movement in a human with quadriplegia. *Nature* 2016.
- Bradley A, Yao J, Dewald J, and Richter CP.** Evaluation of Electroencephalography Source Localization Algorithms with Multiple Cortical Sources. *PLoS one* 11: e0147266, 2016.
- Bradnam LV, Stinear CM, Barber PA, and Byblow WD.** Contralesional hemisphere control of the proximal paretic upper limb following stroke. *Cerebral cortex* 22: 2662-2671, 2012.
- Brinkman C, and Porter R.** Supplementary motor area in the monkey: activity of neurons during performance of a learned motor task. *Journal of neurophysiology* 42: 681-709, 1979.
- Brown P.** Pathophysiology of spasticity. *Journal of neurology, neurosurgery, and psychiatry* 57: 773-777, 1994.
- Buetevisch CM, Pirog Reville K, Haut MW, Kowalski GM, Wischniewski M, Pifer M, Belagaje SR, Nahab F, Cobia DJ, Hu X, Drake D, and Hobbs G.** Abnormally reduced

primary motor cortex output is related to impaired hand function in chronic stroke. *Journal of neurophysiology* 2018.

Buetefisch CM, Revill KP, Shuster L, Hines B, and Parsons M. Motor demand-dependent activation of ipsilateral motor cortex. *Journal of neurophysiology* 112: 999-1009, 2014.

Buffalo EA, Fries P, Landman R, Buschman TJ, and Desimone R. Laminar differences in gamma and alpha coherence in the ventral stream. *Proceedings of the National Academy of Sciences of the United States of America* 108: 11262-11267, 2011.

Buma FE, van Kordelaar J, Raemaekers M, van Wegen EE, Ramsey NF, and Kwakkel G. Brain activation is related to smoothness of upper limb movements after stroke. *Experimental brain research* 234: 2077-2089, 2016.

Bundy DT, Souders L, Baranyai K, Leonard L, Schalk G, Coker R, Moran DW, Huskey T, and Leuthardt EC. Contralesional Brain-Computer Interface Control of a Powered Exoskeleton for Motor Recovery in Chronic Stroke Survivors. *Stroke; a journal of cerebral circulation* 48: 1908-1915, 2017.

Bundy DT, Szrama N, Pahwa M, and Leuthardt EC. Unilateral, 3D Arm Movement Kinematics Are Encoded in Ipsilateral Human Cortex. *The Journal of neuroscience : the official journal of the Society for Neuroscience* 38: 10042-10056, 2018.

Buntin MB, Colla CH, Deb P, Sood N, and Escarce JJ. Medicare spending and outcomes after postacute care for stroke and hip fracture. *Med Care* 48: 776-784, 2010.

Butefisch CM, Wessling M, Netz J, Seitz RJ, and Homberg V. Relationship between interhemispheric inhibition and motor cortex excitability in subacute stroke patients. *Neurorehabilitation and neural repair* 22: 4-21, 2008.

Buzsaki G, and Draguhn A. Neuronal oscillations in cortical networks. *Science* 304: 1926-1929, 2004.

Buzsaki G, and Wang XJ. Mechanisms of gamma oscillations. *Annual review of neuroscience* 35: 203-225, 2012.

Byblow WD, Stinear CM, Barber PA, Petoe MA, and Ackerley SJ. Proportional recovery after stroke depends on corticomotor integrity. *Annals of neurology* 2015.

Cai J, Ji Q, Xin R, Zhang D, Na X, Peng R, and Li K. Contralesional Cortical Structural Reorganization Contributes to Motor Recovery after Sub-Cortical Stroke: A Longitudinal Voxel-Based Morphometry Study. *Frontiers in human neuroscience* 10: 393, 2016.

Calautti C, Leroy F, Guincestre JY, and Baron JC. Dynamics of motor network overactivation after striatocapsular stroke: a longitudinal PET study using a fixed-performance paradigm. *Stroke; a journal of cerebral circulation* 32: 2534-2542, 2001.

Calautti C, Naccarato M, Jones PS, Sharma N, Day DD, Carpenter AT, Bullmore ET, Warburton EA, and Baron JC. The relationship between motor deficit and hemisphere activation balance after stroke: A 3T fMRI study. *NeuroImage* 34: 322-331, 2007.

Carter AR, Astafiev SV, Lang CE, Connor LT, Rengachary J, Strube MJ, Pope DL, Shulman GL, and Corbetta M. Resting interhemispheric functional magnetic resonance imaging connectivity predicts performance after stroke. *Annals of neurology* 67: 365-375, 2010.

Cassim F, Monaca C, Szurhaj W, Bourriez JL, Defebvre L, Derambure P, and Guieu JD. Does post-movement beta synchronization reflect an idling motor cortex? *Neuroreport* 12: 3859-3863, 2001.

Chen CC, Kiebel SJ, and Friston KJ. Dynamic causal modelling of induced responses. *NeuroImage* 41: 1293-1312, 2008.

- Chen CC, Kilner JM, Friston KJ, Kiebel SJ, Jolly RK, and Ward NS.** Nonlinear coupling in the human motor system. *The Journal of neuroscience : the official journal of the Society for Neuroscience* 30: 8393-8399, 2010.
- Chen CF, Kreutz-Delgado K, Sereno MI, and Huang RS.** Unraveling the spatiotemporal brain dynamics during a simulated reach-to-eat task. *NeuroImage* 185: 58-71, 2019.
- Chen R, Gerloff C, Hallett M, and Cohen LG.** Involvement of the ipsilateral motor cortex in finger movements of different complexities. *Annals of neurology* 41: 247-254, 1997.
- Cheyne D, Bells S, Ferrari P, Gaetz W, and Bostan AC.** Self-paced movements induce high-frequency gamma oscillations in primary motor cortex. *NeuroImage* 42: 332-342, 2008.
- Churchland MM, Cunningham JP, Kaufman MT, Foster JD, Nuyujukian P, Ryu SI, and Shenoy KV.** Neural population dynamics during reaching. *Nature* 487: 51-56, 2012.
- Clarkson AN, Lopez-Valdes HE, Overman JJ, Charles AC, Brennan KC, and Thomas Carmichael S.** Multimodal examination of structural and functional remapping in the mouse photothrombotic stroke model. *J Cereb Blood Flow Metab* 33: 716-723, 2013.
- Conrad MO, and Kamper DG.** Isokinetic strength and power deficits in the hand following stroke. *Clinical neurophysiology : official journal of the International Federation of Clinical Neurophysiology* 123: 1200-1206, 2012.
- Crone NE, Miglioretti DL, Gordon B, and Lesser RP.** Functional mapping of human sensorimotor cortex with electrocorticographic spectral analysis. II. Event-related synchronization in the gamma band. *Brain : a journal of neurology* 121 (Pt 12): 2301-2315, 1998a.
- Crone NE, Miglioretti DL, Gordon B, Sieracki JM, Wilson MT, Uematsu S, and Lesser RP.** Functional mapping of human sensorimotor cortex with electrocorticographic spectral analysis. I. Alpha and beta event-related desynchronization. *Brain : a journal of neurology* 121 (Pt 12): 2271-2299, 1998b.
- Cunningham DA, Machado A, Janini D, Varnerin N, Bonnett C, Yue G, Jones S, Lowe M, Beall E, Sakaie K, and Plow EB.** Assessment of inter-hemispheric imbalance using imaging and noninvasive brain stimulation in patients with chronic stroke. *Archives of physical medicine and rehabilitation* 96: S94-103, 2015.
- Darling WG, Ge J, Stilwell-Morecraft KS, Rotella DL, Pizzimenti MA, and Morecraft RJ.** Hand Motor Recovery Following Extensive Frontoparietal Cortical Injury Is Accompanied by Upregulated Corticoreticular Projections in Monkey. *The Journal of neuroscience : the official journal of the Society for Neuroscience* 38: 6323-6339, 2018.
- Datta A, Bansal V, Diaz J, Patel J, Reato D, and Bikson M.** Gyri-precise head model of transcranial direct current stimulation: improved spatial focality using a ring electrode versus conventional rectangular pad. *Brain stimulation* 2: 201-207, 207 e201, 2009.
- Davare M, Duque J, Vandermeeren Y, Thonnard JL, and Olivier E.** Role of the ipsilateral primary motor cortex in controlling the timing of hand muscle recruitment. *Cerebral cortex* 17: 353-362, 2007.
- Davidson AG, and Buford JA.** Bilateral actions of the reticulospinal tract on arm and shoulder muscles in the monkey: stimulus triggered averaging. *Experimental brain research* 173: 25-39, 2006.
- Davidson AG, Schieber MH, and Buford JA.** Bilateral spike-triggered average effects in arm and shoulder muscles from the monkey pontomedullary reticular formation. *The Journal of neuroscience : the official journal of the Society for Neuroscience* 27: 8053-8058, 2007.

- Dechaumont-Palacin S, Marque P, De Boissezon X, Castel-Lacanal E, Carel C, Berry I, Pastor J, Albucher JF, Chollet F, and Loubinoux I.** Neural correlates of proprioceptive integration in the contralesional hemisphere of very impaired patients shortly after a subcortical stroke: an fMRI study. *Neurorehabilitation and neural repair* 22: 154-165, 2008.
- Deecke L, and Kornhuber HH.** An electrical sign of participation of the mesial 'supplementary' motor cortex in human voluntary finger movement. *Brain research* 159: 473-476, 1978.
- Derambure P, Defebvre L, Dujardin K, Bourriez JL, Jacquesson JM, Destee A, and Guieu JD.** Effect of aging on the spatio-temporal pattern of event-related desynchronization during a voluntary movement. *Electroencephalography and clinical neurophysiology* 89: 197-203, 1993.
- Dewald JP, Pope PS, Given JD, Buchanan TS, and Rymer WZ.** Abnormal muscle coactivation patterns during isometric torque generation at the elbow and shoulder in hemiparetic subjects. *Brain : a journal of neurology* 118 (Pt 2): 495-510, 1995.
- Douaud G, Smith S, Jenkinson M, Behrens T, Johansen-Berg H, Vickers J, James S, Voets N, Watkins K, Matthews PM, and James A.** Anatomically related grey and white matter abnormalities in adolescent-onset schizophrenia. *Brain : a journal of neurology* 130: 2375-2386, 2007.
- Dum RP, and Strick PL.** Motor areas in the frontal lobe of the primate. *Physiol Behav* 77: 677-682, 2002.
- Dum RP, and Strick PL.** The origin of corticospinal projections from the premotor areas in the frontal lobe. *The Journal of neuroscience : the official journal of the Society for Neuroscience* 11: 667-689, 1991.
- Duncan PW, Goldstein LB, Matchar D, Divine GW, and Feussner J.** Measurement of motor recovery after stroke. Outcome assessment and sample size requirements. *Stroke; a journal of cerebral circulation* 23: 1084-1089, 1992.
- Ebbesen CL, and Brecht M.** Motor cortex - to act or not to act? *Nat Rev Neurosci* 18: 694-705, 2017.
- Ellis MD, Carmona C, Drogos J, and Dewald JPA.** Progressive Abduction Loading Therapy with Horizontal-Plane Viscous Resistance Targeting Weakness and Flexion Synergy to Treat Upper Limb Function in Chronic Hemiparetic Stroke: A Randomized Clinical Trial. *Front Neurol* 9: 71, 2018.
- Ellis MD, Sukal-Moulton T, and Dewald JP.** Progressive shoulder abduction loading is a crucial element of arm rehabilitation in chronic stroke. *Neurorehabilitation and neural repair* 23: 862-869, 2009.
- Evarts EV.** Relation of pyramidal tract activity to force exerted during voluntary movement. *Journal of neurophysiology* 31: 14-27, 1968.
- Fan YT, Lin KC, Liu HL, Chen YL, and Wu CY.** Changes in structural integrity are correlated with motor and functional recovery after post-stroke rehabilitation. *Restorative neurology and neuroscience* 33: 835-844, 2015a.
- Fan YT, Wu CY, Liu HL, Lin KC, Wai YY, and Chen YL.** Neuroplastic changes in resting-state functional connectivity after stroke rehabilitation. *Frontiers in human neuroscience* 9: 546, 2015b.
- Favre I, Zeffiro TA, Detante O, Krainik A, Hommel M, and Jaillard A.** Upper limb recovery after stroke is associated with ipsilesional primary motor cortical activity: a meta-analysis. *Stroke; a journal of cerebral circulation* 45: 1077-1083, 2014.

- Fields RD.** A new mechanism of nervous system plasticity: activity-dependent myelination. *Nat Rev Neurosci* 16: 756-767, 2015.
- Filatova OG, Yang Y, Dewald JPA, Tian R, Maceira-Elvira P, Takeda Y, Kwakkel G, Yamashita O, and van der Helm FCT.** Dynamic Information Flow Based on EEG and Diffusion MRI in Stroke: A Proof-of-Principle Study. *Frontiers in neural circuits* 12: 79, 2018.
- Fogassi L, and Luppino G.** Motor functions of the parietal lobe. *Current opinion in neurobiology* 15: 626-631, 2005.
- Fregosi M, Contestabile A, Hamadjida A, and Rouiller EM.** Corticobulbar projections from distinct motor cortical areas to the reticular formation in macaque monkeys. *The European journal of neuroscience* 2017.
- Fries P.** Rhythms for Cognition: Communication through Coherence. *Neuron* 88: 220-235, 2015.
- Fujiwara T, Kawakami M, Honaga K, Tochikura M, and Abe K.** Hybrid Assistive Neuromuscular Dynamic Stimulation Therapy: A New Strategy for Improving Upper Extremity Function in Patients with Hemiparesis following Stroke. *Neural Plast* 2017: 2350137, 2017.
- Fukushima K, Peterson BW, and Wilson VJ.** Vestibulospinal, reticulospinal and interstitiospinal pathways in the cat. *Progress in brain research* 50: 121-136, 1979.
- Gadidi V, Katz-Leurer M, Carmeli E, and Bornstein NM.** Long-term outcome poststroke: predictors of activity limitation and participation restriction. *Archives of physical medicine and rehabilitation* 92: 1802-1808, 2011.
- Gallego JA, Perich MG, Miller LE, and Solla SA.** Neural Manifolds for the Control of Movement. *Neuron* 94: 978-984, 2017.
- Ganguly K, Secundo L, Ranade G, Orsborn A, Chang EF, Dimitrov DF, Wallis JD, Barbaro NM, Knight RT, and Carmena JM.** Cortical representation of ipsilateral arm movements in monkey and man. *The Journal of neuroscience : the official journal of the Society for Neuroscience* 29: 12948-12956, 2009.
- Garmirian LRP, Acosta AM, Hill NM, and Dewald JPA.** Estimating Voluntary Activation Of The Elbow And Wrist Muscles In Chronic Hemiparetic Stroke Using Twitch Interpolation Methodology. *Conference proceedings : Annual International Conference of the IEEE Engineering in Medicine and Biology Society IEEE Engineering in Medicine and Biology Society Annual Conference* 2018: 2244-2247, 2018.
- Gauthier LV, Taub E, Perkins C, Ortmann M, Mark VW, and Uswatte G.** Remodeling the brain: plastic structural brain changes produced by different motor therapies after stroke. *Stroke; a journal of cerebral circulation* 39: 1520-1525, 2008.
- Gemperline JJ, Allen S, Walk D, and Rymer WZ.** Characteristics of motor unit discharge in subjects with hemiparesis. *Muscle & nerve* 18: 1101-1114, 1995.
- Georgopoulos AP, Kalaska JF, Caminiti R, and Massey JT.** On the relations between the direction of two-dimensional arm movements and cell discharge in primate motor cortex. *The Journal of neuroscience : the official journal of the Society for Neuroscience* 2: 1527-1537, 1982.
- Gerloff C, Cohen LG, Floeter MK, Chen R, Corwell B, and Hallett M.** Inhibitory influence of the ipsilateral motor cortex on responses to stimulation of the human cortex and pyramidal tract. *The Journal of physiology* 510 (Pt 1): 249-259, 1998.

- Gevins A, Smith ME, McEvoy L, and Yu D.** High-resolution EEG mapping of cortical activation related to working memory: effects of task difficulty, type of processing, and practice. *Cerebral cortex* 7: 374-385, 1997.
- Gibson EM, Purger D, Mount CW, Goldstein AK, Lin GL, Wood LS, Inema I, Miller SE, Bieri G, Zuchero JB, Barres BA, Woo PJ, Vogel H, and Monje M.** Neuronal activity promotes oligodendrogenesis and adaptive myelination in the mammalian brain. *Science* 344: 1252304, 2014.
- Gilbertson T, Lalo E, Doyle L, Di Lazzaro V, Cioni B, and Brown P.** Existing motor state is favored at the expense of new movement during 13-35 Hz oscillatory synchrony in the human corticospinal system. *The Journal of neuroscience : the official journal of the Society for Neuroscience* 25: 7771-7779, 2005.
- Golestani AM, Tymchuk S, Demchuk A, Goodyear BG, and Group V-S.** Longitudinal evaluation of resting-state fMRI after acute stroke with hemiparesis. *Neurorehabilitation and neural repair* 27: 153-163, 2013.
- Grefkes C, Eickhoff SB, Nowak DA, Dafotakis M, and Fink GR.** Dynamic intra- and interhemispheric interactions during unilateral and bilateral hand movements assessed with fMRI and DCM. *NeuroImage* 41: 1382-1394, 2008a.
- Grefkes C, and Fink GR.** Reorganization of cerebral networks after stroke: new insights from neuroimaging with connectivity approaches. *Brain : a journal of neurology* 134: 1264-1276, 2011.
- Grefkes C, Nowak DA, Eickhoff SB, Dafotakis M, Kust J, Karbe H, and Fink GR.** Cortical connectivity after subcortical stroke assessed with functional magnetic resonance imaging. *Annals of neurology* 63: 236-246, 2008b.
- Hamzei F, Dettmers C, Rijntjes M, and Weiller C.** The effect of cortico-spinal tract damage on primary sensorimotor cortex activation after rehabilitation therapy. *Experimental brain research* 190: 329-336, 2008.
- Harvey RL, Edwards D, Dunning K, Fregni F, Stein J, Laine J, Rogers LM, Vox F, Durand-Sanchez A, Bockbrader M, Goldstein LB, Francisco GE, Kinney CL, Liu CY, and * NTI.** Randomized Sham-Controlled Trial of Navigated Repetitive Transcranial Magnetic Stimulation for Motor Recovery in Stroke. *Stroke; a journal of cerebral circulation* 49: 2138-2146, 2018.
- Hasegawa K, Kasuga S, Takasaki K, Mizuno K, Liu M, and Ushiba J.** Ipsilateral EEG mu rhythm reflects the excitability of uncrossed pathways projecting to shoulder muscles. *Journal of neuroengineering and rehabilitation* 14: 85, 2017.
- Hawe RL, Scott SH, and Dukelow SP.** Taking Proportional Out of Stroke Recovery. *Stroke; a journal of cerebral circulation* STROKEAHA118023006, 2018.
- Herbert WJ, Powell K, and Buford JA.** Evidence for a role of the reticulospinal system in recovery of skilled reaching after cortical stroke: initial results from a model of ischemic cortical injury. *Experimental brain research* 233: 3231-3251, 2015.
- Herz DM, Christensen MS, Reck C, Florin E, Barbe MT, Stahlhut C, Pauls KA, Tittgemeyer M, Siebner HR, and Timmermann L.** Task-specific modulation of effective connectivity during two simple unimanual motor tasks: a 122-channel EEG study. *NeuroImage* 59: 3187-3193, 2012.

- Hirschauer TJ, and Buford JA.** Bilateral force transients in the upper limbs evoked by single-pulse microstimulation in the pontomedullary reticular formation. *Journal of neurophysiology* 113: 2592-2604, 2015.
- Honeycutt CF, and Perreault EJ.** Deficits in startle-evoked arm movements increase with impairment following stroke. *Clinical neurophysiology : official journal of the International Federation of Clinical Neurophysiology* 125: 1682-1688, 2014.
- Hope TMH, Friston K, Price CJ, Leff AP, Rotshtein P, and Bowman H.** Recovery after stroke: not so proportional after all? *Brain : a journal of neurology* 142: 15-22, 2019.
- Horenstein C, Lowe MJ, Koenig KA, and Phillips MD.** Comparison of unilateral and bilateral complex finger tapping-related activation in premotor and primary motor cortex. *Human brain mapping* 30: 1397-1412, 2009.
- Hotson G, Fifer MS, Acharya S, Benz HL, Anderson WS, Thakor NV, and Crone NE.** Coarse electrocorticographic decoding of ipsilateral reach in patients with brain lesions. *PloS one* 9: e115236, 2014.
- Hu XL, Tong KY, Song R, Zheng XJ, and Leung WW.** A comparison between electromyography-driven robot and passive motion device on wrist rehabilitation for chronic stroke. *Neurorehabilitation and neural repair* 23: 837-846, 2009.
- Hu XL, Tong RK, Ho NS, Xue JJ, Rong W, and Li LS.** Wrist Rehabilitation Assisted by an Electromyography-Driven Neuromuscular Electrical Stimulation Robot After Stroke. *Neurorehabilitation and neural repair* 29: 767-776, 2015.
- Huang MX, Harrington DL, Paulson KM, Weisend MP, and Lee RR.** Temporal dynamics of ipsilateral and contralateral motor activity during voluntary finger movement. *Human brain mapping* 23: 26-39, 2004.
- Hubbard IJ, Carey LM, Budd TW, Levi C, McElduff P, Hudson S, Bateman G, and Parsons MW.** A Randomized Controlled Trial of the Effect of Early Upper-Limb Training on Stroke Recovery and Brain Activation. *Neurorehabilitation and neural repair* 29: 703-713, 2015.
- Hubbard IJ, Parsons MW, Neilson C, and Carey LM.** Task-specific training: evidence for and translation to clinical practice. *Occup Ther Int* 16: 175-189, 2009.
- Hummel F, Kirsammer R, and Gerloff C.** Ipsilateral cortical activation during finger sequences of increasing complexity: representation of movement difficulty or memory load? *Clinical neurophysiology : official journal of the International Federation of Clinical Neurophysiology* 114: 605-613, 2003.
- Hummel FC, Steven B, Hoppe J, Heise K, Thomalla G, Cohen LG, and Gerloff C.** Deficient intracortical inhibition (SICI) during movement preparation after chronic stroke. *Neurology* 72: 1766-1772, 2009.
- Igarashi J, Isomura Y, Arai K, Harukuni R, and Fukai T.** A theta-gamma oscillation code for neuronal coordination during motor behavior. *The Journal of neuroscience : the official journal of the Society for Neuroscience* 33: 18515-18530, 2013.
- Jahanshahi M, Jenkins IH, Brown RG, Marsden CD, Passingham RE, and Brooks DJ.** Self-initiated versus externally triggered movements. I. An investigation using measurement of regional cerebral blood flow with PET and movement-related potentials in normal and Parkinson's disease subjects. *Brain : a journal of neurology* 118 (Pt 4): 913-933, 1995.
- Jankelowitz SK, and Colebatch JG.** The acoustic startle reflex in ischemic stroke. *Neurology* 62: 114-116, 2004.

- Jenkins IH, Jahanshahi M, Jueptner M, Passingham RE, and Brooks DJ.** Self-initiated versus externally triggered movements. II. The effect of movement predictability on regional cerebral blood flow. *Brain : a journal of neurology* 123 (Pt 6): 1216-1228, 2000.
- Jensen O, and Tesche CD.** Frontal theta activity in humans increases with memory load in a working memory task. *The European journal of neuroscience* 15: 1395-1399, 2002.
- Johansen-Berg H, Dawes H, Guy C, Smith SM, Wade DT, and Matthews PM.** Correlation between motor improvements and altered fMRI activity after rehabilitative therapy. *Brain : a journal of neurology* 125: 2731-2742, 2002a.
- Johansen-Berg H, Rushworth MF, Bogdanovic MD, Kischka U, Wimalaratna S, and Matthews PM.** The role of ipsilateral premotor cortex in hand movement after stroke. *Proceedings of the National Academy of Sciences of the United States of America* 99: 14518-14523, 2002b.
- Johnson MD, and Heckman CJ.** Gain control mechanisms in spinal motoneurons. *Frontiers in neural circuits* 8: 81, 2014.
- Jones TA.** Motor compensation and its effects on neural reorganization after stroke. *Nat Rev Neurosci* 2017.
- Jones TA.** Multiple synapse formation in the motor cortex opposite unilateral sensorimotor cortex lesions in adult rats. *J Comp Neurol* 414: 57-66, 1999.
- Jones TA, and Schallert T.** Use-dependent growth of pyramidal neurons after neocortical damage. *The Journal of neuroscience : the official journal of the Society for Neuroscience* 14: 2140-2152, 1994.
- Jorgensen HS, Nakayama H, Raaschou HO, Vive-Larsen J, Stoier M, and Olsen TS.** Outcome and time course of recovery in stroke. Part II: Time course of recovery. The Copenhagen Stroke Study. *Archives of physical medicine and rehabilitation* 76: 406-412, 1995.
- Joundi RA, Jenkinson N, Brittain JS, Aziz TZ, and Brown P.** Driving oscillatory activity in the human cortex enhances motor performance. *Current biology : CB* 22: 403-407, 2012.
- Jurgens U.** The efferent and afferent connections of the supplementary motor area. *Brain research* 300: 63-81, 1984.
- Kamper DG, Fischer HC, Cruz EG, and Rymer WZ.** Weakness is the primary contributor to finger impairment in chronic stroke. *Archives of physical medicine and rehabilitation* 87: 1262-1269, 2006.
- Kandel ER, Schwartz JH, Jessell TM, Siegelbaum SA, and Hudspeth AJ.** *Principles of Neural Science*. McGraw-Hill Companies, Inc., 2013.
- Karbasforoushan H, Cohen-Adad J, and Dewald JPA.** Brainstem and spinal cord MRI identifies altered sensorimotor pathways post-stroke. *Nature communications* (In Press).
- Khanna P, and Carmena JM.** Beta band oscillations in motor cortex reflect neural population signals that delay movement onset. *Elife* 6: 2017.
- Kilner JM, Alonso-Alonso M, Fisher R, and Lemon RN.** Modulation of synchrony between single motor units during precision grip tasks in humans. *The Journal of physiology* 541: 937-948, 2002.
- Kim SY, Allred RP, Adkins DL, Tennant KA, Donlan NA, Kleim JA, and Jones TA.** Experience with the "good" limb induces aberrant synaptic plasticity in the perilesion cortex after stroke. *The Journal of neuroscience : the official journal of the Society for Neuroscience* 35: 8604-8610, 2015.

- Kitago T, Liang J, Huang VS, Hayes S, Simon P, Tenteromano L, Lazar RM, Marshall RS, Mazzoni P, Lennihan L, and Krakauer JW.** Improvement after constraint-induced movement therapy: recovery of normal motor control or task-specific compensation? *Neurorehabilitation and neural repair* 27: 99-109, 2013.
- Klamroth-Marganska V, Blanco J, Campen K, Curt A, Dietz V, Ettlin T, Felder M, Fellinghauer B, Guidali M, Kollmar A, Luft A, Nef T, Schuster-Amft C, Stahel W, and Riener R.** Three-dimensional, task-specific robot therapy of the arm after stroke: a multicentre, parallel-group randomised trial. *Lancet Neurol* 13: 159-166, 2014.
- Kleim JA, Barbay S, Cooper NR, Hogg TM, Reidel CN, Remple MS, and Nudo RJ.** Motor learning-dependent synaptogenesis is localized to functionally reorganized motor cortex. *Neurobiol Learn Mem* 77: 63-77, 2002.
- Kleim JA, Barbay S, and Nudo RJ.** Functional reorganization of the rat motor cortex following motor skill learning. *Journal of neurophysiology* 80: 3321-3325, 1998.
- Kokotilo KJ, Eng JJ, McKeown MJ, and Boyd LA.** Greater activation of secondary motor areas is related to less arm use after stroke. *Neurorehabilitation and neural repair* 24: 78-87, 2010.
- Kopell N, Ermentrout GB, Whittington MA, and Traub RD.** Gamma rhythms and beta rhythms have different synchronization properties. *Proceedings of the National Academy of Sciences of the United States of America* 97: 1867-1872, 2000.
- Kopell N, Kramer MA, Malerba P, and Whittington MA.** Are different rhythms good for different functions? *Frontiers in human neuroscience* 4: 187, 2010.
- Krakauer JW, Carmichael ST, Corbett D, and Wittenberg GF.** Getting neurorehabilitation right: what can be learned from animal models? *Neurorehabilitation and neural repair* 26: 923-931, 2012.
- Kurata K, and Wise SP.** Premotor and supplementary motor cortex in rhesus monkeys: neuronal activity during externally- and internally-instructed motor tasks. *Experimental brain research* 72: 237-248, 1988.
- Kuypers HG, Fleming WR, and Farinholt JW.** Subcorticospinal projections in the rhesus monkey. *J Comp Neurol* 118: 107-137, 1962.
- Kwakkel G, Veerbeek JM, van Wegen EE, and Wolf SL.** Constraint-induced movement therapy after stroke. *Lancet Neurol* 14: 224-234, 2015.
- Kwakkel G, Winters C, van Wegen EE, Nijland RH, van Kuijk AA, Visser-Meily A, de Groot J, de Vlugt E, Arendzen JH, Geurts AC, Meskers CG, and Consortium EX-S.** Effects of Unilateral Upper Limb Training in Two Distinct Prognostic Groups Early After Stroke: The EXPLICIT-Stroke Randomized Clinical Trial. *Neurorehabilitation and neural repair* 2016.
- Lacey MG, Gooding-Williams G, Prokic EJ, Yamawaki N, Hall SD, Stanford IM, and Woodhall GL.** Spike firing and IPSPs in layer V pyramidal neurons during beta oscillations in rat primary motor cortex (M1) in vitro. *PloS one* 9: e85109, 2014.
- Lan Y, Yao J, and Dewald JPA.** The Impact of Shoulder Abduction Loading on Volitional Hand Opening and Grasping in Chronic Hemiparetic Stroke. *Neurorehabilitation and neural repair* 31: 521-529, 2017.
- Lang CE, and Beebe JA.** Relating movement control at 9 upper extremity segments to loss of hand function in people with chronic hemiparesis. *Neurorehabilitation and neural repair* 21: 279-291, 2007.

- Lang CE, Wagner JM, Bastian AJ, Hu Q, Edwards DF, Sahrman SA, and Dromerick AW.** Deficits in grasp versus reach during acute hemiparesis. *Experimental brain research* 166: 126-136, 2005.
- Lang CE, Wagner JM, Edwards DF, Sahrman SA, and Dromerick AW.** Recovery of grasp versus reach in people with hemiparesis poststroke. *Neurorehabilitation and neural repair* 20: 444-454, 2006.
- Langer N, Hanggi J, Muller NA, Simmen HP, and Jancke L.** Effects of limb immobilization on brain plasticity. *Neurology* 78: 182-188, 2012.
- Lara AH, Cunningham JP, and Churchland MM.** Different population dynamics in the supplementary motor area and motor cortex during reaching. *Nature communications* 9: 2754, 2018.
- Lawrence DG, and Kuypers HG.** The functional organization of the motor system in the monkey. I. The effects of bilateral pyramidal lesions. *Brain : a journal of neurology* 91: 1-14, 1968.
- Lemon RN.** Descending pathways in motor control. *Annual review of neuroscience* 31: 195-218, 2008.
- Lemon RN.** The G. L. Brown Prize Lecture. Cortical control of the primate hand. *Exp Physiol* 78: 263-301, 1993.
- Levin MF, Kleim JA, and Wolf SL.** What do motor "recovery" and "compensation" mean in patients following stroke? *Neurorehabilitation and neural repair* 23: 313-319, 2009.
- Li S, Chen YT, Francisco GE, Zhou P, and Rymer WZ.** A Unifying Pathophysiological Account for Post-stroke Spasticity and Disordered Motor Control. *Front Neurol* 10: 468, 2019.
- Li S, and Francisco GE.** New insights into the pathophysiology of post-stroke spasticity. *Frontiers in human neuroscience* 9: 192, 2015.
- Liepert J, Hamzei F, and Weiller C.** Motor cortex disinhibition of the unaffected hemisphere after acute stroke. *Muscle & nerve* 23: 1761-1763, 2000.
- Lin LY, Ramsey L, Metcalf NV, Rengachary J, Shulman GL, Shimony JS, and Corbetta M.** Stronger prediction of motor recovery and outcome post-stroke by cortico-spinal tract integrity than functional connectivity. *PloS one* 13: e0202504, 2018.
- Lo AC, Guarino PD, Richards LG, Haselkorn JK, Wittenberg GF, Federman DG, Ringer RJ, Wagner TH, Krebs HI, Volpe BT, Bever CT, Jr., Bravata DM, Duncan PW, Corn BH, Maffucci AD, Nadeau SE, Conroy SS, Powell JM, Huang GD, and Peduzzi P.** Robot-assisted therapy for long-term upper-limb impairment after stroke. *N Engl J Med* 362: 1772-1783, 2010.
- Loehrer PA, Nettersheim FS, Jung F, Weber I, Huber C, Dembek TA, Pelzer EA, Fink GR, Tittgemeyer M, and Timmermann L.** Ageing changes effective connectivity of motor networks during bimanual finger coordination. *NeuroImage* 143: 325-342, 2016.
- Lotze M, Beutling W, Loibl M, Domin M, Platz T, Schminke U, and Byblow WD.** Contralesional motor cortex activation depends on ipsilesional corticospinal tract integrity in well-recovered subcortical stroke patients. *Neurorehabilitation and neural repair* 26: 594-603, 2012.
- Loubinoux I, Carel C, Pariente J, Dechaumont S, Albucher JF, Marque P, Manelfe C, and Chollet F.** Correlation between cerebral reorganization and motor recovery after subcortical infarcts. *NeuroImage* 20: 2166-2180, 2003.

- Macpherson J, Wiesendanger M, Marangoz C, and Miles TS.** Corticospinal neurones of the supplementary motor area of monkeys. A single unit study. *Experimental brain research* 48: 81-88, 1982.
- Maier IC, Baumann K, Thallmair M, Weinmann O, Scholl J, and Schwab ME.** Constraint-induced movement therapy in the adult rat after unilateral corticospinal tract injury. *The Journal of neuroscience : the official journal of the Society for Neuroscience* 28: 9386-9403, 2008.
- Maier MA, Armand J, Kirkwood PA, Yang HW, Davis JN, and Lemon RN.** Differences in the corticospinal projection from primary motor cortex and supplementary motor area to macaque upper limb motoneurons: an anatomical and electrophysiological study. *Cerebral cortex* 12: 281-296, 2002.
- Maldonado MA, Allred RP, Felthouser EL, and Jones TA.** Motor skill training, but not voluntary exercise, improves skilled reaching after unilateral ischemic lesions of the sensorimotor cortex in rats. *Neurorehabilitation and neural repair* 22: 250-261, 2008.
- Maraka S, Jiang Q, Jafari-Khouzani K, Li L, Malik S, Hamidian H, Zhang T, Lu M, Soltanian-Zadeh H, Chopp M, and Mitsias PD.** Degree of corticospinal tract damage correlates with motor function after stroke. *Ann Clin Transl Neurol* 1: 891-899, 2014.
- Matelli M, Luppino G, Fogassi L, and Rizzolatti G.** Thalamic input to inferior area 6 and area 4 in the macaque monkey. *J Comp Neurol* 280: 468-488, 1989.
- Matsuyama K, Mori F, Kuze B, and Mori S.** Morphology of single pontine reticulospinal axons in the lumbar enlargement of the cat: a study using the anterograde tracer PHA-L. *J Comp Neurol* 410: 413-430, 1999.
- Matsuyama K, Takakusaki K, Nakajima K, and Mori S.** Multi-segmental innervation of single pontine reticulospinal axons in the cervico-thoracic region of the cat: anterograde PHA-L tracing study. *J Comp Neurol* 377: 234-250, 1997.
- Mayka MA, Corcos DM, Leurgans SE, and Vaillancourt DE.** Three-dimensional locations and boundaries of motor and premotor cortices as defined by functional brain imaging: a meta-analysis. *NeuroImage* 31: 1453-1474, 2006.
- McCabe J, Monkiewicz M, Holcomb J, Pundik S, and Daly JJ.** Comparison of robotics, functional electrical stimulation, and motor learning methods for treatment of persistent upper extremity dysfunction after stroke: a randomized controlled trial. *Archives of physical medicine and rehabilitation* 96: 981-990, 2015.
- McCombe Waller S, Whittall J, Jenkins T, Magder LS, Hanley DF, Goldberg A, and Luft AR.** Sequencing bilateral and unilateral task-oriented training versus task oriented training alone to improve arm function in individuals with chronic stroke. *BMC Neurol* 14: 236, 2014.
- McPherson JG, Chen A, Ellis MD, Yao J, Heckman CJ, and Dewald JPA.** Progressive recruitment of contralesional cortico-reticulospinal pathways drives motor impairment post stroke. *The Journal of physiology* 596: 1211-1225, 2018a.
- McPherson JG, Ellis MD, Harden RN, Carmona C, Drogos JM, Heckman CJ, and Dewald JPA.** Neuromodulatory Inputs to Motoneurons Contribute to the Loss of Independent Joint Control in Chronic Moderate to Severe Hemiparetic Stroke. *Front Neurol* 9: 470, 2018b.
- McPherson JG, Ellis MD, Heckman CJ, and Dewald JP.** Evidence for increased activation of persistent inward currents in individuals with chronic hemiparetic stroke. *Journal of neurophysiology* 100: 3236-3243, 2008.

- McPherson JG, Stienen AHA, Drogos JM, and Dewald JPA.** Modification of spastic stretch reflexes at the elbow by flexion synergy expression in individuals with chronic hemiparetic stroke. *Archives of physical medicine and rehabilitation* 2017.
- McPherson LM, and Dewald JPA.** Differences between flexion and extension synergy-driven coupling at the elbow, wrist, and fingers of individuals with chronic hemiparetic stroke. *Clinical neurophysiology : official journal of the International Federation of Clinical Neurophysiology* 130: 454-468, 2019.
- Mehrholtz J, Pohl M, Platz T, Kugler J, and Elsner B.** Electromechanical and robot-assisted arm training for improving activities of daily living, arm function, and arm muscle strength after stroke. *Cochrane Database Syst Rev* CD006876, 2015.
- Michielsen ME, Selles RW, van der Geest JN, Eckhardt M, Yavuzer G, Stam HJ, Smits M, Ribbers GM, and Bussmann JB.** Motor recovery and cortical reorganization after mirror therapy in chronic stroke patients: a phase II randomized controlled trial. *Neurorehabilitation and neural repair* 25: 223-233, 2011.
- Miller LC, and Dewald JP.** Involuntary paretic wrist/finger flexion forces and EMG increase with shoulder abduction load in individuals with chronic stroke. *Clinical neurophysiology : official journal of the International Federation of Clinical Neurophysiology* 123: 1216-1225, 2012.
- Moisa M, Polania R, Grueschow M, and Ruff CC.** Brain Network Mechanisms Underlying Motor Enhancement by Transcranial Entrainment of Gamma Oscillations. *The Journal of neuroscience : the official journal of the Society for Neuroscience* 36: 12053-12065, 2016.
- Montgomery LR, Herbert WJ, and Buford JA.** Recruitment of ipsilateral and contralateral upper limb muscles following stimulation of the cortical motor areas in the monkey. *Experimental brain research* 230: 153-164, 2013.
- Morecraft RJ, and Van Hoesen GW.** Frontal granular cortex input to the cingulate (M3), supplementary (M2) and primary (M1) motor cortices in the rhesus monkey. *J Comp Neurol* 337: 669-689, 1993.
- Mozaffarian D, Benjamin EJ, Go AS, Arnett DK, Blaha MJ, Cushman M, de Ferranti S, Despres JP, Fullerton HJ, Howard VJ, Huffman MD, Judd SE, Kissela BM, Lackland DT, Lichtman JH, Lisabeth LD, Liu S, Mackey RH, Matchar DB, McGuire DK, Mohler ER, 3rd, Moy CS, Muntner P, Mussolino ME, Nasir K, Neumar RW, Nichol G, Palaniappan L, Pandey DK, Reeves MJ, Rodriguez CJ, Sorlie PD, Stein J, Towfighi A, Turan TN, Virani SS, Willey JZ, Woo D, Yeh RW, Turner MB, American Heart Association Statistics C, and Stroke Statistics S.** Heart disease and stroke statistics--2015 update: a report from the American Heart Association. *Circulation* 131: e29-322, 2015.
- Muakkassa KF, and Strick PL.** Frontal lobe inputs to primate motor cortex: evidence for four somatotopically organized 'premotor' areas. *Brain research* 177: 176-182, 1979.
- Murase N, Duque J, Mazzocchio R, and Cohen LG.** Influence of interhemispheric interactions on motor function in chronic stroke. *Annals of neurology* 55: 400-409, 2004.
- Murata Y, Higo N, Oishi T, Yamashita A, Matsuda K, Hayashi M, and Yamane S.** Effects of motor training on the recovery of manual dexterity after primary motor cortex lesion in macaque monkeys. *Journal of neurophysiology* 99: 773-786, 2008.
- Murphy TH, and Corbett D.** Plasticity during stroke recovery: from synapse to behaviour. *Nat Rev Neurosci* 10: 861-872, 2009.

- Nachev P, Kennard C, and Husain M.** Functional role of the supplementary and pre-supplementary motor areas. *Nat Rev Neurosci* 9: 856-869, 2008.
- Nair DG, Hutchinson S, Fregni F, Alexander M, Pascual-Leone A, and Schlaug G.** Imaging correlates of motor recovery from cerebral infarction and their physiological significance in well-recovered patients. *NeuroImage* 34: 253-263, 2007.
- Nathan PW, and Smith MC.** Long descending tracts in man. I. Review of present knowledge. *Brain : a journal of neurology* 78: 248-303, 1955.
- Ng KL, Gibson EM, Hubbard R, Yang J, Caffo B, O'Brien RJ, Krakauer JW, and Zeiler SR.** Fluoxetine Maintains a State of Heightened Responsiveness to Motor Training Early After Stroke in a Mouse Model. *Stroke; a journal of cerebral circulation* 46: 2951-2960, 2015.
- Nowak M, Hinson E, van Ede F, Pogosyan A, Guerra A, Quinn A, Brown P, and Stagg CJ.** Driving Human Motor Cortical Oscillations Leads to Behaviorally Relevant Changes in Local GABAA Inhibition: A tACS-TMS Study. *The Journal of neuroscience : the official journal of the Society for Neuroscience* 37: 4481-4492, 2017.
- Nudo RJ.** Recovery after brain injury: mechanisms and principles. *Frontiers in human neuroscience* 7: 887, 2013.
- Nudo RJ, and Milliken GW.** Reorganization of movement representations in primary motor cortex following focal ischemic infarcts in adult squirrel monkeys. *Journal of neurophysiology* 75: 2144-2149, 1996.
- Nudo RJ, Milliken GW, Jenkins WM, and Merzenich MM.** Use-dependent alterations of movement representations in primary motor cortex of adult squirrel monkeys. *The Journal of neuroscience : the official journal of the Society for Neuroscience* 16: 785-807, 1996a.
- Nudo RJ, Wise BM, SiFuentes F, and Milliken GW.** Neural substrates for the effects of rehabilitative training on motor recovery after ischemic infarct. *Science* 272: 1791-1794, 1996b.
- O'Dwyer NJ, Ada L, and Neilson PD.** Spasticity and muscle contracture following stroke. *Brain : a journal of neurology* 119 (Pt 5): 1737-1749, 1996.
- Ohara S, Ikeda A, Kunieda T, Yazawa S, Baba K, Nagamine T, Taki W, Hashimoto N, Mihara T, and Shibasaki H.** Movement-related change of electrocorticographic activity in human supplementary motor area proper. *Brain : a journal of neurology* 123 (Pt 6): 1203-1215, 2000.
- Okano K, and Tanji J.** Neuronal activities in the primate motor fields of the agranular frontal cortex preceding visually triggered and self-paced movement. *Experimental brain research* 66: 155-166, 1987.
- Owen M, Ingo C, and Dewald JPA.** Upper Extremity Motor Impairments and Microstructural Changes in Bulbosplinal Pathways in Chronic Hemiparetic Stroke. *Front Neurol* 8: 257, 2017.
- Page SJ, Levine PG, and Basobas BA.** "Reps" Aren't Enough: Augmenting Functional Electrical Stimulation With Behavioral Supports Significantly Reduces Impairment in Moderately Impaired Stroke. *Archives of physical medicine and rehabilitation* 97: 747-752, 2016.
- Pagnussat AS, Simao F, Anastacio JR, Mestriner RG, Michaelsen SM, Castro CC, Salbego C, and Netto CA.** Effects of skilled and unskilled training on functional recovery and brain plasticity after focal ischemia in adult rats. *Brain research* 1486: 53-61, 2012.
- Park CH, Chang WH, Ohn SH, Kim ST, Bang OY, Pascual-Leone A, and Kim YH.** Longitudinal changes of resting-state functional connectivity during motor recovery after stroke. *Stroke; a journal of cerebral circulation* 42: 1357-1362, 2011.

- Pekna M, Pekny M, and Nilsson M.** Modulation of neural plasticity as a basis for stroke rehabilitation. *Stroke; a journal of cerebral circulation* 43: 2819-2828, 2012.
- Penny WD, Stephan KE, Mechelli A, and Friston KJ.** Comparing dynamic causal models. *NeuroImage* 22: 1157-1172, 2004.
- Peterson BW, Maunz RA, Pitts NG, and Mackel RG.** Patterns of projection and branching of reticulospinal neurons. *Experimental brain research* 23: 333-351, 1975.
- Picard N, and Strick PL.** Activation of the supplementary motor area (SMA) during performance of visually guided movements. *Cerebral cortex* 13: 977-986, 2003.
- Picazio S, Veniero D, Ponso V, Caltagirone C, Gross J, Thut G, and Koch G.** Prefrontal control over motor cortex cycles at beta frequency during movement inhibition. *Current biology : CB* 24: 2940-2945, 2014.
- Platz T, van Kaick S, Mehrholz J, Leidner O, Eickhof C, and Pohl M.** Best conventional therapy versus modular impairment-oriented training for arm paresis after stroke: a single-blind, multicenter randomized controlled trial. *Neurorehabilitation and neural repair* 23: 706-716, 2009.
- Plautz EJ, Milliken GW, and Nudo RJ.** Effects of repetitive motor training on movement representations in adult squirrel monkeys: role of use versus learning. *Neurobiol Learn Mem* 74: 27-55, 2000.
- Po C, Kalthoff D, Kim YB, Nelles M, and Hoehn M.** White matter reorganization and functional response after focal cerebral ischemia in the rat. *PloS one* 7: e45629, 2012.
- Pogosyan A, Gaynor LD, Eusebio A, and Brown P.** Boosting cortical activity at Beta-band frequencies slows movement in humans. *Current biology : CB* 19: 1637-1641, 2009.
- Prabhakaran S, Zarahn E, Riley C, Speizer A, Chong JY, Lazar RM, Marshall RS, and Krakauer JW.** Inter-individual variability in the capacity for motor recovery after ischemic stroke. *Neurorehabilitation and neural repair* 22: 64-71, 2008.
- Ralston DD, and Ralston HJ, 3rd.** The terminations of corticospinal tract axons in the macaque monkey. *J Comp Neurol* 242: 325-337, 1985.
- Rehme AK, Eickhoff SB, Rottschy C, Fink GR, and Grefkes C.** Activation likelihood estimation meta-analysis of motor-related neural activity after stroke. *NeuroImage* 59: 2771-2782, 2012.
- Rehme AK, and Grefkes C.** Cerebral network disorders after stroke: evidence from imaging-based connectivity analyses of active and resting brain states in humans. *The Journal of physiology* 591: 17-31, 2013.
- Riddle CN, Edgley SA, and Baker SN.** Direct and indirect connections with upper limb motoneurons from the primate reticulospinal tract. *The Journal of neuroscience : the official journal of the Society for Neuroscience* 29: 4993-4999, 2009.
- Riehle A, and Requin J.** Monkey primary motor and premotor cortex: single-cell activity related to prior information about direction and extent of an intended movement. *Journal of neurophysiology* 61: 534-549, 1989.
- Ritter P, Moosmann M, and Villringer A.** Rolandic alpha and beta EEG rhythms' strengths are inversely related to fMRI-BOLD signal in primary somatosensory and motor cortex. *Human brain mapping* 30: 1168-1187, 2009.
- Rizzolatti G, Camarda R, Fogassi L, Gentilucci M, Luppino G, and Matelli M.** Functional organization of inferior area 6 in the macaque monkey. II. Area F5 and the control of distal movements. *Experimental brain research* 71: 491-507, 1988.

- Roger VL, Go AS, Lloyd-Jones DM, Benjamin EJ, Berry JD, Borden WB, Bravata DM, Dai S, Ford ES, Fox CS, Fullerton HJ, Gillespie C, Hailpern SM, Heit JA, Howard VJ, Kissela BM, Kittner SJ, Lackland DT, Lichtman JH, Lisabeth LD, Makuc DM, Marcus GM, Marelli A, Matchar DB, Moy CS, Mozaffarian D, Mussolino ME, Nichol G, Paynter NP, Soliman EZ, Sorlie PD, Sotoodehnia N, Turan TN, Virani SS, Wong ND, Woo D, Turner MB, American Heart Association Statistics C, and Stroke Statistics S.** Heart disease and stroke statistics--2012 update: a report from the American Heart Association. *Circulation* 125: e2-e220, 2012.
- Romo R, and Schultz W.** Neuronal activity preceding self-initiated or externally timed arm movements in area 6 of monkey cortex. *Experimental brain research* 67: 656-662, 1987.
- Roopun AK, Middleton SJ, Cunningham MO, LeBeau FE, Bibbig A, Whittington MA, and Traub RD.** A beta2-frequency (20-30 Hz) oscillation in nonsynaptic networks of somatosensory cortex. *Proceedings of the National Academy of Sciences of the United States of America* 103: 15646-15650, 2006.
- Rossiter HE, Boudrias MH, and Ward NS.** Do movement-related beta oscillations change after stroke? *Journal of neurophysiology* 112: 2053-2058, 2014.
- Rouiller EM, Babalian A, Kazennikov O, Moret V, Yu XH, and Wiesendanger M.** Transcallosal connections of the distal forelimb representations of the primary and supplementary motor cortical areas in macaque monkeys. *Experimental brain research* 102: 227-243, 1994.
- Sanes JN, and Donoghue JP.** Plasticity and primary motor cortex. *Annual review of neuroscience* 23: 393-415, 2000.
- Sathian K, Buxbaum LJ, Cohen LG, Krakauer JW, Lang CE, Corbetta M, and Fitzpatrick SM.** Neurological principles and rehabilitation of action disorders: common clinical deficits. *Neurorehabilitation and neural repair* 25: 21S-32S, 2011.
- Sawaki L, Butler AJ, Leng X, Wassenaar PA, Mohammad YM, Blanton S, Sathian K, Nichols-Larsen DS, Wolf SL, Good DC, and Wittenberg GF.** Constraint-induced movement therapy results in increased motor map area in subjects 3 to 9 months after stroke. *Neurorehabilitation and neural repair* 22: 505-513, 2008.
- Schaechter JD, Perdue KL, and Wang R.** Structural damage to the corticospinal tract correlates with bilateral sensorimotor cortex reorganization in stroke patients. *NeuroImage* 39: 1370-1382, 2008.
- Schell GR, and Strick PL.** The origin of thalamic inputs to the arcuate premotor and supplementary motor areas. *The Journal of neuroscience : the official journal of the Society for Neuroscience* 4: 539-560, 1984.
- Schmit BD, Dewald JP, and Rymer WZ.** Stretch reflex adaptation in elbow flexors during repeated passive movements in unilateral brain-injured patients. *Archives of physical medicine and rehabilitation* 81: 269-278, 2000.
- Schulz R, Park CH, Boudrias MH, Gerloff C, Hummel FC, and Ward NS.** Assessing the integrity of corticospinal pathways from primary and secondary cortical motor areas after stroke. *Stroke; a journal of cerebral circulation* 43: 2248-2251, 2012.
- Seidler RD, Noll DC, and Thiers G.** Feedforward and feedback processes in motor control. *NeuroImage* 22: 1775-1783, 2004.
- Sharma N, Baron JC, and Rowe JB.** Motor imagery after stroke: relating outcome to motor network connectivity. *Annals of neurology* 66: 604-616, 2009.

- Shibasaki H, and Hallett M.** What is the Bereitschaftspotential? *Clinical neurophysiology : official journal of the International Federation of Clinical Neurophysiology* 117: 2341-2356, 2006.
- Singer BJ, Vallence AM, Cleary S, Cooper I, and Loftus AM.** The effect of EMG triggered electrical stimulation plus task practice on arm function in chronic stroke patients with moderate-severe arm deficits. *Restorative neurology and neuroscience* 31: 681-691, 2013.
- Smith SM, Jenkinson M, Woolrich MW, Beckmann CF, Behrens TE, Johansen-Berg H, Bannister PR, De Luca M, Drobnjak I, Flitney DE, Niazy RK, Saunders J, Vickers J, Zhang Y, De Stefano N, Brady JM, and Matthews PM.** Advances in functional and structural MR image analysis and implementation as FSL. *NeuroImage* 23 Suppl 1: S208-219, 2004.
- Soteropoulos DS, Edgley SA, and Baker SN.** Lack of evidence for direct corticospinal contributions to control of the ipsilateral forelimb in monkey. *The Journal of neuroscience : the official journal of the Society for Neuroscience* 31: 11208-11219, 2011.
- Soteropoulos DS, Williams ER, and Baker SN.** Cells in the monkey ponto-medullary reticular formation modulate their activity with slow finger movements. *The Journal of physiology* 590: 4011-4027, 2012.
- Sowell ER, Thompson PM, Tessner KD, and Toga AW.** Mapping continued brain growth and gray matter density reduction in dorsal frontal cortex: Inverse relationships during postadolescent brain maturation. *The Journal of neuroscience : the official journal of the Society for Neuroscience* 21: 8819-8829, 2001.
- Stancak A, Jr., Feige B, Lucking CH, and Kristeva-Feige R.** Oscillatory cortical activity and movement-related potentials in proximal and distal movements. *Clinical neurophysiology : official journal of the International Federation of Clinical Neurophysiology* 111: 636-650, 2000.
- Starkey ML, and Schwab ME.** How Plastic Is the Brain after a Stroke? *Neuroscientist* 20: 359-371, 2014.
- Stephan KE, Penny WD, Daunizeau J, Moran RJ, and Friston KJ.** Bayesian model selection for group studies. *NeuroImage* 46: 1004-1017, 2009.
- Stinear CM, Barber PA, Smale PR, Coxon JP, Fleming MK, and Byblow WD.** Functional potential in chronic stroke patients depends on corticospinal tract integrity. *Brain : a journal of neurology* 130: 170-180, 2007.
- Sukal TM, Ellis MD, and Dewald JP.** Shoulder abduction-induced reductions in reaching work area following hemiparetic stroke: neuroscientific implications. *Experimental brain research* 183: 215-223, 2007.
- Sullivan JE, Drogos J, Carmona C, and Yao J.** The Post Stroke Upper Limb Improvement Effort Survey (IMPETUS): A Survey of individuals with Chronic Stroke. *Topics in stroke rehabilitation* Accepted.
- Sun H, Blakely TM, Darvas F, Wander JD, Johnson LA, Su DK, Miller KJ, Fetz EE, and Ojemann JG.** Sequential activation of premotor, primary somatosensory and primary motor areas in humans during cued finger movements. *Clinical neurophysiology : official journal of the International Federation of Clinical Neurophysiology* 126: 2150-2161, 2015.
- Szurhaj W, Labyt E, Bourriez JL, Kahane P, Chauvel P, Mauguiere F, and Derambure P.** Relationship between intracerebral gamma oscillations and slow potentials in the human sensorimotor cortex. *The European journal of neuroscience* 24: 947-954, 2006.
- Takahashi CD, Der-Yeghiaian L, Le V, Motiwala RR, and Cramer SC.** Robot-based hand motor therapy after stroke. *Brain : a journal of neurology* 131: 425-437, 2008.

- Takahashi K, Best MD, Huh N, Brown KA, Tobaa AA, and Hatsopoulos NG.** Encoding of both reaching and grasping kinematics in dorsal and ventral premotor cortices. *The Journal of neuroscience : the official journal of the Society for Neuroscience* 2017.
- Takemi M, Masakado Y, Liu M, and Ushiba J.** Event-related desynchronization reflects downregulation of intracortical inhibition in human primary motor cortex. *Journal of neurophysiology* 110: 1158-1166, 2013.
- Takemi M, Masakado Y, Liu M, and Ushiba J.** Sensorimotor event-related desynchronization represents the excitability of human spinal motoneurons. *Neuroscience* 297: 58-67, 2015.
- Tamakoshi K, Ishida A, Takamatsu Y, Hamakawa M, Nakashima H, Shimada H, and Ishida K.** Motor skills training promotes motor functional recovery and induces synaptogenesis in the motor cortex and striatum after intracerebral hemorrhage in rats. *Behav Brain Res* 260: 34-43, 2014.
- Tanji J.** Sequential organization of multiple movements: involvement of cortical motor areas. *Annual review of neuroscience* 24: 631-651, 2001.
- Tanji J, and Kurata K.** Comparison of movement-related activity in two cortical motor areas of primates. *Journal of neurophysiology* 48: 633-653, 1982.
- Tanji J, Okano K, and Sato KC.** Neuronal activity in cortical motor areas related to ipsilateral, contralateral, and bilateral digit movements of the monkey. *Journal of neurophysiology* 60: 325-343, 1988.
- Tanne-Gariepy J, Rouiller EM, and Boussaoud D.** Parietal inputs to dorsal versus ventral premotor areas in the macaque monkey: evidence for largely segregated visuomotor pathways. *Experimental brain research* 145: 91-103, 2002.
- Taub E, Uswatte G, and Elbert T.** New treatments in neurorehabilitation founded on basic research. *Nat Rev Neurosci* 3: 228-236, 2002.
- Taub E, Uswatte G, and Mark VW.** The functional significance of cortical reorganization and the parallel development of CI therapy. *Frontiers in human neuroscience* 8: 396, 2014.
- Tavakoli AV, and Yun K.** Transcranial Alternating Current Stimulation (tACS) Mechanisms and Protocols. *Front Cell Neurosci* 11: 214, 2017.
- Teasell R, Foley N, Salter K, Bhogal S, Jutai J, and Speechley M.** Evidence-Based Review of Stroke Rehabilitation: executive summary, 12th edition. *Topics in stroke rehabilitation* 16: 463-488, 2009.
- Thickbroom GW, Byrnes ML, Archer SA, and Mastaglia FL.** Motor outcome after subcortical stroke: MEPs correlate with hand strength but not dexterity. *Clinical neurophysiology : official journal of the International Federation of Clinical Neurophysiology* 113: 2025-2029, 2002.
- van Kerkoerle T, Self MW, Dagnino B, Gariel-Mathis MA, Poort J, van der Togt C, and Roelfsema PR.** Alpha and gamma oscillations characterize feedback and feedforward processing in monkey visual cortex. *Proceedings of the National Academy of Sciences of the United States of America* 111: 14332-14341, 2014.
- van Meer MP, van der Marel K, Wang K, Otte WM, El Bouazati S, Roeling TA, Viergever MA, Berkelbach van der Sprenkel JW, and Dijkhuizen RM.** Recovery of sensorimotor function after experimental stroke correlates with restoration of resting-state interhemispheric functional connectivity. *The Journal of neuroscience : the official journal of the Society for Neuroscience* 30: 3964-3972, 2010.

van Wijk BC, Beek PJ, and Daffertshofer A. Neural synchrony within the motor system: what have we learned so far? *Frontiers in human neuroscience* 6: 252, 2012.

Verstynen T, Diedrichsen J, Albert N, Aparicio P, and Ivry RB. Ipsilateral motor cortex activity during unimanual hand movements relates to task complexity. *Journal of neurophysiology* 93: 1209-1222, 2005.

Verstynen T, and Ivry RB. Network dynamics mediating ipsilateral motor cortex activity during unimanual actions. *J Cogn Neurosci* 23: 2468-2480, 2011.

von Stein A, and Sarnthein J. Different frequencies for different scales of cortical integration: from local gamma to long range alpha/theta synchronization. *Int J Psychophysiol* 38: 301-313, 2000.

Wang L, Yu C, Chen H, Qin W, He Y, Fan F, Zhang Y, Wang M, Li K, Zang Y, Woodward TS, and Zhu C. Dynamic functional reorganization of the motor execution network after stroke. *Brain : a journal of neurology* 133: 1224-1238, 2010.

Ward N. Assessment of cortical reorganisation for hand function after stroke. *The Journal of physiology* 589: 5625-5632, 2011.

Ward NS, Brander F, and Kelly K. Intensive upper limb neurorehabilitation in chronic stroke: outcomes from the Queen Square programme. *Journal of neurology, neurosurgery, and psychiatry* 90: 498-506, 2019.

Ward NS, Brown MM, Thompson AJ, and Frackowiak RS. Neural correlates of motor recovery after stroke: a longitudinal fMRI study. *Brain : a journal of neurology* 126: 2476-2496, 2003.

Ward NS, Newton JM, Swayne OB, Lee L, Thompson AJ, Greenwood RJ, Rothwell JC, and Frackowiak RS. Motor system activation after subcortical stroke depends on corticospinal system integrity. *Brain : a journal of neurology* 129: 809-819, 2006.

Wei K, Glaser JI, Deng L, Thompson CK, Stevenson IH, Wang Q, Hornby TG, Heckman CJ, and Kording KP. Serotonin affects movement gain control in the spinal cord. *The Journal of neuroscience : the official journal of the Society for Neuroscience* 34: 12690-12700, 2014.

Weilke F, Spiegel S, Boecker H, von Einsiedel HG, Conrad B, Schwaiger M, and Erhard P. Time-resolved fMRI of activation patterns in M1 and SMA during complex voluntary movement. *Journal of neurophysiology* 85: 1858-1863, 2001.

Wilkins KB, Owen M, Ingo C, Carmona C, Dewald JPA, and Yao J. Neural Plasticity in Moderate to Severe Chronic Stroke Following a Device-Assisted Task-Specific Arm/Hand Intervention. *Front Neurol* 8: 284, 2017.

Windhoff M, Opitz A, and Thielscher A. Electric field calculations in brain stimulation based on finite elements: an optimized processing pipeline for the generation and usage of accurate individual head models. *Human brain mapping* 34: 923-935, 2013.

Winkler AM, Ridgway GR, Webster MA, Smith SM, and Nichols TE. Permutation inference for the general linear model. *NeuroImage* 92: 381-397, 2014.

Winship IR, and Murphy TH. In vivo calcium imaging reveals functional rewiring of single somatosensory neurons after stroke. *The Journal of neuroscience : the official journal of the Society for Neuroscience* 28: 6592-6606, 2008.

Winstein CJ, Stein J, Arena R, Bates B, Cherney LR, Cramer SC, Deruyter F, Eng JJ, Fisher B, Harvey RL, Lang CE, MacKay-Lyons M, Ottenbacher KJ, Pugh S, Reeves MJ, Richards LG, Stiers W, Zorowitz RD, American Heart Association Stroke Council CoC, Stroke Nursing CoCC, Council on Quality of C, and Outcomes R. Guidelines for Adult

Stroke Rehabilitation and Recovery: A Guideline for Healthcare Professionals From the American Heart Association/American Stroke Association. *Stroke; a journal of cerebral circulation* 47: e98-e169, 2016a.

Winstein CJ, Wolf SL, Dromerick AW, Lane CJ, Nelsen MA, Lewthwaite R, Cen SY, Azen SP, and Interdisciplinary Comprehensive Arm Rehabilitation Evaluation Investigative T. Effect of a Task-Oriented Rehabilitation Program on Upper Extremity Recovery Following Motor Stroke: The ICARE Randomized Clinical Trial. *JAMA* 315: 571-581, 2016b.

Winters C, van Wegen EE, Daffertshofer A, and Kwakkel G. Generalizability of the Proportional Recovery Model for the Upper Extremity After an Ischemic Stroke. *Neurorehabilitation and neural repair* 29: 614-622, 2015.

Wise SP. The primate premotor cortex: past, present, and preparatory. *Annual review of neuroscience* 8: 1-19, 1985.

Wise SP, Boussaoud D, Johnson PB, and Caminiti R. Premotor and parietal cortex: corticocortical connectivity and combinatorial computations. *Annual review of neuroscience* 20: 25-42, 1997.

Wolf SL, Winstein CJ, Miller JP, Taub E, Uswatte G, Morris D, Giuliani C, Light KE, Nichols-Larsen D, and Investigators E. Effect of constraint-induced movement therapy on upper extremity function 3 to 9 months after stroke: the EXCITE randomized clinical trial. *JAMA* 296: 2095-2104, 2006.

Wu J, Quinlan EB, Dodakian L, McKenzie A, Kathuria N, Zhou RJ, Augsburger R, See J, Le VH, Srinivasan R, and Cramer SC. Connectivity measures are robust biomarkers of cortical function and plasticity after stroke. *Brain : a journal of neurology* 138: 2359-2369, 2015.

Yanagisawa T, Yamashita O, Hirata M, Kishima H, Saitoh Y, Goto T, Yoshimine T, and Kamitani Y. Regulation of motor representation by phase-amplitude coupling in the sensorimotor cortex. *The Journal of neuroscience : the official journal of the Society for Neuroscience* 32: 15467-15475, 2012.

Yao J, Chen A, Carmona C, and Dewald JP. Cortical overlap of joint representations contributes to the loss of independent joint control following stroke. *NeuroImage* 45: 490-499, 2009.

Yao J, and Dewald JP. Evaluation of different cortical source localization methods using simulated and experimental EEG data. *NeuroImage* 25: 369-382, 2005.

Yao J, and Dewald JPA. The Increase in Overlap of Cortical Activity Preceding Static Elbow/Shoulder Motor Tasks Is Associated With Limb Synergies in Severe Stroke. *Neurorehabilitation and neural repair* 32: 624-634, 2018.

Yao J, Drogos J, Veltink F, Anderson C, Concha Urday Zaa J, Hanson LI, and Dewald JP. The effect of transcranial direct current stimulation on the expression of the flexor synergy in the paretic arm in chronic stroke is dependent on shoulder abduction loading. *Frontiers in human neuroscience* 9: 262, 2015.

Yuan H, Liu T, Szarkowski R, Rios C, Ashe J, and He B. Negative covariation between task-related responses in alpha/beta-band activity and BOLD in human sensorimotor cortex: an EEG and fMRI study of motor imagery and movements. *NeuroImage* 49: 2596-2606, 2010.

Zaaimi B, Edgley SA, Soteropoulos DS, and Baker SN. Changes in descending motor pathway connectivity after corticospinal tract lesion in macaque monkey. *Brain : a journal of neurology* 135: 2277-2289, 2012.

Zaaimi B, Soteropoulos DS, Fisher KM, Riddle CN, and Baker SN. Classification of Neurons in the Primate Reticular Formation and Changes after Recovery from Pyramidal Tract Lesion. *The Journal of neuroscience : the official journal of the Society for Neuroscience* 38: 6190-6206, 2018.

Zatorre RJ, Fields RD, and Johansen-Berg H. Plasticity in gray and white: neuroimaging changes in brain structure during learning. *Nature neuroscience* 15: 528-536, 2012.

Zeiler SR, Hubbard R, Gibson EM, Zheng T, Ng K, O'Brien R, and Krakauer JW. Paradoxical Motor Recovery From a First Stroke After Induction of a Second Stroke: Reopening a Postischemic Sensitive Period. *Neurorehabilitation and neural repair* 2015.

Zhu LL, Lindenberg R, Alexander MP, and Schlaug G. Lesion load of the corticospinal tract predicts motor impairment in chronic stroke. *Stroke; a journal of cerebral circulation* 41: 910-915, 2010.

Zito K, and Svoboda K. Activity-dependent synaptogenesis in the adult Mammalian cortex. *Neuron* 35: 1015-1017, 2002.

Appendix

Analysis scripts can be found at <https://github.com/KevinBWilkins>.

EEG Analysis

Dynamic Causal Modeling for Induced Responses

Prior to running Dynamic Causal Modeling for Induced Responses (DCM-IR), EEG data was converted to the proper format. First, markers were placed at EMG onset using the program BrainVision Analyzer. The unfiltered continuous data was then down sampled from 2048 Hz to 256 Hz to reduce file size. DCM will do this automatically at a later stage if this is not done here. Finally, data was exported from BrainVision Analyzer as a .eeg file, including both a header and marker file, in a binary data file format with multiplexed data orientation. This process was repeated for each block of trials.

Once the data was exported as a .eeg file, it was converted to SPM format in SPM12, which allows for faster and more efficient processing for the subsequent steps. We then used the ‘prepare’ feature for the following:

1. Add the channel locations from separate .mat files for the electrodes and fiducials (x, y, z coordinates; electrodes = 160x3 matrix; fiducials = 3x3 matrix)
2. Create a Trial Definition .mat file to create epochs from -2200 ms to +500 ms relative to EMG onset markers
3. Create an Average Reference .mat file for all good channels

The continuous data was then preprocessed in batch with the following parameters:

1. Bandpass filtered between 1 and 50 Hz using a 5th order, zero-phase Butterworth filter

2. Montaged with Average Reference File
3. Epoched using the Trial Definition file, with no baseline correction and no padding (epoch was already long enough and did not need further padding)
4. Baseline corrected between -2180 and -1800 ms

Following this preprocessing, bad trials were removed. This process was repeated with the other blocks for that condition and then trials were merged. Lastly, bad channels were removed from further analysis.

Preprocessed and artifact-free trials were then loaded into the DCM-IR (**DCM_Ind.m**). We used a time window of -1000 to 0 ms. Note, the spectrogram was computed across the entire epoch (-2200 to +500 ms), and then cut to only include -1000 to 0 ms. This way there were no edge artifacts from the wavelet. Settings for detrend (=1) and subsample (=1) were left as defaults, and the number of modes was changed to 4. This choice was verified in a post-hoc analysis to ensure that 4 modes captured enough of the data. We selected an onset of -400 ms and a duration of 400 ms. Source locations were then set and then a forward model was created using SPM's software. This required a T1 MRI image of the participant in a .nii format, which was then used to create a Boundary Element Method model and co-registered with EEG electrode location. Following creation of the forward model, we set the model connections for both linear and nonlinear connections as well as the input to the model. Wavelets were computed between 4 and 48 Hz with a cycle number of 7. Once these parameters were set, the model was inverted to solve for the A coupling matrix. Results of the DCM as well as the images of coupling matrices were saved.

Once all possible models for all subjects were inverted, we used Bayesian Model Selection (BMS) to evaluate which model best explained the observed data. We used Random Effects since this allows for intragroup heterogeneity which is likely the case in stroke. We first set up a family-level inference to compare two groups of models (with and without nonlinear intrinsic connections). We then ran a follow-up analysis to compare all of the models within that winning family.

After determining the best model using BMS, images of coupling matrices for that model were smoothed using a Gaussian smoothing kernel with a Full Width at Half Maximum of 8 x 8 x 8 mm in the x, y, and z direction. The MATLAB script **stats_batch_5regECD.m** then evaluated the necessary one-sample, two-sample, or paired t-test comparison depending on the analysis. The MATLAB script **ANOVA_batch_script.m** evaluated a 2x2 flexible factorial for group (control/stroke) and task (open/lift+open).

The following scripts were used in follow-up analyses:

1. DCM_VarianceExplained.m

- a. Calculate Variance Explained for best model based on residuals
- b. Calculate Variance Explained for the number of frequency modes chosen

2. couplingmat.m

- a. Plots exceedance probabilities for BMS results
- b. Extracts coupling values from individual A matrices in particular connections/frequencies
- c. Recreates Frequency-Frequency coupling figures
- d. Recreates Frequency-Frequency coupling figures with only significant voxels

- e. Recreates Time-Frequency maps for both observed and simulated data

3. Avg_CouplingAmatrix.m

- a. Creates average A coupling matrix for all subjects

4. TF_ObservedPredictued_Group.m

- a. Creates an average Time-Frequency map for observed and simulated data

5. ExtractValues.m

- a. Extracts out significant values from A matrix

6. CreateSigMaps.m

- a. Need **loadcolorscheme.m** to run
- b. Creates frequency-frequency matrix image for significant voxels

Pressure Analysis

Pressure was measured using the TactArray Pressure mat from Pressure Profile Systems (PPS) in conjunction with the ACT3D robot. Each trial, .mat files were created for the robotic measurements (lift_##_**) and PPS measurements (lift_##_**_ppsPressure and **_##_condition_ppsTime). ## represents the trial number and ** represents the condition (table or SABD load). The MATLAB program **PPS_newSensoryMat_BC.m** calculated the pressure of each finger based on either the user's selection or autodetection of where the greatest pressure occurred during the trial. These values were then normalized by the max grasping pressure.

Robotic metrics were not used for analyses in this thesis, but were saved with the following format: Row 1= current iteration, Row 2 = current period, Rows 3-5 = end effector position (x, y, z), Rows 6-8 = end effector velocity (x, y, z), Rows 9-11 = end effector force (x, y, z), Row 12 = shoulder

flexion angle, Row 13 = elbow flexion angle, Row 14= shoulder abduction angle, Row 15 = end effector rotation, Rows 16-18 = reach percentage value, Row 19 = is arm on the table, Row 20 = TTL, Row 21 = end effector rotation.

Gray Matter Density Analysis

Prior to running the Voxel-Based Morphometry (VBM) analysis, we flipped the T1 structural image so that all stroke participants had the lesion in the same hemisphere. To do this, we used **load_untouch_nii.m**, the function **flipdim**, and **save_untouch_nii.m** which are located on the department's cluster.

Once all brains were in the correct orientation, each T1 image was placed in an FSL-VBM directory. Stroke participants were labeled 's_INITIALS' and control participants were labeled 'c_INITIALS'. A subset of images from the stroke group (equal to the total number of control participants) chosen randomly were put into an additional folder called 'template_list' to account for differences in group size along with all of the control group images.

We first ran the command **fsl_vbm_q_bet -b** in the terminal to move all the images to a new 'struc' folder and then run brain extraction of the images (separate the brain tissue from skull/skin). Each brain extracted image was visually inspected to ensure the quality of the extraction. Additional options were added to **bet** if the extraction was poor.

Next, we created a study-specific gray matter template using the command **fslvbm_2_template -a**. This segments the brain into gray matter, white matter, and CSF. The gray matter images in the

template list are affine-registered to the gray matter ICBM-152 template, concatenated, and averaged. This provides a first-pass, study-specific “affine” gray matter template. The gray matter images are re-registered to this gray matter template using non-linear registration. The resulting study-specific gray matter template is $2 \times 2 \times 2 \text{ mm}^3$ in standard space.

After creating the template, we non-linearly registered all the gray matter images to the study-specific template using the command **fslvbm_3_proc**. This also introduces a compensation for the contraction/enlargement due to the non-linear component of the transformation. Images are then smoothed by a Gaussian kernel with a sigma = 3mm. A gray matter mask is also created.

Finally, we quantified group differences in gray matter density using threshold-free cluster analysis (TFCE) and permutation testing (n=5000). We did this by running the command **randomize -i GM_mod_merg_s3 -m GM_mask -o fslvbm -d design.mat -t design.con -T -n 5000**.

We accounted for sex and age by including these as covariates in the design file. To do this, we demeaned sex and age in Excel and created the new contrast file (see picture below). We then ran the command **randomize -i GM_mod_merg_s3 -m GM_mask -o fslvbm_cov -d design_cov.mat -t design_cov.con -T -D**. For analyses restricted to only a particular region, we added on a mask on the top of the GM_mask.

General Linear Model

EVs **Contrasts & F-tests**

Number of main EVs 4

Number of additional, voxel-dependent EVs 0

Paste

	Group	EV1		EV2		EV3		EV4	
		group A	group B	Age	Sex				
Input 1	1	1	0	-11.1	0.7E				
Input 2	1	1	0	1.7E	-0.2E				
Input 3	1	1	0	-0.2	-0.2E				
Input 4	1	1	0	1.7E	-0.2E				
Input 5	1	1	0	1.7E	-0.2E				
Input 6	1	1	0	6.7E	-0.2E				
Input 7	1	1	0	-14.1	0.7E				
Input 8	1	1	0	-5.2	0.7E				
Input 9	1	1	0	14.7	-0.2E				
Input 10	1	1	0	8.7E	0.7E				
Input 11	1	1	0	0.7E	-0.2E				
Input 12	1	0	1	2.7E	0.7E				
Input 13	1	0	1	-10.1	-0.2E				
Input 14	1	0	1	0.7E	-0.2E				
Input 15	1	0	1	0.7E	-0.2E				
Input 16	1	0	1	0.7E	-0.2E				
Input 17	1	0	1	3.7E	-0.2E				
Input 18	1	0	1	8.7E	-0.2E				
Input 19	1	0	1	-2.2	-0.2E				
Input 20	1	0	1	0.7E	0.7E				
Input 21	1	0	1	6.7E	0.2E				

View design Efficiency

General Linear Model

EVs **Contrasts & F-tests**

Contrasts 4 F-tests 0

Paste

	Title	EV1	EV2	EV3	EV4
C1	Control > Str	1	-1	0	0
C2	Stroke > Cor	-1	1	0	0
C3	group A mea	1	0	0	0
C4	group B mea	0	1	0	0

View design Efficiency